QUANTIFICATION OF THE ACTIVITIES OF

BCL-2 AND BCL-XL

QUANTIFICATION OF THE ACTIVITIES OF THE ANTI-APOPTOTIC PROTEINS BCL-2 AND BCL-XL

By

ALINE A. FIEBIG, B.SC.

A Thesis

Submitted to the School of Graduate Studies

In Partial Fulfillment of the Requirements

For the Degree

Master of Science

McMaster Univeristy

Master of Science (2003) McMaster University

(Biochemistry) Hamilton, Ontario

TITLE: Quantification of the Activities of the Anti-Apoptotic Proteins Bcl-2 and Bcl-XL

AUTHOR: Aline A. Fiebig, B.Sc. (University of Waterloo)

SUPERVISOR: Dr. David W. Andrews

NUMBER OF PAGES: XIV, 127

Abstract

Apoptosis is the process by which organisms eliminate excess, damaged or hazardous cells in a controlled manner. This process is controlled by the Bcl-2 family of proteins. Bcl-2 and Bcl-XL are anti-apoptotic paralogues that can replace CED-9, the sole homologue in *C. elegans*. It has therefore been assumed that Bcl-2 and Bcl-XL are replaceable and functionally identical. However, evidence in some mammalian cells indicates that this may not be the case. The purpose of this project was to exhaustively compare the anti-apoptotic activities of Bcl-2 and Bcl-XL in one cell type. As Bcl-2 and Bcl-XL have been found to localize to the ER and the outer mitochondrial membrane, we also determined whether subcellular location affects the function of these proteins differently. MCF-7 breast cancer cells were stably transfected with Bcl-2 and Bcl-XL alternatively targeted to the ER or mitochondria, and exposed to various doses of doxorubicin; PARP cleavage was measured using quantitative Western blotting as an indication of apoptosis to obtain EC_{50} values in the different cell lines. The levels of both Bcl-2 and Bcl-XL affected anti-apoptotic activity; specific degradation of both proteins was noted at higher doses of doxorubicin. Nevertheless, the results indicated clearly that there was a difference between Bcl-2 and Bcl-XL. Using EC_{50} values Bcl-XL mutants were at least 8 times more protective than Bcl-2 mutants. Furthermore, most of the cleavage products of PARP in Bcl-XL expressing clones were due to non-caspase-7 proteases, a pattern not seen with Bcl-2. Bcl-2 and Bcl-XL localized to mitochondria

were most effective, while cytosolic and ER localized Bcl-XL were less effective, and Bcl-2 at these sites did not inhibit apoptosis.

Acknowledgments

There are many souls who have made the completion of this project possible, academically, emotionally and spiritually.

My deepest thanks go to my committee members: Dr. David Andrews, Dr. Brian Leber and Dr. Eric Brown. Each has given me advice and encouragement in their own ways.

A few necessary components for this project were obtained from members of the scientific community outside of McMaster University. The original plasmid containing Bcl-XL was obtained from Dr. G. Nunez at the University of Michigan and the MCF-7 cell line expressing procaspase-3 was obtained from Dr. C. J. Froelich at Evanston Northwestern Healthcare Research Institute.

My thanks also go out to faculty members of the Biochemistry and Biology departments at McMaster University, especially Dr. Dino Trigatti, Dr. John Hassel, Dr. Eric Brown, Dr. Ray Truant, Dr. Gerry Wright and Dr. John Capone for use of laboratory equipment throughout the course of my work.

I would also like to thank the many members of the Andrews' lab, both past and present. Mina Falcone was a constant companion during time spent in the Central Animal Facility. Weijia Zhu, the tissue culture goddess of the lab, has been there to help me on numerous occasions. I would also like to thank Catherine Hollerbach and Alison Cowie, Weijia Zhu, Helen Atkinson, Bomina Yu and Mina Falcone for constructing the plasmids used in this investigation. A declaration of appreciation would not be complete without acknowledging Iain Mainprize for his stimulating conversations, his expertise in

Table of Contents

Abbreviations

acta – carboxyl terminal insertion sequence of the ActA protein

αM – Cell lysates made from cells maintained in αMEM + 10 % FBS for two days

αMEM – Alpha-minimal essential medium

B6 – vitamin B6

BH – Bcl-2 homology

BID – Bcl-2 interacting domain

BSA – Bovine serum albumin

cb5 – ER specific isoform of cytochrome b5

CBD – Chitin binding domain

CHAPS – 3-[(3-cholamidopropyl) dimethylammonio]-1-propane sulfonate

$\Delta\Psi m$ – mitochondrial membrane potential

ΔTM – Carboxyl hydrophobic terminal tail deletion

DISC – Death inducing signaling complex

Dox – Doxorubicin (Adriamycin)

DTT – Dithiothreitol

EC_{50} – Effective concentration; concentration of agent that will induce 50 % of desired response

EDTA – Ethylenediaminetetraacetic acid

ER – Endoplasmic reticulum

est- – Cell lysates made from cells maintained for 6 days in estrogen depleted condtions

ETOP – Etoposide (VP-16)

FITC – fluorescein-5-isothiocyanate

HI-FBS – Heat inactivated fetal bovine serum

HRP – Horseradish peroxidase

IAP – Inhibitor of apoptosis protein

LB – Luria broth

MMP – Mitochondrial membrane potential

Neo – Denotes MCF-7 cells transfected with pRcCMV vector only

nt – no tail; analogous to ΔTM

PARP – Poly ADP-ribose polymerase

PBS – Phosphate buffered saline

PIN – Protease inhibitor cocktail

RAG – Recombination activating gene

ROS – Reactive oxygen radicals

SDS-PAGE – Sodium dodecylsulphate polyacrylamine gel electrophoresis

SPF – Specific pathogen free

TB3 – Test bleed number 3

TBS-T – Buffer for washing Western blot membranes; contains Tris-HCl, NaCl and Tween 20

TLB – Tricene SDS-PAGE loading buffer

TNF – Tumour necrosis factor

Tris – Tris (hydroxymethyl) amino methane

VDAC – Voltage dependent anion channel

wt – Wild type

YS – Yosemite Sam

List of Figures

List of Tables

1 Introduction

Multicellular organisms regulate cell death by both intra- and extra-cellular signals. This occurs both during development, and in adults for tissue maintenance and survival. This process of programmed cell death is termed apoptosis (reviewed in Adams and Cory, 1998). Apoptosis enables an organism to eliminate excess, damaged or hazardous cells in an organized manner such that dead cells are packaged and disposed of without inflammation (reviewed in Adams and Cory, 1998). A set of morphological and biochemical characteristics accompanies apoptosis, including chromatin condensation, internucleosomal DNA cleavage (Wyllie, 1980), cell shrinkage, membrane blebbing and often diverse yet specific protein cleavage (reviewed in Zornig et al., 2001).

Aberrations in the apoptotic process can cause major pathologies. If apoptosis is suppressed, cancer and autoimmune diseases can result, while AIDS and neurodegenerative disorders such as Huntington's disease and Alzheimer's disease can result from excess apoptosis (reviewed in Zornig et al., 2001)

1.1 The Two Pathways of Apoptosis

Apoptosis has been described in all multicellular organisms, including plants, nematodes, insects and vertebrates. The current model recognizes that the process of apoptosis is more complex than previously thought, and that cross talk between different elements exists.

Apoptosis is now described as proceeding either by an intrinsic or extrinsic pathway. The extrinsic pathway is initiated by ligand association with death receptors like Fas or TNF receptor that then activate procaspase-8 (see left side of Figure 1). The intrinsic pathway is engaged by chemotherapeutic agents, oncoproteins, DNA damage, hypoxia and survival factor deprivation and involves the disruption of the mitochondrial membrane and eventual formation of the apoptosome (Apaf-1, procaspase-9 and cytochrome c) (see right side of Figure 1) (reviewed in Johnstone et al., 2002; reviewed in Wang, 2001).This figure outlines some of the cellular factors known to be involved in doxorubicin induced apoptosis and is therefore highly simplified.

Ligand association with a death receptor triggers the formation of a death inducing signalling complex (DISC). Adapter proteins are recruited to the DISC, which in turn recruits initiator procaspases (e.g. procaspase-8) that are subsequently proteolytically activated. Active caspase-8 can then activate the executioner caspases (procaspase-3 and procaspase-7), leading to apoptosis. Activation of procaspase-8 can be inhibited by both FLIP and inhibitor of apoptosis proteins (IAP) (reviewed in Johnstone et al., 2002). Some cell types require that the apoptotic signal be amplified at the mitochondria through BID. Caspase-8 cleaves the amino-terminal portion of BID to generate the carboxyl terminal p15 tBID. tBID translocates from the cytosol to the mitochondria where it can initiate cytochrome c release (Gross et al., 1999b).

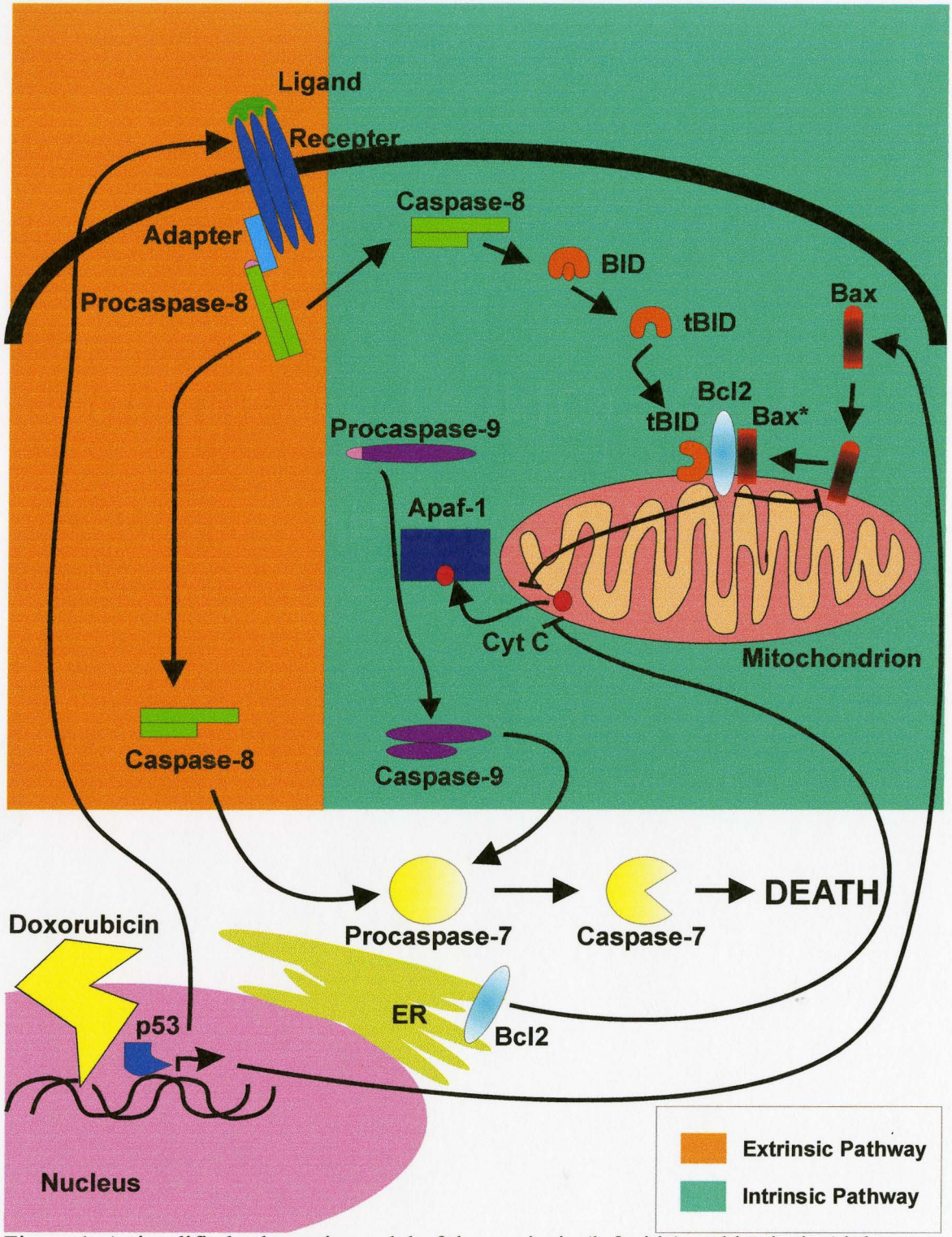

Figure 1: A simplified schematic model of the extrinsic (left side) and intrinsic (right side) pathways of apoptosis. For a complete description refer to text in the introduction. Modified from Johnstone *et al.*, 2002; Gross *et al.*, 1999a; as reviewed by Wang, 2001.

The intrinsic apoptotic pathway centres on the mitochondrion. The Bcl-2 family of proteins is thought to regulate mitochondrial membrane permeability by the opposing actions of the pro- and anti-apoptotic members of this family. Bcl-2 and Bcl-XL are integral membrane anti-apoptotic proteins that can inhibit tBID and Bax-induced cytochrome c release (Desagher et al., 1999) as well as the release of SMAC/Diablo from the mitochondrial intermembrane space (Sun et al., 2002). Bcl-2 and Bcl-XL inhibit Bax activation (Annis et al., 2001; Kuwana et al., 2002) as well as translocation from the cytosol to mitochondria, thereby inhibiting cytochrome c release (Annis et al., 2001). In both the intrinsic and extrinsic pathways, if cytochrome c is released into the cytosol, it allows Apaf-1 to bind ATP and activate procaspase-9. Active caspase-9 can then activate further downstream executioner caspases (reviewed in Johnstone et al., 2002; reviewed in Wang et al., 2001).

1.2 The Bcl-2 Protein Family

The Bcl-2 family of proteins is a subset of proteins that regulate apoptosis. Members of this family are either death agonists (Bax, Bak, Egl-1, etc.) or antagonists (Bcl-2, Bcl-XL, Ced-9, etc.) (see Table 1). The first member of this family to be discovered was Bcl-2. It was found that 80 % of patients with human follicular B-cell lymphoma have a t(14;18) chromosomal translocation breakpoint that places the *bcl-2* gene under the control of the immunoglobin heavy chain enhancer, leading to its activation and constitutive expression (Pegoraro et al., 1984).

Table 1: Members of the Bcl-2 protein family from mammalian, avian, nematode, and viral sources. Antiapoptotic Bcl-2 proteins suppress cell death, while proapoptotic family members promote death. The proapoptotic family members can be subdivided according to the presence or absence of conserved Bcl-2 homology domains 1 and 2, where the Bax subfamily contains three BH domains (BH1, BH2 and BH3) and the BH3 subfamily is missing two of the three domains.

Antiapoptotic		**Proapoptotic**	
		Bax Subfamily	**BH3 Subfamily**
Bcl-2	Bcl-XL	Bax	Bik
Bcl-w	Mcl-1	Bak	Blk
A1	NR-13	Bok	Hrk
BHRF1	LMW5-HL	Bcl-XS	Bad
ORF16	KS-Bcl-2		Bid
E1B-19K	Ced-9		Egl-1

Mammalian: Bcl-2, Bcl-XL, Bcl-w, Mcl-1, A1, Bax, Bak, Bok, Bcl-XS, Bik, Blk, Hrk, Bad, Bid; Avian: NR-13; Nematode: Ced-9 , Egl-1; Viral: BHRF1, LMW5-HL, ORF16, KS-Bcl2, E1B-19K. Modified from Adams and Cory, 1998 and Gross *et al.*, 1999b.

The discovery of Bcl-2 lead to the identification of a new class of oncoproteins. Unlike those previously described that increase proliferation, like c-Myc, Bcl-2 prevents cell death (Pegoraro et al., 1984). Other members of the family were subsequently discovered, including: Bcl-XL and Bcl-XS that are alternative splice variants of the *bcl-X* gene (Boise et al., 1993), Bax (Oltvai et al., 1993) and Bak (Kiefer et al., 1995). To date the family contains 16 members in mammals (Petros et al., 2001).

Bcl-2 and Bcl-XL display both structural and functional similarities, leading to generalizations regarding their participation in a common pathway to inhibit cell death. These similarities have spurred two theories by which these proteins are thought to act: 1) titration of function either by sequestering of pro-apoptotic family members by Bcl-2 and Bcl-XL via the BH domains, and 2) formation of a pore via two central hydrophobic regions, facilitating ion translocation (reviewed in Gross et al., 1999a). Experimental data is available to support both of these hypotheses that may not be mutually exclusive.

Members of the Bcl-2 family contain at least one of four conserved Bcl-2 homology (BH) domains (see Figure 2A and B). These domains have been shown to mediate protein-protein interactions (reviewed in Adams and Cory, 1998). Those members that inhibit apoptosis contain at least BH domains 1 and 2, while those most similar to Bcl-2 contain all four BH domains and a transmembrane anchor. Only two anti-apoptotic proteins have been identified without a transmembrane region, A1 (mammalian) and LMW5-HL (viral) (reviewed in Gross et al., 1999a). The proapoptotic

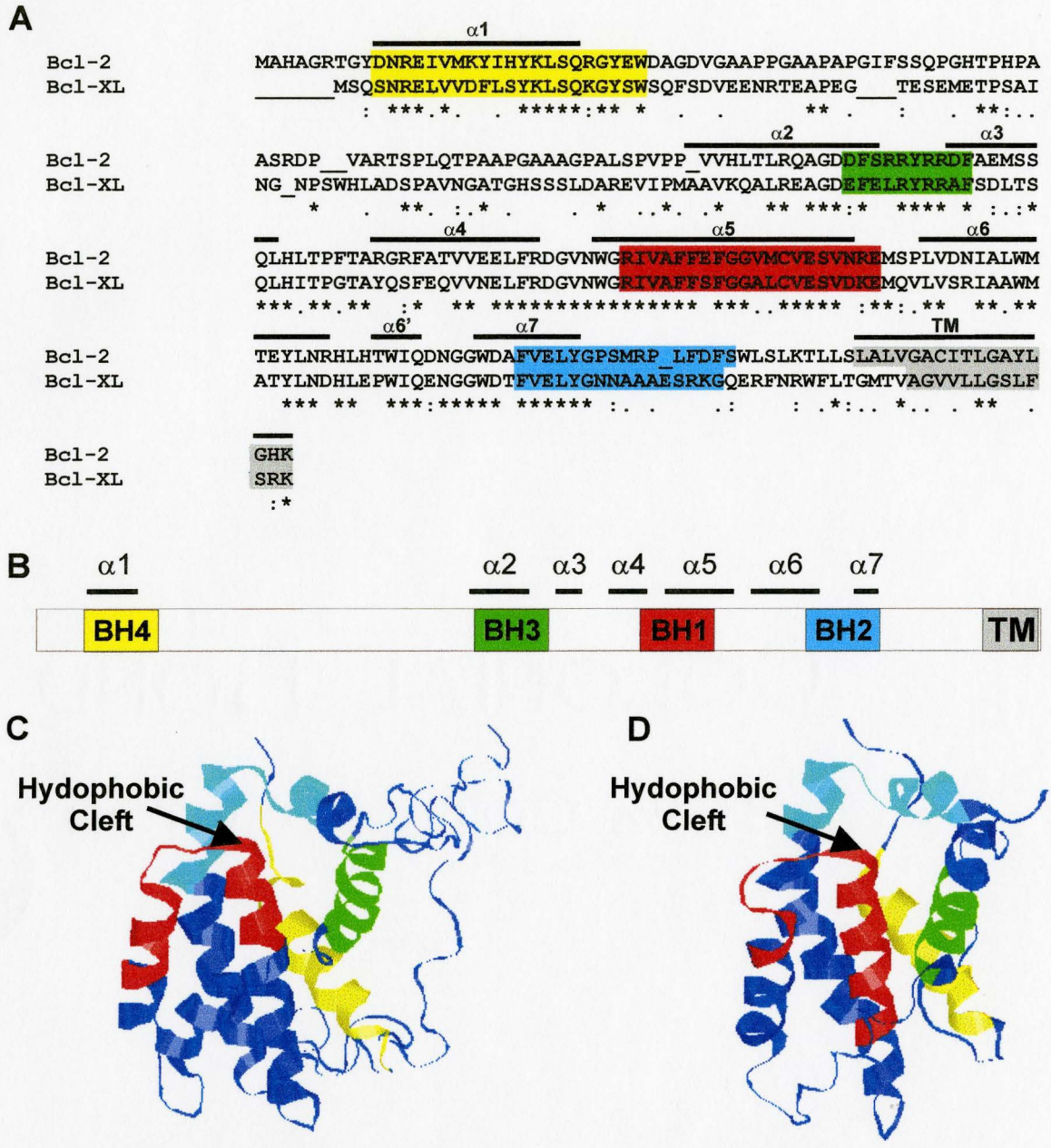

Figure 2: Bcl-2 and Bcl-XL have similar protein sequences and structures. A) A sequence alignment of the Bcl-2 (isoform 2) and Bcl-XL cDNA shows a great deal of identical (*), conserved polar (:) and conserved nonpolar (.) residues between the two proteins (Voet and Voet, 1995). The BH domains and α helices are noted. Alignments made with Clustal 1.7. B) Schematic representation of the Bcl-2 and Bcl-XL proteins. NMR structures of the human C) Bcl-XLΔTM and D) human Bcl-2/Bcl-XL chimera. The Bcl-2/Bcl-XL chimera is composed of human Bcl-2 (isoform 2) with the loop region (amino acids 51 - 91) of Bcl-XL. The last 11 hydrophobic amino acids of Bcl-2 were also removed. Adapted from Muchmore *et al.*, 1996 and Petros *et al.*, 2001). BH1: Bcl-2 homology domain 1, etc; TM: transmembrane region.

Bax subfamily retains all BH domains except BH4 and most resemble Bcl-2, while the BH3subfamily retains only the BH3 domain (see Table 1) (reviewed in Adams and Cory, 1998). The existence of the BH3 subfamily proteins argued that the BH3 is the minimal region required for cell death (reviewed in Adams and Cory, 1998).

Both Bcl-2 and Bcl-XL contain all four BH domains and a C-terminal hydrophobic region required for membrane localization; the two proteins display 56 % nucleotide identity and 43 % amino acid identity (Boise et al., 1993). The NMR and crystal structure of Bcl-XL without the transmembrane region (Bcl-XLΔTM) revealed that the BH1, BH2 and BH3 domains were in close proximity and formed an elongated hydrophobic cleft (see Figure 2C). It was postulated that this cleft could be the site of interaction with pro-apoptotic proteins (Muchmore et al., 1996). Subsequently, the BH3 region of Bak was shown to bind the hydrophobic cleft formed by the BH1, BH2 and BH3 regions of Bcl-XL (Sattler et al., 1997). The authors also state that while the BH3 region binds the cleft with a high affinity, modelling of the full length proteins suggested the necessity of a conformational change to expose the hydrophobic surface of the α2 helix in Bak, which contains the BH3 domain (Sattler et al., 1997). The dimerization function of Bcl-2 and Bcl-XL with Bax has been examined by using immunoprecipitation investigations (Oltvai et al., 1993; Sedlak et al., 1995). It should be noted that these immunoprecipitation investigations showed dimerization capabilities between several of the Bcl-2 family members using non-ionic detergents. However, Hsu and Youle found that the use of non-ionic detergents in immunoprecipitation investigations involving Bcl-2 proteins induced a conformational change in the molecules, facilitating dimerization

(Hsu and Youle, 1997b). Therefore, previous investigations showing dimerization between pro- and anti-apoptotic Bcl-2 family members may only be valid in the presence of the detergent-induced interactions following a conformational change. For example, investigations involving a mutant form of Bax, lacking a C-terminal hydrophobic tail (BaxΔTM), and Bax ΔS184, which constitutively localizes to the mitochondrion, suggest that the conformation of the molecule is determined by the C-terminal tail (Nechushtan et al., 1999). This is confirmed by the solution structure of Bax (Suzuki et al., 2000). The Bax ΔS184 mutant, although constitutively localized at the mitochondrion, undergoes a conformational change only after induction of apoptosis, that can be detected by the conformation-specific monoclonal antibody 6A7. Bcl-XL protects cells transfected with either full length Bax and the Bax ΔS184 mutant (Nechushtan et al., 1999), possibly sequestering active Bax after translocation to the mitochondrial outer membrane.

Mutations within the BH1, BH2 and BH3 domains of Bcl-XL abolish its binding to Bax, yet still protects cells from IL-3 withdrawal induced apoptosis (Cheng et al., 1996; Minn et al., 1999). This suggests that Bcl-2 and Bcl-XL may control apoptosis without binding death agonists. Once the NMR and X-ray structures of Bcl-XLΔTM were obtained, it was noted that they resembled the membrane insertion domain of bacterial toxins like diphtheria toxin and the colicins (Muchmore et al., 1996; Aritomi et al., 1997). As well, the NMR structure of a Bcl-2/Bcl-XL chimera resembles the Bcl-XLΔTM NMR structure (see Figure 2D) (Petros et al., 2001). However, it should be noted that the Bcl-2/Bcl-XL chimera is composed of both Bcl-2 and Bcl-XL templates: amino acids 1 - 34 = Bcl-2, 35 - 50 = Bcl-XL, 92 - 207 = Bcl-2. As well, amino acids 208

- 239 of the C-terminus of Bcl-2 are absent. The substitutions and deletions in the Bcl-2/Bcl-XL chimera were necessary to improve solubility permitting analysis by NMR (Petros et al., 2001). These proteins have two central hydrophobic helices (α5 and α6) surrounded by five amphipathic helices. It was postulated that, like the bacterial toxins, organization of the central hydrophobic core of Bcl-XL allows the proteins to remain water soluble, until a conformational change facilitates insertion of α5 and α6 into membranes (Schendel et al., 1997). Work performed by Atkinson, whereby the cysteine near the C-terminus of α5 (C151) was labelled with an environmentally sensitive fluorescent dye, NBD, showed that this cysteine in the context of full length Bcl-XL inserted into the interior of the membrane bilayer in liposomes and ER microsomes (Atkinson, 2001). Full length Bcl-XL has been shown to form a cation selective channel (Na^+) in planar lipid bilayers that can be inhibited by luminal Ca^{2+} (Lam et al., 1998). Bcl-2ΔTM has also been shown to form cation selective channels in acidic lipid membranes; however, this study was performed at an unphysiologically low pH to provoke membrane insertion of Bcl-2ΔTM (Schendel et al., 1997). Formation of the cation selective channel suggests regulation of membrane permeability by these proteins. When the region surrounding the α5 and α6 hairpin of Bcl-XL (E153 to R165) was replaced with the corresponding region of Bax (K123 to T135), the mutant showed a decreased ability to form channels in planar lipid bilayers (Minn et al., 1999). When this mutant was further mutated to render it incapable of Bax binding, it did not protect FL5.12 cells from apoptosis induced by growth factor withdrawal (Minn et al., 1999).

Previous studies have demonstrated that Bcl-2 is localized to the mitochondrion, endoplasmic reticulum (ER) and the nuclear envelope (Krajewski et al., 1993; Janiak et al., 1994b). Similarly Bcl-XL has been shown to reside in the nuclear envelope, cytosol and extra-nuclear membranes, including the mitochondrion (Gonzalez-Garcia et al., 1994; Hsu et al., 1997a). The subcellular location of these antiapoptotic proteins is physiologically relevant (Zhu et al., 1996; Annis et al., 2001; Soucie et al., 2001). The mitochondrion has been found to play a central role in apoptosis. If the cell is compromised, the mitochondria can undergo dysfunction, including loss of membrane potential, production of reactive oxygen radicals (ROS) and release of proteins into the cytosol that normally reside in the intermembrane space (reviewed in Gross et al., 1999a). These events can be countered by Bcl-2 (Annis et al., 2001). The role of the ER in apoptosis is less clear. It is thought that the ER can be a site of direct caspase activation, or ER involvement in apoptosis could involve intracellular Ca^{2+} homeostasis (reviewed in Rudner et al., 2001).

The Bcl-2 family of proteins are targeted to membranes by insertion sequences (Janiak et al., 1994a) or regions of hydrophobic amino acids at the C-terminal end of proteins that target them to the lipid bilayer of specific organelles (Kutay et al., 1993). The ER specific isoform of cytochrome b5 is one such protein that has been well characterized. It has been shown that the insertion sequence of this protein can target foreign proteins to the ER (Mitoma and Ito, 1992). Pister *et al.*, have shown that when the amino terminal secretory sequence of the *Listeria monocytogenes* actin nucleation protein (ActA) protein is removed, the remainder of the protein binds specifically to the outer

mitochondrial membrane (Pistor et al., 1994). This suggested that the carboxy-terminal transmembrane domain of ActA could function as a mitochondrial specific insertion sequence. These defined sequences were used to construct Bcl-2 mutants with specified targeting. Bcl-2 targeted to either the ER or the mitochondrion by exchanging the endogenous C-terminal insertion sequence of Bcl-2 with those of the rat liver ER cytochrome b5 (Bcl-2-cb5) or the *Listerial* ActA (Bcl-2-acta), respectively (Zhu et al., 1996) (see Figure 3).

The Bcl-2 mutants were used to determine the importance of Bcl-2 subcellular localization in MDCK epithelial and Rat-1/myc fibroblast cells (Zhu et al., 1996). In the epithelial cells, only the wild type (wt) Bcl-2 and Bcl-2-acta protected cells from serum starvation-induced apoptosis. The converse is true in fibroblast cells, where Bcl-2-cb5 was more effective (Zhu et al., 1996). The fact that the Bcl-2-cb5 and Bcl-2-acta chimeras are functional in at least one cell line indicates that protein function was not lost due to misfolding. The cytosolic version of Bcl-2 lacking the transmembrane region (Bcl-2-nt) failed to protect MDCK cells from death induced by serum withdrawal. This data favoured a model where cell death can follow two spatially distinct pathways within a cell, suggesting that this response could be cell type dependent or due to the presence of over-expressed exogenous myc (Zhu et al., 1996). Further studies addressing the latter issue showed that within Rat-1/myc cells two apoptotic pathways exist. Rat-1/myc cells exposed to low serum, ceramide or taxol were preferentially protected from apoptosis by Bcl-2-cb5, while Bcl-2-acta inhibited apoptosis in these cells and in cells treated with

Bcl-2
...SWLSLKTLLSLALVGACITLGAYLSHK

Bcl-2-acta
...SWLSLKLILNAMLAIGVFSLGAFIKIIQLRKN

Bcl-2-cb5
...SWLSLKITTVESNSSWWTNWVIPAISALVVALMYRLYMAED

Bcl-XL
...GQERFNRWFLTGMTVAGVVLLGSLFSRK

Bcl-XL-nt
...GQERFLN

Bcl-XL-acta
...GQERFLILNAMLAIGVFSLGAFIKIIQLRKNN

Bcl-XL-cb5
...GQERFLKITTVESNSWWTNWVIPAISALVVALMYRLYMAED

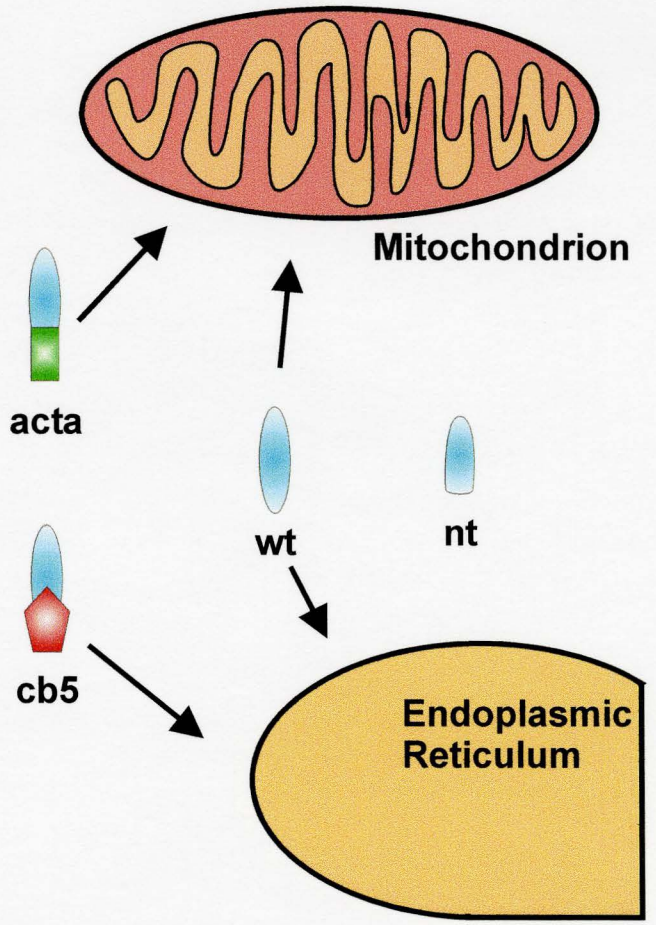

Figure 3: Amino acid sequences of the C-terminal portions of wild type Bcl-2 and Bcl-XL and the Bcl-2 and Bcl-XL mutants. Differentially targeting mutants of Bcl-2 and Bcl-XL were constructed to direct the proteins to either the mitochondria (acta) or the endoplasmic reticulum (cb5). Molecules with a mitochondrial and ER targeting sequences are represented in green and red respectively. Wild type Bcl-2 and Bcl-XL are represented by dark and light blue respectively. Amino acids in black are modified due to subcloning.

etoposide (Lee et al., 1999; Annis et al., 2001; Soucie et al., 2001). C-Myc is a transcription factor that is frequently implicated in carcinogenesis. Deregulation of Myc drives continuous tumour cell proliferation due to a loss of Myc response to growth inhibitory signals (Prendergast, 1999). Furthermore, these pathways can be distinguished by the temporal order of cytochrome c release and loss of mitochondrial membrane potential (MMP) (Annis et al., 2001). Bcl-2-cb5 inhibits apoptosis characterized by an initial decrease in MMP followed by cytochrome c release, while it does not inhibit apoptosis induced by apoptotic agonists that elicit Bax translocation to the mitochondrion and cytochrome c release before MMP decrease (Annis et al., 2001).

1.3 Functional Differences Between Bcl-2 and Bcl-XL

Despite the similarities in structure and function, there are studies that suggest that Bcl-XL and Bcl-2 might not be functionally homologous. Although not proof of different function, the expression patterns of endogenous Bcl-2 and Bcl-XL differ during the development of B cells and thymocytes. For example, thymocyte development follows a path through the thymus whereby pre-thymocytes, characterized by cell surface expression of the pre T-cell receptor, are positively selected. In the next stage of development, double positive thymocytes express both CD4 and CD8. These cells undergo further selection and become either $CD4^+$ or $CD8^+$ single-positive thymocytes (Abbas et al., 2000). Bcl-2 expression increases in pre-thymocytes and single-positive thymocytes, while Bcl-XL expression remains low during these times of development. These expression levels of Bcl-2 and Bcl-XL are reversed in double-positive thymocytes. Studies have been performed on Bcl-2 and Bcl-XL in a knockout mouse model. *Bcl-2*

knockout mice reveal a smaller spleen and thymus than control mice. The maturation of B cells and thymocytes appears to proceed normally, however their cell life span is decreased (Kamada et al., 1995). *Bcl-X* -/- mice die at day 13 of gestation (Motoyama et al., 1995). The *bcl-X* -/- mice showed extensive neuronal and haematopoietic cell death. To further assess the effect of *bcl-X* on lymphocytes, double knock out chimeric mice of *bcl-X* and recombination activating gene (*RAG-2*) were made. The *RAG* genes enable immature B and T lymphocytes to undergo V(D)J recombination. Knockout mice lacking RAG-2 fail to develop any mature B and T lymphocytes, but are viable (Shinkai et al., 1992). Therefore, the effects of the absence of *bcl-X* can be determined. There was a decrease in the number of single-positive thymocytes in the thymus in the *bcl-X* and *RAG-2* deficient mice, and the number of pre-B cells was also decreased in bone marrow. The ratio of mature B and T cells in the lymph node and spleen were decreased, however, the population distribution was considered normal (Motoyama et al., 1995). These studies indicate that *bcl-X* gene products have an essential role during the development of immature lymphoid cells, while the *bcl-2* gene product affects the life span of mature lymphoid cells.

In vitro studies show further evidence of functional differences between Bcl-2 and Bcl-XL. Using lymphoid tissue culture cells, a 2 – 8 fold increase in viability of Bcl-XL transfected cells was compared to Bcl-2 transfected cells following inhibition of protein synthesis (Gottschalk et al., 1994), or IL-3 withdrawal (Boise et al., 1993). This evidence supports, but does not confirm, independent control of different stages of lymphoid development by Bcl-2 and Bcl-XL in a qualitative manner. The levels of Bcl-2

and Bcl-XL expression in cells were not determined, only mRNA levels were observed (Boise et al., 1993); therefore, differences in level of protection could be due to differences in the level of expression of Bcl-2 and Bcl-XL proteins in these studies, which can be unrelated to mRNA expression.

Could there be a link between Bcl-2 or Bcl-XL expression and tumour longevity in cancer patients? Previous clinical studies of breast carcinomas and squamous neck sarcomas have shown that the expression of Bcl-2 in a tumour is a good prognostic indicator of patient survival in some disease types. However, the expression of Bcl-XL in these tumour types is a "death sentence" (Pena et al., 1999; Lipponen et al., 1995). This suggests that even small increases in Bcl-XL expression are more significant than large increases in Bcl-2 expression when considering cell longevity. The increased cell longevity upon Bcl-XL expression could also be relevant in normal physiology. Perhaps this is why the essential function of Bcl-XL is primarily in the nervous and certain types of hematopoietic tissues (Motoyama et al., 1995), and Bcl-2 during stages of hematopoietic tissue development, and in the kidney and intestine (Kamada et al., 1995). Bcl-2 expression remains high in memory B cells, while Bcl-XL expression increases, allowing these cells to survive and to undergo an accelerated secondary immune response (Bovia et al., 1998).

1.4 Thesis Objective

The present work attempts to measure in a precise, reproducible manner the functions of Bcl-2 and Bcl-XL using an *in vitro* system (cultured breast epithelial cells: MCF-7 cells). Previous studies performed in our lab have demonstrated that alternatively

targeted Bcl-2 mutants offer differing degrees of protection from a death stimulus depending on cell type and type of stimulus (Zhu et al., 1996; Annis et al., 2001; Soucie et al., 2001). Stable transfections of Bcl-2 and Bcl-XL in MCF-7 breast cancer epithelial cells were subjected to an apoptotic stimulus (doxorubicin) and then assayed for apoptosis by quantitatively monitoring the cleavage of the caspase substrate PARP.

The use of MCF-7 cells in this study was beneficial for several reasons. Endogenous Bcl-2 levels are down-regulated when estrogen is removed from the medium (Teixeira et al., 1995). This allows for increased sensitivity to apoptosis-inducing agents. MCF-7 cells do not express any endogenous Bcl-XL (see Results). Therefore, background effects due to endogenous molecules are minimal and only the effects of the exogenously expressed proteins are monitored. Due to their flat and adherent nature, MCF-7 cells are also amenable to immunofluorescence studies. These cells lack caspase-3 due to a genomic deletion in exon 3 of *procaspase-3* (Janicke et al., 1998), potentially simplifying the number of pathways that may be acting in parallel during apoptosis. Finally, most human breast cancers originate in epithelial cells that express Bcl-2 or Bcl-XL. Clinical studies have demonstrated that expression of Bcl-2 or Bcl-XL in squamous cell and breast carcinoma have contrasting prognostic values (Pena et al., 1999; Lipponen et al., 1995). Therefore, a breast cancer model system may be ideal to investigate qualitative and quantitative differences between Bcl-2 and Bcl-XL.

At present there are several methods by which apoptosis can be monitored, based on either the classic hallmarks of apoptosis such as DNA laddering and chromatin condensation (Wyllie, 1980), externalization of phosphatidylserine (reviewed in

Reutelingsperger et al., 2002), protein cleavage due to caspase activation, or, changes in mitochondrial function such as altered membrane potential and cytochrome c release from the intermembrane space. However, some of these methods can not be used in this study since doxorubicin fluorescence interferes with the fluorescence of the fluorophores in the assay. Additionally, many of these assays are only capable of determining the status of a small subset of cells, which might not be representative of the status of the entire population of cells, whereas one can determine an average response of all cells to apoptotic stimuli by using quantitative Western blots.

During apoptosis, a family of cysteine proteases, the caspases, is activated that cleave a wide rage of nuclear, cytoplasmic and structural proteins (reviewed in Johnstone et al., 2002; reviewed in Wang, 2001). Poly ADP-ribose polymerase (PARP) is a nuclear enzyme involved in DNA repair that is cleaved by caspase-3 and -7 during apoptosis to generate 89 and 24 kDa fragments (Germain et al., 1999). In MCF-7 cells the use of PARP cleavage as a read out for apoptosis is an indirect method to monitor the apoptotic process via caspase-7 activity levels, since these cells lack caspase-3. Other proteases including calpains and cathepsins are active during apoptosis and could also contribute to PARP degradation without the specific production of the 89 kDa fragment (reviewed in Johnson, 2000; Thomas et al., 2001).

A widely used apoptosis-inducing agent in MCF-7 cells is the chemotherapeutic drug doxorubicin (Adriamycin). This drug can inhibit topoisomerase IIα, intercalate in DNA, and generate ROS (reviewed in Gewirtz, 1999) and is widely used in chemotherapy for breast cancer in patients (Harris et al., 1998). Another drug,

etoposide (VP-16), which also inhibits topoisomerase IIα (Yang et al., 2001) was used in our investigations. Our lab has shown that apoptosis stimulated by these two drugs is inhibited by Bcl-2 located at the mitochondrion in Rat-1 cells (Annis et al., 2001; Soucie et al., 2001).

Bcl-2 and Bcl-XL are located in the outer mitochondrial membrane, the endoplasmic reticulum and the nuclear envelope (Krajewski et al., 1993; Zhu et al., 1996; Wolter et al., 1997; Mizuguchi et al., 1996; Hsu and Youle, 1997b). Specific subcellular organelle targeted mutants were created by assembling plasmids that replace the endogenous hydrophobic carboxyl-terminal sequences of Bcl-2 and Bcl-XL with the targeting sequences of either acta or cytochrome b5 (Zhu et al., 1996; Janiak et al., 1994b) (see left panel of Figure 3). These plasmids were transfected into MCF-7 cells and allow specific targeting of proteins to either the mitochondrion (acta) or the ER (cb5) (see right panel of Figure 3). Using this system, we determined whether a difference exists in the ability of Bcl-2 or Bcl-XL to inhibit apoptosis from these different locations.

To summarize, there is to date no precise, reproducible measure of comparing the function of the two anti-apoptotic proteins Bcl-2 and Bcl-XL. In this report we used an *in vitro* system, MCF-7 cells transfected with alternatively targeted Bcl-2 or Bcl-XL (to either the ER or the mitochondrion), and assayed for apoptosis by monitoring the degree of PARP cleavage via quantitative Western blotting. This method allows us to determine if there is a difference in the anti-apoptotic abilities of Bcl-2 and Bcl-XL, and to see if inhibition of apoptosis is dependent upon subcellular location.

2 Materials and Methods

2.1 Materials

Chemical and tissue culture reagents were obtained from Gibco - Life Sciences or Sigma Chemicals unless otherwise noted. Restriction enzymes were obtained from either New England Biolabs or MBI Fermentas Inc. The IMPACT cloning vectors and chitin beads were obtained from New England Biolabs. SP6 polymerase was obtained from Epicenter Technologies. ^{35}S methionine was obtained from Perkin Elmer Life Sciences. 3-[(3-cholamidopropyl) dimethylammonio]-1-propane sulfonate (CHAPS) was obtained from Boeringer Mannheim and Sigma. The Geneporter transfection system was obtained from Gene Therapy Systems Inc. The untreated endothelial, Hela and HepG2 cell lysates were all obtained from Pharmingen. MCF-7, Jurkat and HL60 lysates were made using the protocol described in Section 2.9. Rat and mouse tissue lysates were obtained from Kathleen Pound, of the Andrew's laboratory. Both etoposide (VP-16) and doxorubicin (Adriamycin) were obtained from the McMaster University Pharmacy.

Rabbit reticulocyte lysate was prepared by Mina Falcone as described in Jackson et al. (Jackson et al., 1983). Cell free transcription-translation reactions were performed as described in Janiak *et al.* (Janiak et al., 1994b).

2.2 SDS-PAGE

Proteins to be visualized by Coomassie staining were separated by SDS-PAGE using 10 % Tricene gels (Schagger and von Jagow, 1987). The gels were placed in

Coomassie stain (35 % methanol, 0.1 % Coomassie blue R-250, 10 % acetic acid, 55 % dH_2O) overnight, then were incubated in destain buffer (35 % methanol, 10 % acetic acid, 55 % dH_2O) overnight. The following day the gels were dried between sheets of cellulose (BioRad).

In vitro ^{35}S methionine labelled proteins were separated using 10 % Tricine gels, and radioactively labelled protein signal detected in dried gels by overnight exposure to Kodak Biomax Film.

2.3 Antibodies

Primary polyclonal antibody against Bcl-2 was generated against GST-Bcl-2ΔTM. Sheep anti-Bcl-2 (Bleed 3) (raised by Dr. Weijia Zhu, a research associate in the laboratory, in collaboration with Capralogics) was used for western blotting at a dilution of 1:10,000. Primary polyclonal antibodies against Bcl-XL were generated against full length Bcl-XL. PARP monoclonal antibody (C-2-10) was obtained from Biomol and used for western blotting at a dilution of 1:10,000. Actin monoclonal antibody (clone C4) was obtained from ICN and used at 1:80,000. HRP linked secondary antibodies (donkey anti-mouse, donkey anti-rabbit and donkey anti-sheep) and the donkey anti-rabbit FITC conjugated antibody were obtained from Jackson Laboratories. All HRP linked antibodies used at dilutions of 1:10,000 except when detecting actin; donkey anti-mouse was used at a dilution of 1:80,000. The donkey anti-rabbit FITC conjugated antibody was used at a dilution of 1:30 for immunofluorescence microscopy.

All animal work was performed in the Central Animal Facility (CAF). Specific Pathogen Free (SPF) New Zealand White rabbits were obtained from Riemans and

acclimatized for a period of 1 week in cages. A primary injection consisting of 500 μg purified Bcl-XL protein and Freund's complete adjuvant was injected subcutaneously into an SPF rabbit following proper animal preparation. Regular monthly injections of Bcl-XL protein in Fruend's incomplete adjuvant were performed; 10 days after each injection small-scale (5 ml) test bleeds were performed using the marginal ear vein. These samples were tested to determine the specificity of the antibody for Bcl-XL protein. Once maximal response was obtained from a rabbit, a terminal bleed was obtained using the cannulation method. The final terminal bleed was clotted by adding 1 unit of thrombin per ml of serum, followed by incubation at 37°C until a clot formed. The clot was separated from the serum using sterile wooden sticks, and serum stored at -20°C and -80°C. Rabbit anti-Bcl-XL (Yosemite Sam Test Bleed 2: YS TB2) was used for western blotting at a dilution of 1:20,000 and for immunoprecipitations at dilutions of 1:400 and 1:800 (i.e. 1:400 = 1 μl serum per 400 μl TXSWB (100 mM Tris-Cl pH 8.0, 150 mM NaCl, 10 mM EDTA, 1 % Triton X-100). Rabbit anti-Bcl-XL (YS TB8) was used for Western blotting at a dilution of 1:20,000, for immunoprecipitations at dilutions of 1:400 and 1:800 and for immunofluorescence at a dilution of 1:100.

2.4 Plasmids

Plasmids encoding the Bcl-2 and Bcl-XL mutants and fusion proteins for over-expression were constructed by Dr. Weijia Zhu, Catherine Hollerbach, Helen Atkinson and Alison Cowie. For the construction of the Bcl-2 mutants in the mammalian expression vector system, see Zhu *et al.* (Zhu et al., 1996). Briefly, to target Bcl-2 and

Bcl-XL to mitochondria, the cDNA of Bcl-2 or Bcl-XL (encoding amino acids 1 – 218 and 1 – 210 respectively) were fused to the carboxyl-terminus of ActA (encoding amino acids 613- 639) (Zhu et al., 1996). The same 5' portion of *bcl-2* and *bcl-XL* were fused to the cytochrome b5 hydrophobic tail sequence (encoding amino acids 100 – 134) (Janiak et al., 1994a). Bcl-XL-nt was generated by inserting a stop codon after nucleotide 630.

pSPUTK is a vector containing the SP6 promoter followed by a 5' untranslated region that permits rapid initiation of translation in *in vitro* eukaryotic systems and thereby increases the amount of protein synthesized (Falcone and Andrews, 1991). For the construction of plasmids encoding the Bcl-XL mutants, the *bcl-XL* gene was amplified using Polymerase Chain Reaction (PCR) from a plasmid obtained as a generous gift from G. Nunez (p1055). All constructs were subcloned into the mammalian expression vector pRcCMV (Invitrogen). For further construction details see the appropriate plasmid sheet identified by an Andrews' plasmid reference number associated with each construct as outlined in Table 2.

2.5 Intein Purification of Bcl-XL for Rabbit Polyclonal Antibody Production

E. coli (DH5α) cells were transformed with plasmid p1132 (Bcl-XL-intein fusion). The Bcl-XL intein fusion protein was over-expressed from the plasmid and subsequently purified as described by Atkinson (Atkinson, 2001) with the following exceptions. Following lysis and removal of non-soluble debris by centrifugation, the intein Bcl-XL fusion protein was bound to chitin resin and cleavage of the Bcl-XL-intein fusion protein was induced with 30 mM DTT instead of 100 mM hydroxylamine. Elution

Table 2: Cross-references between plasmid names and Andrews' Lab plasmid reference numbers of the plasmids used in this project.

Plasmid Name	Andrews Lab reference number	Source
pSPUTK	56	Mina Falcone
pRcCMV	655	Invitrogen
G. Nunez gift plasmid	1055	G. Nunez
Bcl-2-wt (pSPUTK)	584	Alison Cowie
Bcl-2-acta (pSPUTK)	651	Catherine Hollerbach
Bcl-2-cb5 (pSPUTK)	652	Alison Cowie
Bcl-XL-wt (pSPUTK)	1175	Helen Atkinson
Bcl-XL-acta (pSPUTK)	1171	Catherine Hollerbach
Bcl-XL-cb5 (pSPUTK)	1170	Weijia Zhu
Bcl-2-wt (pRcCMV)	656	Alison Cowie
Bcl-2-acta (pRcCMV)	663	Catherine Hollerbach
Bcl-2-cb5 (pRcCMV)	664	Alison Cowie
Bcl-XL-wt (pRcCMV)	1183	Catherine Hollerbach and Weijia Zhu
Bcl-XL-nt (pRcCMV)	1186	Catherine Hollerbach
Bcl-XL-acta (pRcCMV)	1185	Catherine Hollerbach
Bcl-XL-cb5 (pRcCMV)	1184	Catherine Hollerbach
Bcl-XL-wt (intein)	1132	Bomina Yu

fractions from the column were not further purified, but used directly for the injection of SPF rabbits. The following buffers were used for Bcl-XL purification:

Column Buffer: 10 mM Na-HEPES pH 8, 500 mM NaCl, 0.1 mM EDTA, 20 % glycerol and supplemented to a 5x with a cocktail of protease inhibitors (PIN) (200x stock= 20 µg/ml chymostatin, 20 µg/ml antipain, 20 µg/ml leupeptin, 20 µg/ml pepstatin and 40 µg/ml aprotinin).

Wash Buffer: 10 mM Na-HEPES pH 8, 500 mM NaCl, 0.1 mM EDTA, 20 % glycerol, 5x PIN and 0.2 % (w/v) CHAPS.

Cleavage Buffer: 10 mM Na-HEPES pH 8, 500 mM NaCl, 0.1 mM EDTA, 20 % glycerol, 5x PIN, 0.2 % (w/v) CHAPS and 30 mM DTT.

Stripping Buffer: 20 mM Na-HEPES pH 8, 500 mM NaCl, 1 % SDS.

To determine the amount of Bcl-XL in the elution fractions, a serial dilution of a known amount of BSA was loaded on the same SDS-PAGE gel as the elution fractions. The gel was stained with Coomassie brilliant blue and destained with the buffers described in Section 2.2. Using the Kodak Image Station (440CF) system, images of the wet gels were captured and optical density readings obtained using the "net intensity" option of the Kodak Image Station software. Bcl-XL protein concentrations were determined by comparison of the elution fraction net intensities to the ones of the standard BSA curve.

2.6 Immunoprecipitation

The *bcl-XL* gene in the pSPUTK vector (p1175) was transcribed and translated *in vitro* using the rabbit reticulocyte lysate based transcription/translation system.

Aliquotes (9.5 or 9 µl) of translation product were diluted with 400 µl TXSWB supplemented with 1x PIN and 1 mM PMSF. 0.5 or 1 µl of rabbit anti-Bcl-XL antibody (YS TB2 or YS TB8) was added to the reaction mixture. These samples were then incubated overnight with end over end rotation at 4°C. The following morning 2.5 µl of washed protein A agarose beads (BioRad) were added, followed by another 1 hour incubation at 4°C with rotation. The beads were then washed four times with 1 ml TXSWB containing 1x PIN and 1 mM PMSF, followed by 2 washes with 1 ml of 100 mM Tris-HCl pH 8, 100 mM NaCl, 1x PIN and 1mM PMSF. Loading buffer (40 µl) was added to the protein A beads and 10 µl of this mixture was separated by Tris-tricine SDS-PAGE. Radioactive bands were visualized by exposing the gels to film overnight. Rabbit pre-immune serum was used as a control to determine whether any rabbit antibodies present prior to challenge with purified Bcl-XL cross-reacted with protein products generated using the rabbit reticulocyte lysate translation *in vitro* system. To determine the percentage of total product bound, 1 µl of the total products from the rabbit reticulocyte lysate was diluted to 10 µl with loading buffer and analysed on the same SDS-PAGE gel.

2.7 Immunoflourescence

1.0×10^5 MCF-7 cells were grown on cover slips in 6 well tissue culture plates. Following 3 days in alpha-minimal essential medium (αMEM medium), cells were stained with 0.2 µM Mitotracker red (Molecular Probes) for 30 minutes followed by a 30 minute recovery period in regular medium. Cells were then fixed for 30 minutes with 4 % paraformaldehyde followed by permeabilzation with 1 % Triton in PBS for 10

minutes and incubation with rabbit anti-Bcl-XL (1:100) in 3 % BSA-PBS for 1 hour suspended in a 37°C waterbath, followed by secondary antibody (FITC donkey anti-rabbit (1:30 dilution)) for 1 hour suspended in a 37°C waterbath. Cells were analyzed using a Zeiss 510 confocal microscope system and associated software (Carl Zeiss Laser Scanning System LSM510 version 2.3). Confocal images are single scans.

2.8 Cell Culture

MCF-7 cells were transfected with the *bcl-2-wt*, *bcl-2-acta* and *bcl-2-cb5* encoding plasmids by Dr. Weijia Zhu using calcium phosphate precipitation (Zhu et al., 1996). The *bcl-XL* chimeric genes, (*bcl-XL-wt*, *bcl-XL-nt*, *bcl-XL-acta* and *bcl-XL-cb5*), were transfected into MCF-7 cells using either calcium phosphate precipitation (as described in Zhu et al., 1996) or the Geneporter transfection systems (according to the manufacture's protocol) by Dr. Weijia Zhu and myself.

MCF-7 cells constitutively expressing Bcl-XL, Bcl-XL-cb5, Bcl-XL-acta, Bcl-XL-nt, Bcl-2, Bcl-2-cb5, Bcl-2-acta or transfected with the empty pRcCMV vector (Neo) were maintained in αMEM medium supplemented with 10 % heat inactivated fetal bovine serum (HI-FBS) (Life Sciences). Cell lines were selected for further analysis (as discussed in section 2.9) based on Bcl-2 and Bcl-XL expression levels.

2.9 Cell Death Assays

MCF-7 cells (0.9×10^6) were seeded into several 60 mm dishes and grown for a day. One 60 mm dish of each cell line was maintained for an additional day in αMEM (αM lysates) and then harvested (see below); cell confluency was typically ~ 70 – 90 %

at the time of harvest. The remainder of the cells in the other dishes were treated with phenol red minus αMEM supplemented with 10 % charcoal filtered HI-FBS for 6 days, to sensitize the MCF-7 cells to apoptosis by decreasing endogenous Bcl-2 levels (est-lysates) (Teixeira et al., 1995). After 6 days of estrogen depletion, the cells were washed with PBS (2.7 mM KCl; 1.5 mM KH_2PO_4; 7.25 mM $Na_2HPO_4 \cdot 2H_2O$; 137 mM NaCl) and replaced with estrogen free media containing either doxorubicin at the indicated concentrations, or 10 – 500 μM etoposide. After 48 hours of doxorubicin treatment, (or the indicated time of etoposide treatment), both the floating and adherent cells were harvested and pelleted by centrifugation in a Beckman-Coulter centrifuge at 1000 g for 5 minutes (Beckman Coulter: Allegra 6). The cell pellet was washed twice in PBS and resuspended in an appropriate amount of SDS lysis buffer (10 mM Tris-HCl, pH 7.5; 10 mM NaCl; 1 % SDS) supplemented with 5x PIN. Cells in a 60 mm dish at ~ 70 % confluency were lysed in 500 μl of lysis buffer. Cell lysates were diluted 1:1 with 95°C Tricine Loading Buffer (TLB) (4 % SDS, 0.1 M Tris-HCl pH 8.9, 2 mM EDTA, 0.1 % bromophenol blue, 20 % glycerol and 0.25 M DTT), and snap frozen using liquid nitrogen and stored at –80°C. Protein concentration in each lysate was measured using the standard (37°C) protocol of the BCA protein assay (Pierce) on aliquots removed prior to adding TLB.

2.10 Quantitative Immunoblot Analysis

2.10.1 Western Blotting

Samples to be separated by SDS-PAGE electrophoresis were diluted in Tricine Loading Buffer prior to electrophoresis. Proteins to be detected by Western blotting were separated using 10 % Tricine gels and then transferred to either PVDF or nitrocellulose membrane for 1 hour at 100 mA per membrane using a semi-dry blotter (Pharmacia Biotech: Hoefer SemiPhor semi-dry transfer unit). Membranes were blocked in a buffer containing casein (blocking buffer: 10 mM K_2PO_4 pH 7.4, 140 mM NaCl, 0.02 % NaN_3 and 5 g/L powdered milk) at room temperature for 30 minutes. The blots were incubated overnight at 4°C in primary antibody diluted in either polyclonal antibody buffer (10 mM K_2PO_4 pH 7.4, 560 mM NaCl, 0.1 % Triton X-100, 0.02 % SDS and 1 % BSA) or monoclonal antibody buffer (10 mM K_2PO_4 pH 7.4, 0.1 % Triton X-100, 140 mM NaCl, 1 % BSA), depending on the antibody. The next day the blots were washed twice in wash buffer (10 mM K_2PO_4 pH 7.4, 140 mM NaCl, 0.1 % Triton X-100) followed by two additional washes in TBS-T (10mM Tris-HCl pH 7.4, 500 mM NaCl and 0.2 % Tween 20). The blots were then incubated in horseradish peroxidase-conjugated secondary antibodies diluted in TBS-T with 1 % BSA for 2 hours at room temperature. The blots were washed 3 times for 5 minutes in TBS-T and then developed using the ECL method (NEN Life Sciences).

2.10.2 Samples for Absolute Comparisons

Known quantities of purified Bcl-XL and GST-Bcl-2ΔTM were used as standards that were compared to the amount of exogenous protein expressed in MCF-7

lysates (see panels A and E in Figure 4). The lower bands in the GST-Bcl-2ΔTM standard lanes of Figure 4B represent ~ 33 % of total net intensity in the lane (16.3 ng GST-Bcl-2ΔTM lane in Figure 4B). Although the GST-Bcl-2ΔTM was determined to be > 95 % pure by visual inspection of a Coomassie stained gel, there are some lower molecular weight bands around 35 kDa. It should be noted that the sheep anti-Bcl-2 antibody was generated against GST-Bcl-2, and that anti-GST antibodies in the serum were not removed. As well, the GST-Bcl-2ΔTM protein is not very stable and can only be frozen and thawed up to three times before the R^2 values of the linear regression for the GST-Bcl-2ΔTM standards falls below 0.95. Therefore, purified GST-Bcl-2ΔTM protein was frozen in small aliquots and discarded after the third use. Due to the unknown nature of the 33 % of protein below the GST-Bcl-2ΔTM band (see Figure 4B), all absolute values of Bcl-2 in the MCF-7 cell lines were corrected by the fraction of protein below the GST-Bcl-2ΔTM band or 33.3 ± 8.7 %. This value is an average of optical density readings (Kodak Image Station) of the bands below GST-Bcl-2ΔTM as a fraction of total lane optical density from 10 different gels. Using the Kodak Image station, "net intensity" readings of the standards were obtained, corrected as described above, and a linear regression performed using MS Excel software (see panels C and G in Figure 4). Only lines of best fit with R^2 values ≥ 0.95 were utilized to ensure that the readings were within the linear range of the equipment. The line of best fit was also inspected visually and sample readings that fell within the linear portion of the curve were used from the equation of the line of best fit to determine exogenous protein levels in MCF-7 lysates.

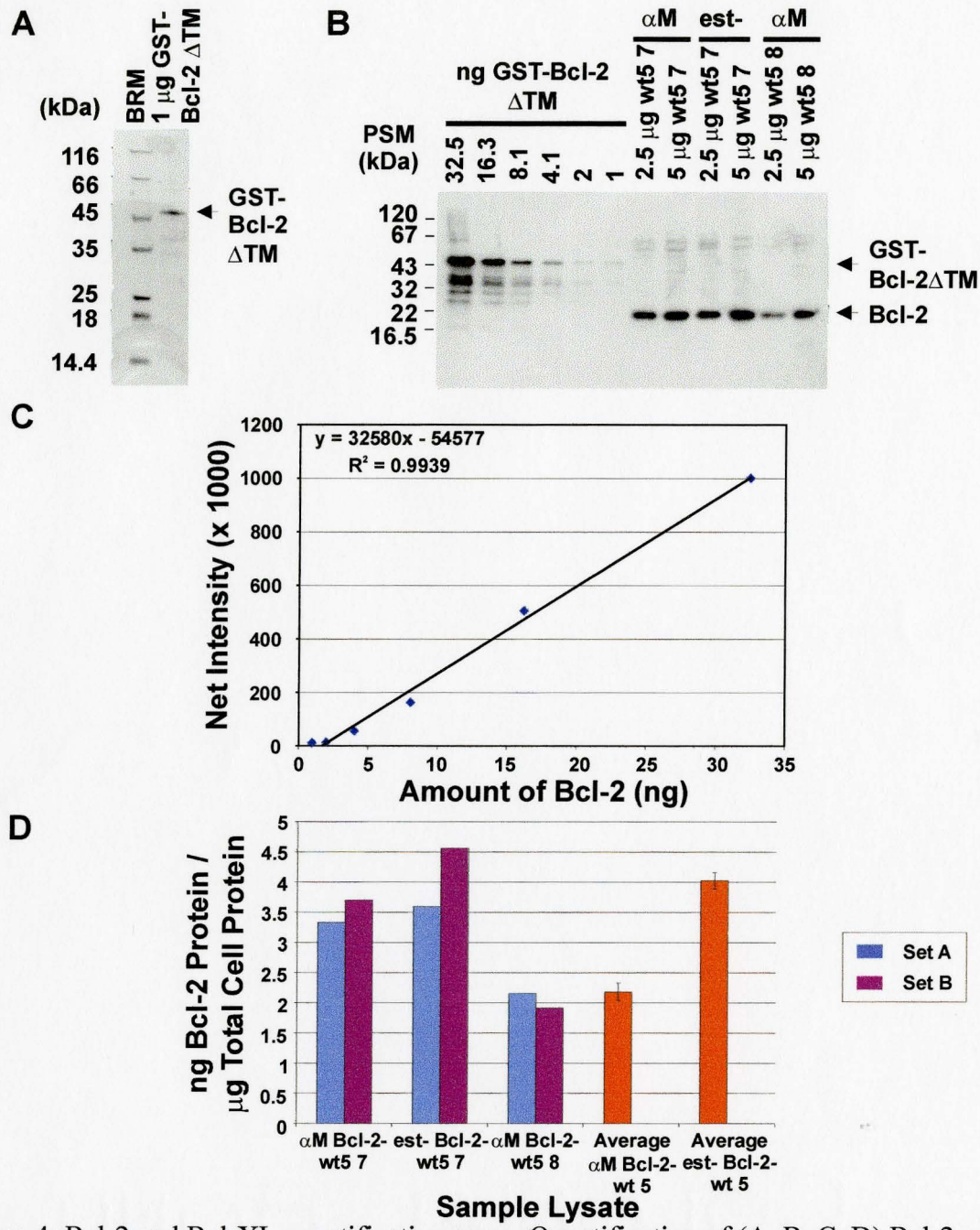

Figure 4: Bcl-2 and Bcl-XL quantification assay. Quantification of (A, B, C, D) Bcl-2 and (E, F, G, H) Bcl-XL expressed in MCF-7 cell lysates. Coomassie stained SDS-PAGE gels of 1 µg of purified A) GST-Bcl-2ΔTM and E) Bcl-XL were determined to be > 95 % pure by visual inspection. Serial dilutions of these standards were resolved on the same SDS-PAGE gel as sample lysates expressing either B) Bcl-2 mutants or F) Bcl-XL mutants. Either 2.5, 5 or 10 µg of total cell protein (determined by BCA assay) of each lysate was loaded. Kodak Image Station data from the sample lysates are compared to the standard curve generated from the C) GST-Bcl-2ΔTM or G) Bcl-XL. In all determinations, data

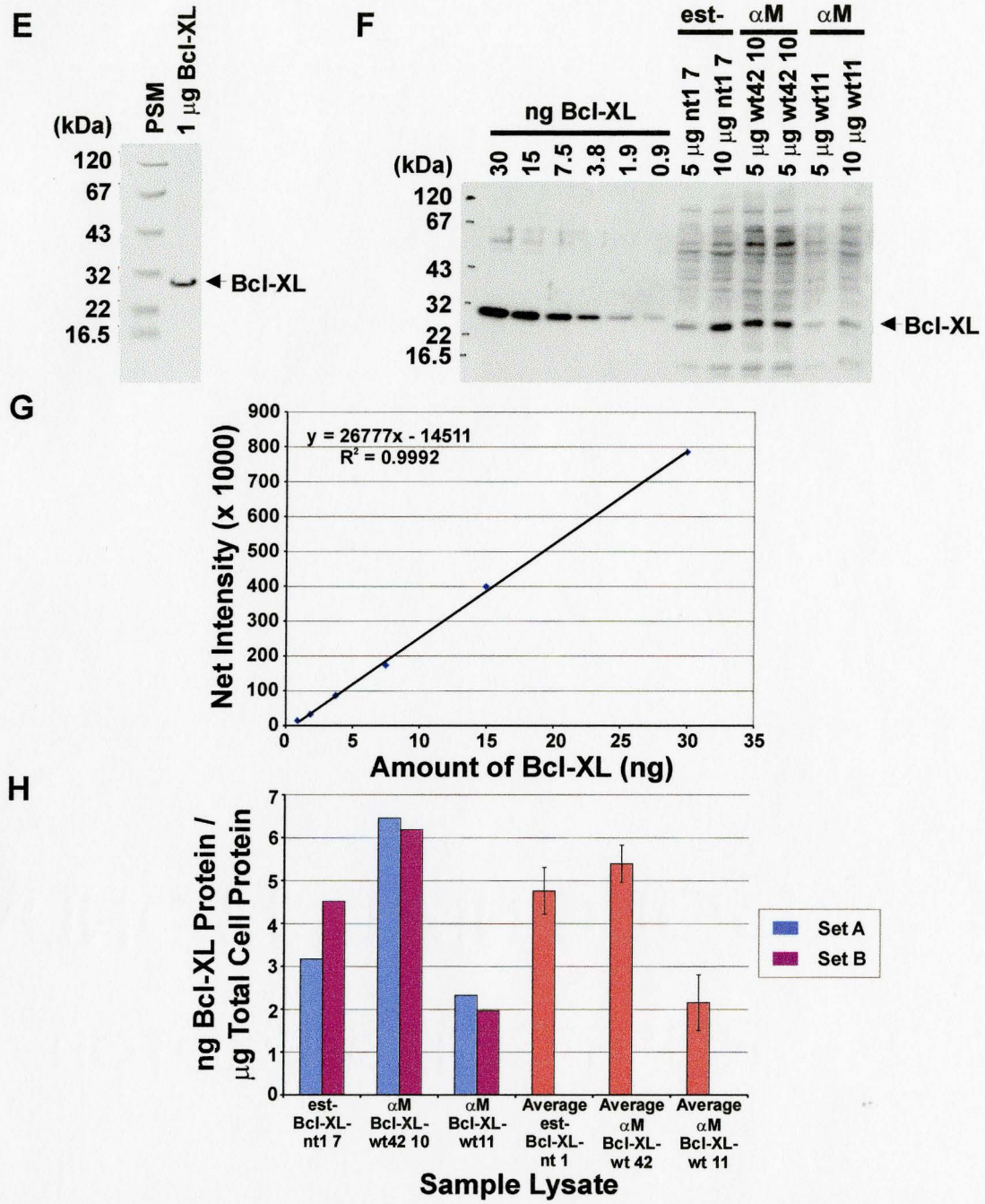

Figure 4 (con't): was only used if R^2 values were > 95 %. Using the equation for the linear regression of the intensity readings of the standard bands, the amounts of exogenous D) Bcl-2 or H) Bcl-XL (in ng) per mg of total cell protein was determined. Values obtained for Bcl-2 cell lines were corrected for the intensity of unknown protein below GST-Bcl-2ΔTM (33.3 % ± 8.7). Blue and mauve bars represent duplicates resolved on the same gel. The average concentration of exogenous Bcl-2 or Bcl-XL for each cell line are represented by orange bars on the right containing at least 5 separate samples. Error bars are standard error of the mean.

Serial dilutions of known amounts of GST-Bcl-2ΔTM (provided by Matt Annis) and Bcl-XL (provided by Helen Atkinson) were loaded on the same gel as unknown samples and transferred to nitrocellulose membrane. The standards were used to construct either a GST-Bcl-2ΔTM or a Bcl-XL standard curve, from which the amounts of Bcl-2 or Bcl-XL in the unknown samples could be calculated (see panels D and H in Figure 4).

2.10.3 Samples for Relative Comparisons

Protein samples (5 μg total cell protein per lane) were separated on a 10 % polyacrylamide tricine gel, followed by transfer to either a PVDF membrane (for the detection of PARP), or a nitrocellulose membrane (for the detection of Bcl-2 and Bcl-XL). To correct for differences in total protein between samples, a smaller aliquot of the same lysates (1 μg total cell protein) was processed as above, transferred to nitrocellulose membranes and probed for actin. These membranes were developed after incubation and washing as described above.

2.10.4 Visualization of Western Blots on the Kodak Image Station

Immunoblots were photographed using the Kodak Image Station system (440CF) and the visual image stored digitally. Analysis of the band intensities was performed using the associated Image Analysis Software. The camera was set for optimal western blot image capture conditions (F-stop: 1.2, zoom: 20, no filter, focus: 1.8). Ten samples of the images were taken at optimal exposure times for the specific antibody (PARP: 1.5 minutes, Bcl-XL: 1.5 minutes, Bcl-2: 35 seconds and actin: ~5 seconds).

Captured images were adjusted for optimal contrast for viewing, and unadjusted band intensities acquired by selection of lanes, bands and background using the Kodak Image Station software. Using the "net intensity" selection in the Image Analysis software, which automatically adjusts for selected background readings, net band intensities were recorded. The results were entered into an MS Excel (Microsoft) spreadsheet for graphical and statistical analysis.

2.11 Calculations

Values for the percent PARP cleaved or degraded were determined using the assay illustrated in Figure 5. During apoptosis PARP is cleaved into 24 and 89 kDa fragments by caspase-3 and -7 by most cells (Germain et al., 1999). MCF-7 cells do not contain functional caspase-3 due to a genomic deletion (Janicke et al., 1998). Following apoptotic treatment PARP can also be cleaved by lysosomal proteases to 62 and 55 kDa or 74 and 42 kDa fragments (Gobeil et al., 2001). Therefore, to assay the effects of doxorubicin on MCF-7 cells it is necessary to measure both cleavage of PARP by caspases as well as degradation by other proteases that may be activated during apoptosis. MCF-7 cells were treated with increasing doses of doxorubicin at a single time point (48 hours) to determine the concentration of doxorubicin at which 50 % of the 116 kDa PARP remains; which will henceforth be referred to as the EC_{50} (as illustrated on the left side of Figure 5). Using the C-2-10 monoclonal antibody, the 116 (full length) and 89 kDa species of PARP can be detected on a Western blot. This antibody therefore recognizes the uncleaved protein, but may not recognize cleavage products generated by proteases other than caspases-3 or -7.

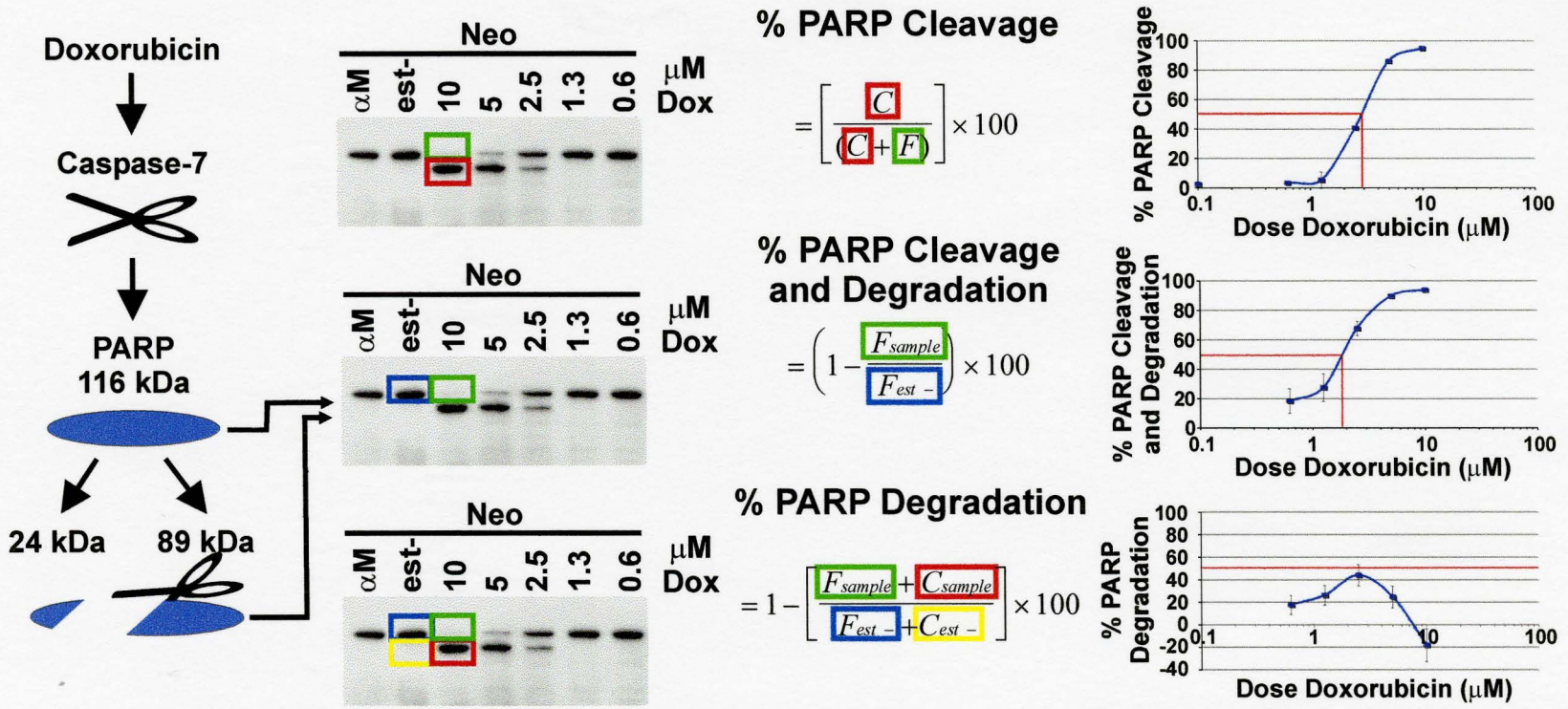

Figure 5: Quantitative determination of PARP cleavage and degradation in MCF-7 cells following induction of apoptosis by treatment with doxorubicin. Vector transfected MCF-7 cells (Neo) treated with doxorubicin undergo PARP cleavage due to active caspase-7, resulting in 24 and 89 kDa fragments. Using the C-2-10 monoclonal PARP antibody directed against the N-terminal portion of the 89 kDa PARP fragment, the 116 (full length) and 89 kDa fragments can be detected (Lazebnik *et al.*, 1994). Band intensities were recorded using a Kodak Image Station. The % PARP cleavage is calculated by comparing the 116 kDa PARP in a doxorubicin treated sample (red box) to the sum of the 116 and 89 kDa bands in the same lane (red and green boxes respectively). Data from several experiments was combined and presented graphically, as shown on the right. The EC_{50} for doxorubicin was estimated from these graphs as shown by the red line. The % PARP cleavage and degradation and the amount of PARP degradation were determined similarly using the indicated band intensities and formulas. In this example the EC_{50} are 2.9 μM % for PARP cleavage and 1.9 μM for % PARP cleavage and degradation. Thus the addition of PARP degradation and specific cleavage of PARP by caspases shifts the EC_{50} from 2.9 to 1.9 μM.

2.11.1 % PARP Cleavage (due to Caspase-7)

$$\% \text{ PARP Cleavage} = \left[\frac{C}{(C+F)}\right] \times 100$$

PARP cleavage was estimated by measuring the full length 116 kDa and 89 kDa cleavage product of PARP at the indicated dose of doxorubicin, as shown in the top panel of Figure 5. *C* corresponds to a net intensity reading of the 89 kDa fragment of PARP at a particular dose of doxorubicin (red box in Figure 5). *F* corresponds to the optical density of full length PARP at the same dose of doxorubicin as *C* above (green box in Figure 5). Once these calculations were performed over a range of doses of doxorubicin, several independent experiments were combined to generate the graph at the right hand side of the top panel in Figure 5. From this graph an EC_{50} was obtained by interpolation as shown by the red line in the graph in Figure 5.

2.11.2 % PARP Cleavage and Degradation

$$\% \text{ PARP Cleavage and Degradation} = \left(1 - \frac{F_{sample}}{F_{est-}}\right) \times 100$$

Combined PARP cleavage and degradation were estimated by comparing the band intensities for 116 kDa full length PARP in untreated (*est-*) cells with that in cells treated with doxorubicin as shown in the middle panel of Figure 5 (dark blue and green boxes respectively). This measurement assesses the toxicity of doxorubicin. The terms F_{est-} and F_{sample} refer the 116 kDa PARP band on Western blots of lysates of cells that had been maintained in estrogen depleted medium for 6 days and to the 116 kDa PARP band

on a Western blot of lysates of cells that had been treated with a dose of doxorubicin respectively. The EC_{50} was determined by interpolation (red line) as above (2.11.1).

2.11.3 % PARP Degradation

$$\% \text{ PARP Degradation} = 1 - \left[\frac{F_{sample} + C_{sample}}{F_{est-} + C_{est-}} \right] \times 100$$

The amount of PARP degradation was estimated as shown in the bottom panel of Figure 5 by measuring the band intensities for the 116 kDa full length PARP and 89 kDa fragment in both untreated and doxorubicin treated cells. The sum of the 116 and 89 kDa PARP species in the doxorubicin treated sample (Figure 5, green and red boxes, respectively) was divided by the sum of the 116 and 89 kDa PARP species in the untreated cells (dark blue and yellow boxes in Figure 5, respectively). The EC_{50} was determined by interpolation (red line) as above (2.11.1). Values below zero indicate an apparent increase in the amount of PARP present. Unlike other values the EC_{50} for degradation may not be observed.

2.11.4 Actin and Bcl-2 or Bcl-XL Ratio

The ratio of total actin in a doxorubicin treated sample was compared to the total actin in an untreated sample within an experiment (a loading standard). Actin is degraded late in apoptosis (Brown et al., 1997); therefore, degradation of actin was also used as an end point.

$$\text{Ratio} = \frac{actin_{sample}}{actin_{est-}}$$

A similar calculation was used to determine the ratio of Bcl-2 or Bcl-XL in a given sample as compared to the est- lysate. To determine the absolute amounts of Bcl-2 or Bcl-XL in a sample, the ratio value obtained above was multiplied by the absolute value of Bcl-2 or Bcl-XL protein that was measured for the est- sample for that experiment.

$$\text{Ratio} = \frac{Bcl2_{sample}}{Bcl2_{est-}} \quad \text{or} = \frac{BclXL_{sample}}{BclXL_{est-}}$$

2.11.5 PARP Remaining Following Estrogen Depletion

$$\%\ \text{PARP Available} = \left(\frac{F_{sample}}{F_{\alpha M}}\right) \times 100$$

The amount of PARP cleavage and degradation due to growth for a period of 6 to 8 days in media that did not include phenol red, and other components removed from charcoal-filtered serum, were calculated. F_{sample} corresponds to the intensity of the 116 kDa PARP band on a Western blot from lysates of that had been grown for 6 to 8 days in charcoal filtered media. $F_{\alpha M}$ corresponds to the 116 kDa PARP band on a Western blot from lysates of that had been grown in αMEM media supplemented with regular HI-FBS.

2.11.6 Data Exclusion/Outlier Analysis (Dixon's Test)

Experiments were designed such that overlapping doses of doxorubicin treated samples were present in multiple experiments to allow comparison between experiments. Occasionally an experiment was excluded due to inconsistencies in individual data points compared to those from other experiments. In such cases, the entire experiment was

eliminated. Of the 53 total experiments performed, only seven were discarded: (Bcl-2-wt 2 4, Bcl-2-wt 5 1, Bcl-2-acta 24 8, Bcl-XL-wt 42 6, Bcl-XL-nt 1 7, Bcl-XL-acta 6 1 and Bcl-XL-cb5 24 5). Sources of the inconsistent data included unequal actin levels between samples in the same experiment (Bcl-2-wt 2 4, Bcl-XL-wt 42 6, Bcl-XL-nt 1 7, Bcl-XL-acta 6 1 and Bcl-XL-cb5 24 5) and occasionally PARP cleavage and degradation data in a single experiment that was not consistent with all other experiments involving the same cell line and treatment conditions (Bcl-2-acta 24 8).

In this study, individual data points were excluded only from experimental results used to calculate the absolute amounts of Bcl-2 and Bcl-XL expressed in a cell line. There was a 0.2 ng difference in absolute protein determination between two SDS-PAGE gels for a single sample (see Appendix, Figure A5). Outlier analysis was used to eliminate 7 of 795 total data points. Outlier analysis can be performed when one can make the assumption that the population is normally distributed, which is a reasonable assumption commonly made for repeated measurements of a single protein concentration. For a normal binomial distribution the following three criteria are necessary: each trial in an experiment is performed the same way, each trial has either a successful or unsuccessful outcome and the probability of success of one trial does not influence another trail (Sternstein M., 1996). For example, the probability that one cell line expresses 1 ng of Bcl-XL / μg of total cell protein has one of two outcomes, success or failure, and the ability of a collection of cells in a dish to express a defined amount of Bcl-XL has no effect on the protein expression levels in cells in another dish. The

procedure for the determination of the amount of exogenous protein expressed is the same for each experiment (see Table 3).

For sample sizes below 25 for a single dish of cells, a Dixon's test was employed as follows. The samples are ordered sequentially, in ascending and descending order, so that the first value (Y_1) is the suspected outlier. For example, consider the following sample set of data: 2.5, 3.5, 2, 1 and 5. The Dixon test would be used to determine if either the highest or lowest data points are outliers (data points 1 and 5). Therefore, in ascending order, (1, 2, 2.5, 3.5, 5) and descending order (5, 3.5, 2.5, 2, 1) the first value of the series would be designated Y_1, the second Y_2 and so forth. The following formulas can then be used to calculate ratios for the given suspected outlier in a sample (Rohlf and Sokal R.R., 1981). A result is not considered deviant if the calculated ratio obtained for the suspect outlier is less than the tabular critical value.

If n=3 to 7 $$r_{10} = \frac{Y_2 - Y_1}{Y_n - Y_1}$$

If n=8 to 10 $$r_{11} = \frac{Y_2 - Y_1}{Y_{n-1} - Y_1}$$

If n=11 to 13 $$r_{21} = \frac{Y_3 - Y_1}{Y_{n-1} - Y_1}$$

Calculated ratios are compared to critical ratios, usually found in a table format (see Table 4).

Table 3: Outlier analysis of total data used to calculate the absolute amounts of Bcl-2 and Bcl-XL in cell lysates from the PARP cleavage and degradation assays.

Cell Line	Total Number of Measurements		Number of Values Eliminated with Dixon Test	
	αM	est-	αM	est-
Bcl-2-wt 2	37	37	1	0
Bcl-2-wt 5	74	51	1	0
Bcl-2-acta 24	47	52	0	0
Bcl-2-cb5 18	30	33	1	1
Bcl-XL-wt 42	58	46	0	0
Bcl-XL-nt 1	35	36	1	1
Bcl-XL-acta 6	25	29	0	0
Bcl-XL-cb5 24	44	39	0	0

αM denotes samples grown in regular αMEM medium; est- denotes cells grown for 6 days in estrogen-free medium.

Table 4: Critical values for testing outliers (Dixon's Test).

Sample Size (n)	95 % Critical Value
3	0.941
4	0.765
5	0.642
6	0.56
7	0.507
8	0.554
9	0.512
10	0.477
11	0.576
12	0.546
13	0.521

Modified from Sokal and Rohlf, 1995.

3 Results

3.1 Exogenous Expression and Subcellular Localization of Bcl-2 and Bcl-XL Mutants in MCF-7 Cells

The structures of both Bcl-2 and Bcl-XL consist of two central hydrophobic helices surrounded by five amphipathic helices. However, comparison of the primary sequences as amino acid alignments reveals that the two proteins share only 43 % identity (Muchmore et al., 1996) and 62 % similarity (see Figure 2A). The subcellular localization of these two proteins is also similar; they both have been found in the ER and mitochondria (Janiak et al., 1994b; Zhu et al., 1996; Wolter et al., 1997; Hsu et al., 1997a). However, Bcl-XL has also been reported in the cytosol (Wolter et al., 1997; Hsu et al., 1997a). Given these differences, we hypothesised that there would be quantitative differences in the function of the proteins. As Bcl-2 has been shown to have different functions at the ER and mitochondria (Zhu et al., 1996) we compared quantitatively the function of Bcl-2 and Bcl-XL at the ER and mitochondria by utilizing mutants of these proteins with restricted subcellular localization.

Studies have shown that the insertion sequence of the ER specific isoform of cytochrome b5 (cb5) can target foreign proteins specifically to the ER (Pistor et al., 1994). A Bcl-2 mutant in which the endogenous insertion sequence was replaced with that from cb5 (Bcl-2-cb5) was shown to localize to the ER when expressed in mammalian cell lines (Zhu et al., 1996). Similarly Bcl-2 was targeted specifically to the outer mitochondrial membrane when the endogenous insertion sequence was replaced with the

carboxy-terminal transmembrane sequence of the *Listeria* ActA protein (Bcl-2-acta) (Zhu et al., 1996).

It has been previously shown that the expression levels of Bcl-2 or Bcl-XL correlate with the level of protection from apoptosis (Gottschalk et al., 1994). Therefore, to accurately measure the ability of wild-type Bcl-2 and wild-type Bcl-XL to prevent apoptosis, we selected cell lines expressing similar amounts of Bcl-2 and Bcl-XL, as well as mutants with restricted localization of these proteins.

To simplify the assay a single drug and time point of treatment was employed. Apoptotic stimuli for which Bcl-2-acta has previously been shown to confer protection were used in this study (etoposide and doxorubicin) (Annis et al., 2001). All cells treated with drugs for a set time of 48 hours, because preliminary results showed that the levels of exogenous Bcl-2 and Bcl-XL decreased with treatment with doxorubicin over extended periods of time. However, expression levels remained relatively stable in preliminary dose response trials with Bcl-2-wt and Bcl-XL-wt at shorter intervals such as 48 hours. Furthermore, a doxorubicin treatment time of 48 hours demonstrated a significant difference in PARP cleavage between the Bcl-2 and Bcl-XL, as well for the mutants with restricted localizations.

The expression levels of exogenous Bcl-2 and Bcl-XL were measured before and after 6 days of growth in estrogen free medium. MCF-7 cells are grown in this medium to decrease endogenous levels of Bcl-2 (Teixeira et al., 1995). Western blots of sample lysates from the Bcl-2 and Bcl-XL cell lines are shown in Figure 6A and B respectively. All cell lines have detectable levels of Bcl-2 or Bcl-XL, except Neo. While

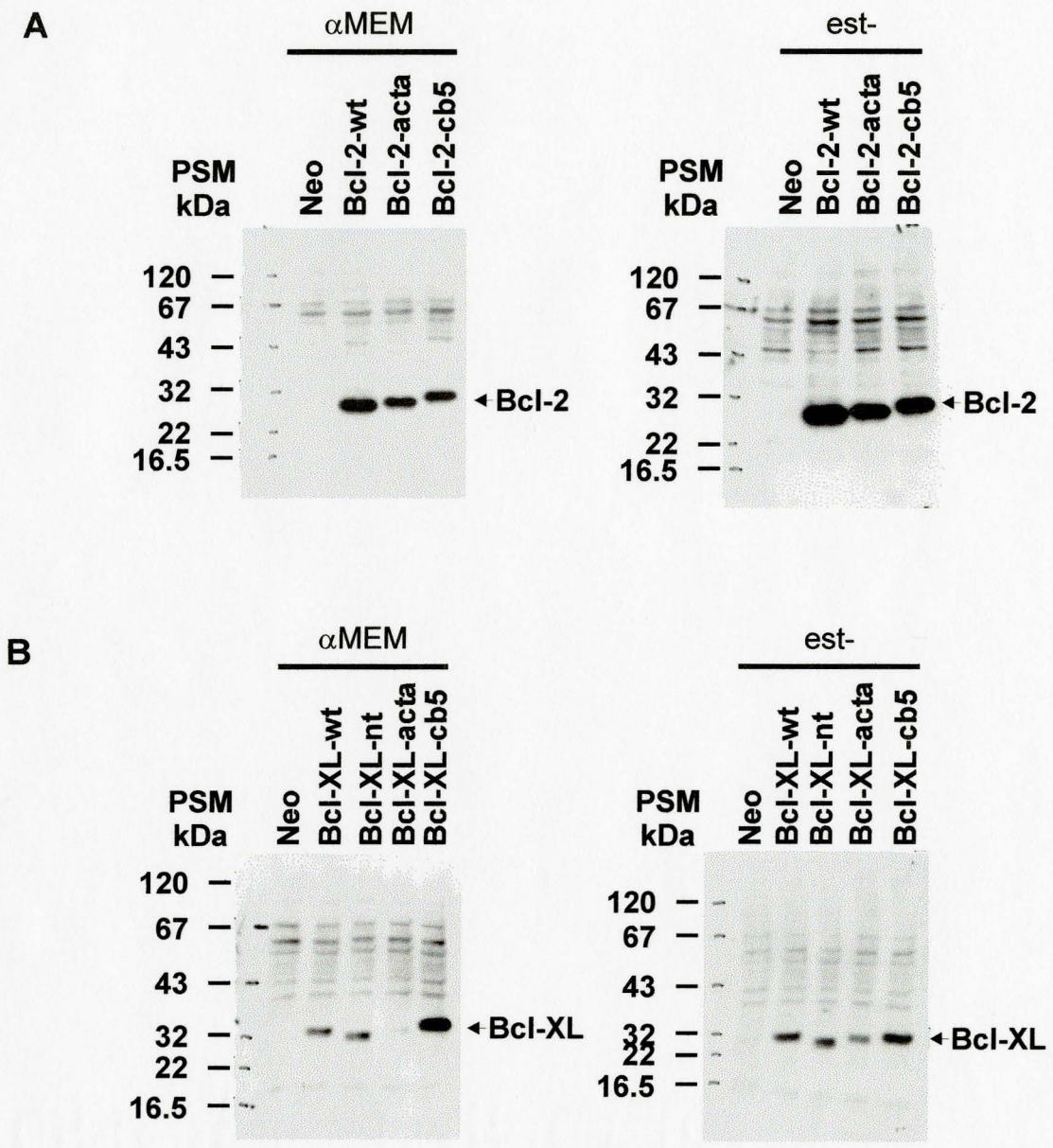

Figure 6: Expression of Bcl-2 and Bcl-XL in MCF-7 cells. MCF-7 cells transfected with plasmids encoding stable lines of either the A) Bcl-2 or B) Bcl-XL mutants were maintained in either regular αMEM medium or for 6 days in phenol red free αMEM supplemented with charcoal filtered HI-FBS (est-). Expression of Bcl-2 and Bcl-XL generally increases following growth in estrogen-free media. For all cell lines, the difference in sizes of the protein expressed on SDS-PAGE is a consequence of the substitution or removal of the C-terminal portion of Bcl-2 or Bcl-XL. The Bcl-2-wt 5, Bcl-2-acta 24, Bcl-2-cb5 18, Bcl-XL-wt 42, Bcl-XL-nt 1, Bcl-XL-acta 6 and Bcl-XL-cb5 24 cell lines are represented in these Western blots.

wild type Bcl-2 and Bcl-XL are both approximately 26 kDa in length, differences in sizes on the Western blots are a consequence of the sizes of the different targeting signals on the mutants. Following 6 days in estrogen free media, the expression levels of the wt and the different mutants generally increase, except in the MCF-7 cell line expressing Bcl-XL-cb5. The expression of exogenous proteins are roughly equal following 6 days growth in estrogen free conditions in all cell lines except Bcl-2-wt 2 and Bcl-2-wt 5, which express approximately 6 - 7 fold more.

Analysis of results with these cell lines depends on proper targeting of the Bcl-2 and Bcl-XL mutants to either the ER or the mitochondrion. Zhu *et al.* have previously shown by immunofluorescence that the Bcl-2 mutants used here target to the mitochondrion or the ER as expected in a variety of cell types including MCF-7 (Zhu et al., 1996; W. Zhu, unpublished data). A similar approach was used to study the localization of Bcl-XL-wt, Bcl-XL-nt, Bcl-XL-acta and Bcl-XL-cb5 in MCF-7 cells. Cells expressing mutants of Bcl-XL were stained with an unpurified polyclonal antiserum to Bcl-XL and analysed by immunofluorescence using confocal microscopy (see Figure 7). The same cells were incubated with Mitotracker Red to identify mitochondria in the transfected cells. In cells expressing Bcl-XL-wt (Figure 7A), the staining for Bcl-XL and mitochondria are similar. Bcl-XL-acta also co-localized with Mitotracker Red at mitochondria (Figure 7C). In contrast, Bcl-XL-nt is diffusely distributed throughout the entire cell, as well is in distinct cytoplasmic granules that do not resemble mitochondria (Figure 7B). Two different MCF-7 cell lines expressing high (Bcl-XL-cb5 20) and low (Bcl-XL-cb5 24) levels of

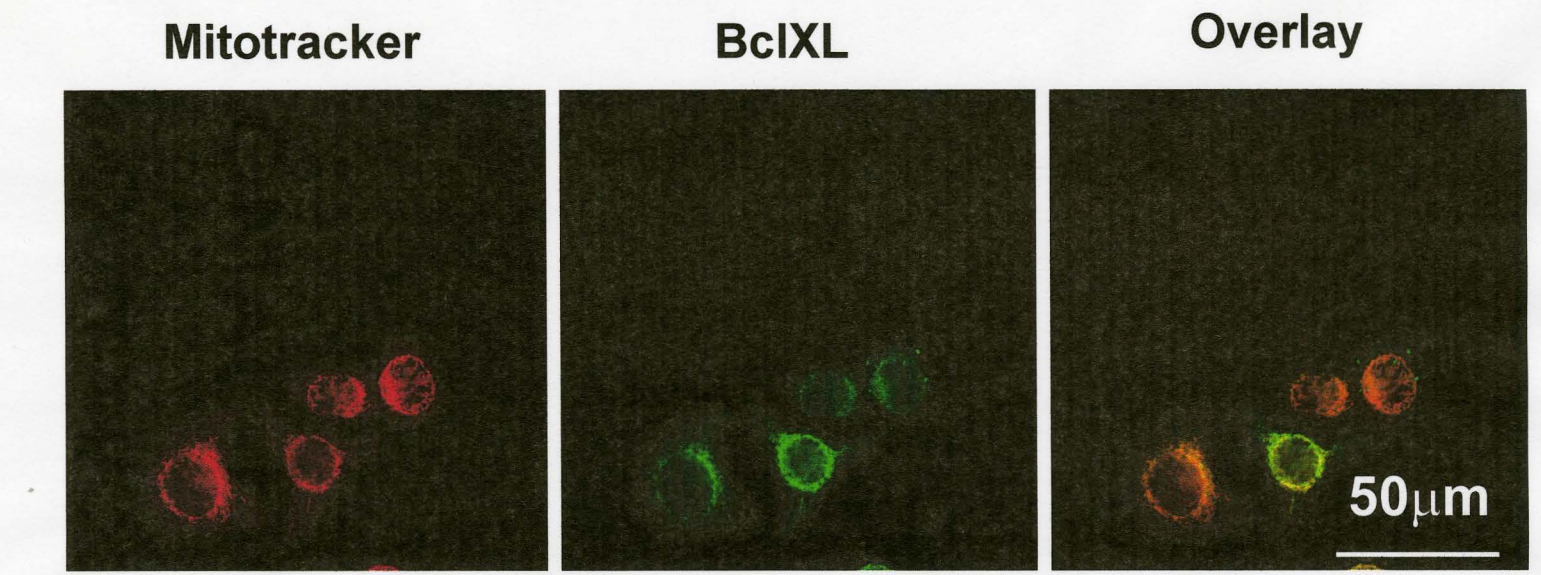

Figure 7: Expression and localization of the Bcl-XL mutants in MCF-7 cells. MCF-7 cells transfected with wild type A) *bcl-XL*, B) *bcl-XL-nt*, C) *bcl-XL-acta* and D) and E) *bcl-XL-cb5* were doubly labeled with Mitotracker Red and Bcl-XL polyclonal antibody following 3 days growth in αMEM. Confocal images of the cells stained with Mitotracker Red are shown in the first column. Images of the same cells labelled with fluorescein (Bcl-XL) are shown in the second column. An overlay of the Mitotracker Red and fluorescein staining is shown in the last column. The two panels of cells transfected with *bcl-XL-cb5* are clonal populations of MCF-7 cells expressing low and high amounts of Bcl-XL-cb5 respectively.

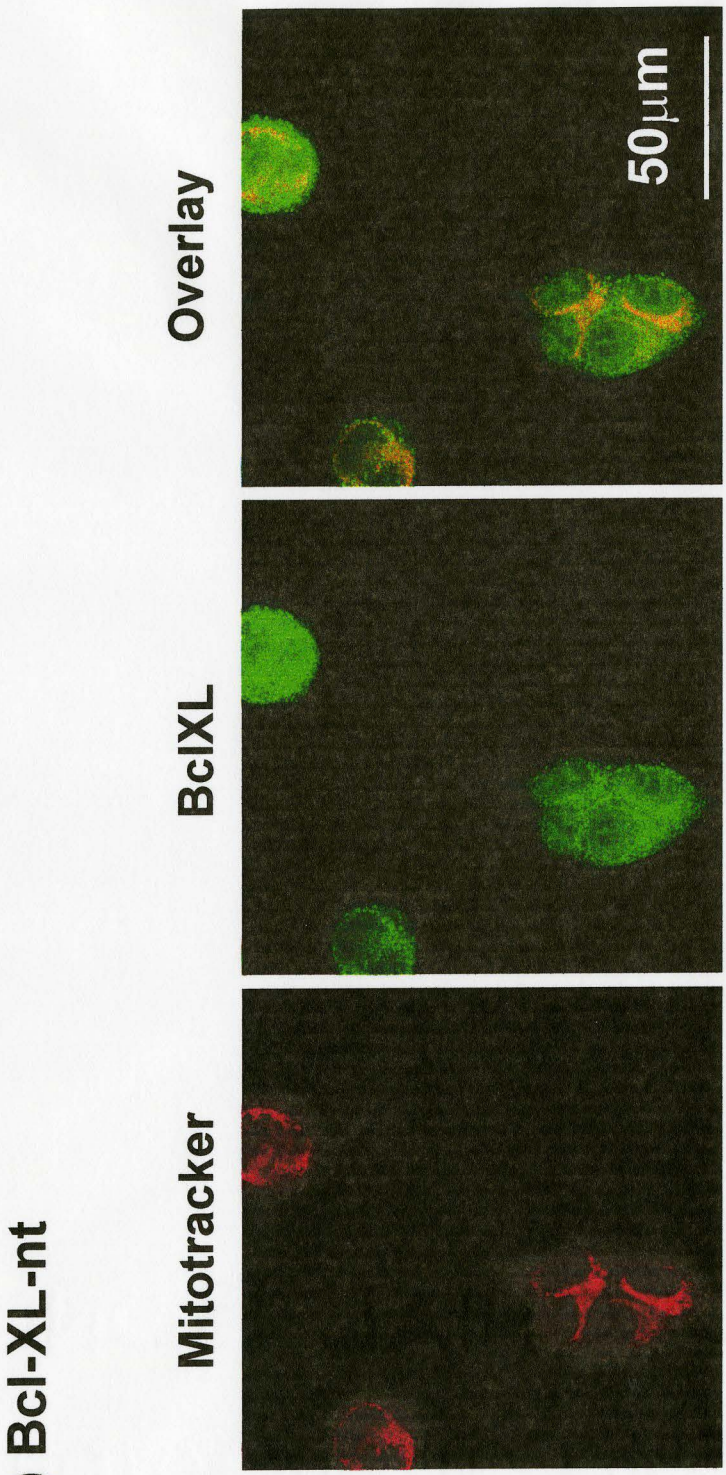
B) Bcl-XL-nt
Mitotracker
BclXL
Overlay
50μm

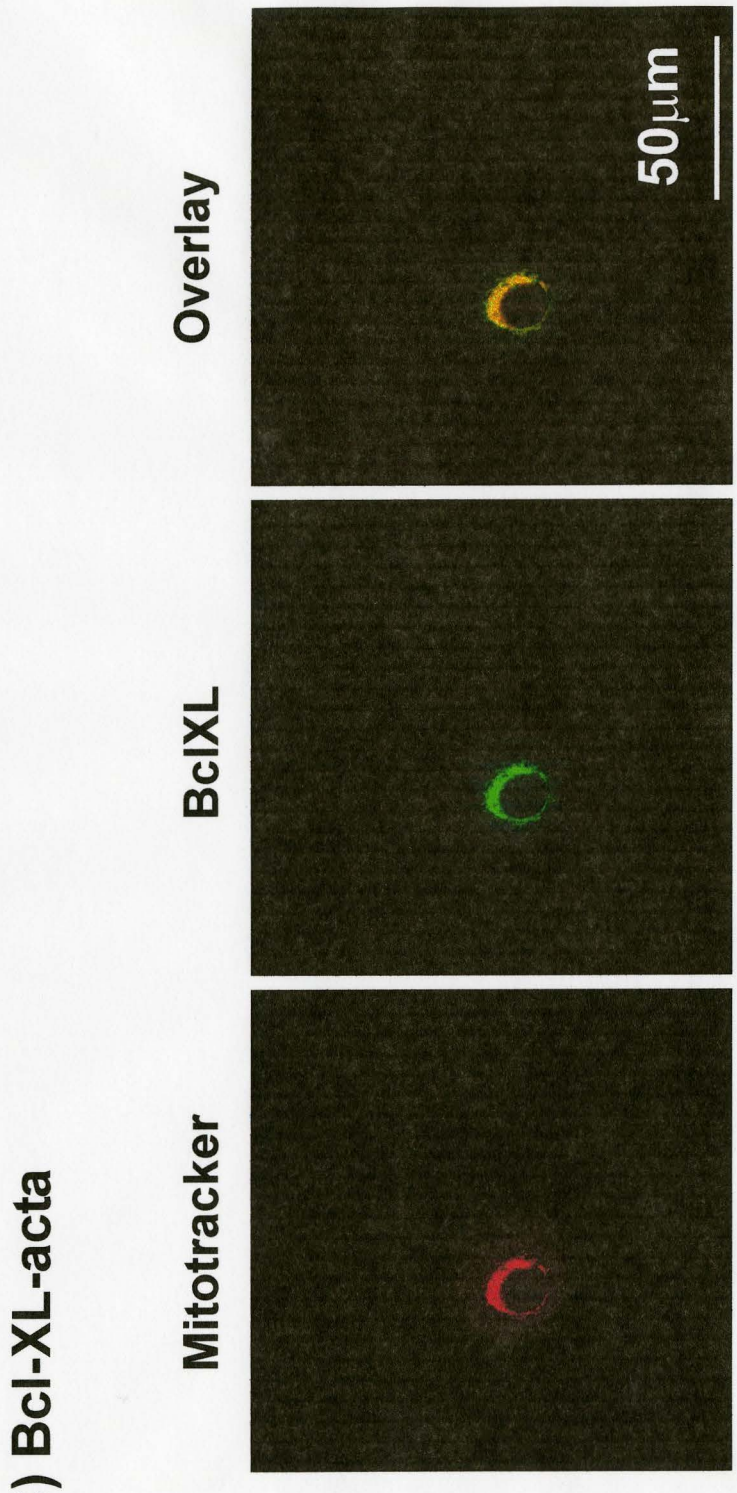
C) Bcl-XL-acta
Mitotracker
BclXL
Overlay
50µm

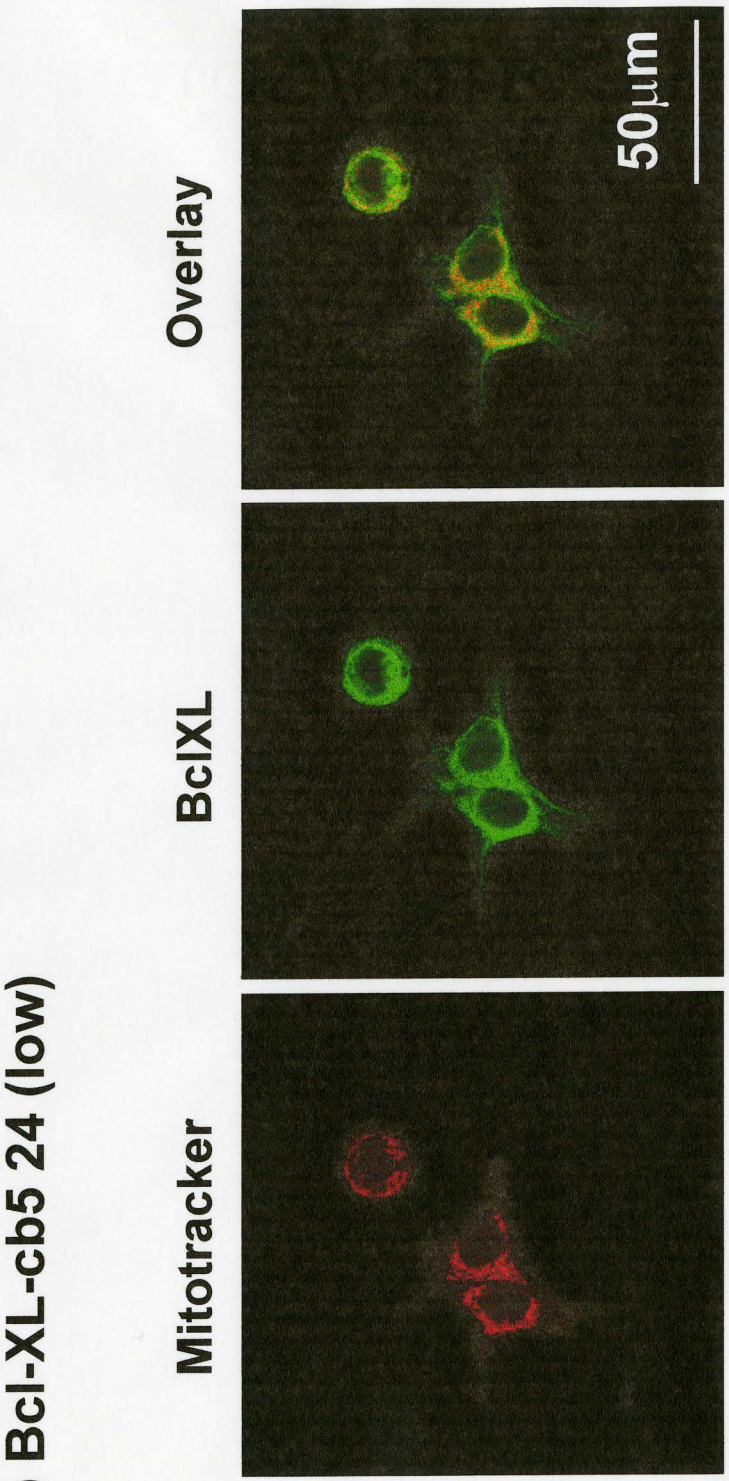
D) Bcl-XL-cb5 24 (low)
Mitotracker
BclXL
Overlay
50µm

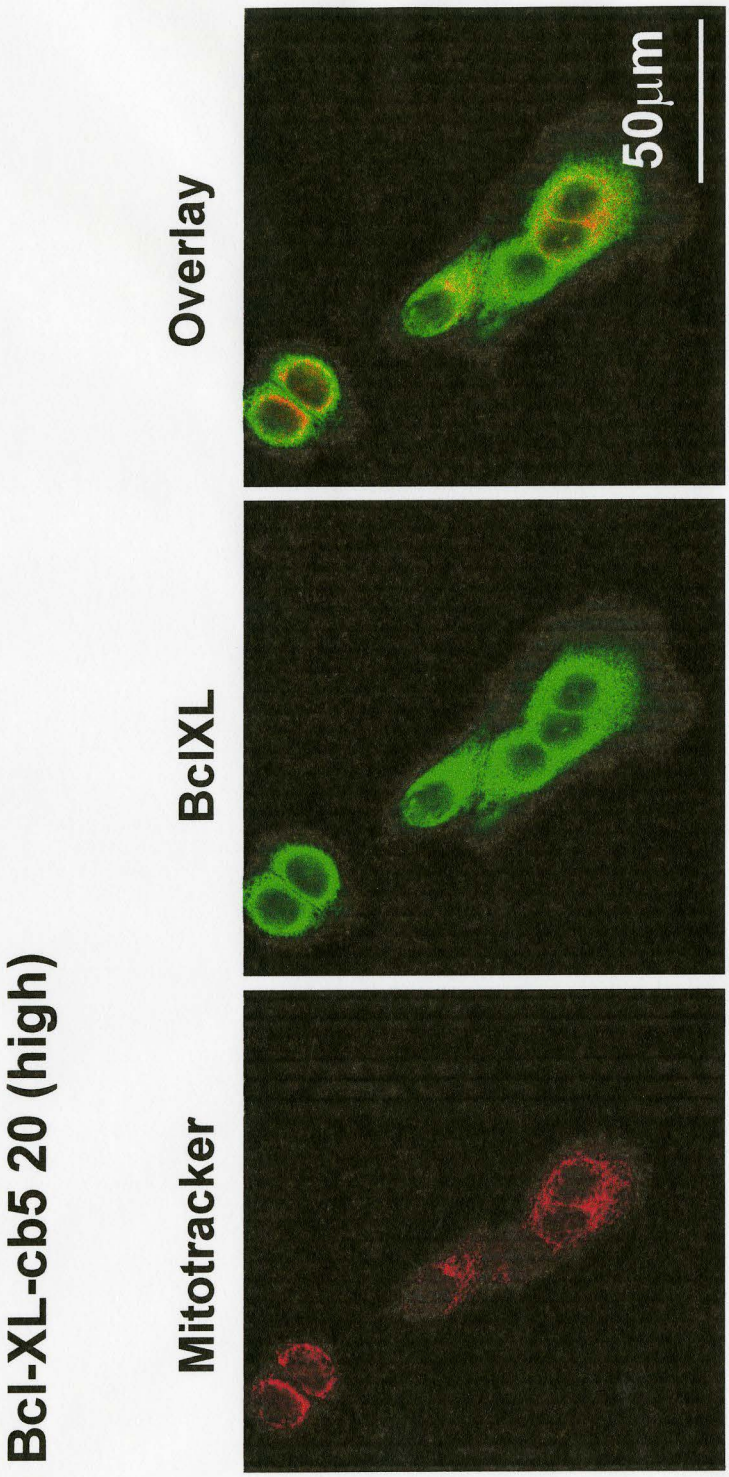
E) Bcl-XL-cb5 20 (high)
Mitotracker
BclXL
Overlay
50μm

Bcl-XL-cb5 (Figures 7E and 7D respectively) were examined. In both cases Bcl-XL-cb5 does not localize to mitochondria, but exhibits a net-like cytoplasmic staining that is more intense around the nucleus. This is consistent with the organization of the ER around the nucleus suggesting Bcl-XL-cb5 localization in the ER. Bcl-XL-cb5 24 was used in all future experimental work. It should be noted that the Bcl-XL antibody used for immunofluorescence was not affinity purified. Use of such an antibody could contribute to background staining in the images.

Bcl-2 and Bcl-XL concentrations in MCF-7 lysates were determined for 43 cell lines (see Figure 8); of these 8 failed to express detectable levels of exogenous protein. The number of independent experiments and the total number of measurements for each cell line are indicated in Table 5. Bcl-2 cell lines had been analyzed previously by W. Zhu and a series of 7 cell lines (out of a total of 36 assayed) were stored that expressed roughly similar amounts of the different Bcl-2 mutants in MCF-7 cells maintained in αMEM (W. Zhu, personal communication). This was confirmed in cells growing in both αMEM and in estrogen depleted media (see Figure 8A). Surprisingly, in cells growing in estrogen depleted media, expression of one of two Bcl-2-wt and all Bcl-2-cb5 cell lines increased. Of the cell lines expressing Bcl-2-wt, there were no significant differences in the amount of Bcl-2 detected. Therefore, Bcl-2-wt 5 and Bcl-2-wt 2 were chosen for analysis. Only one line expressing Bcl-2-acta was available for study. The Bcl-2-cb5 line selected showed the least variation in expression between αMEM and estrogen depleted media (Bcl-2-cb5 18).

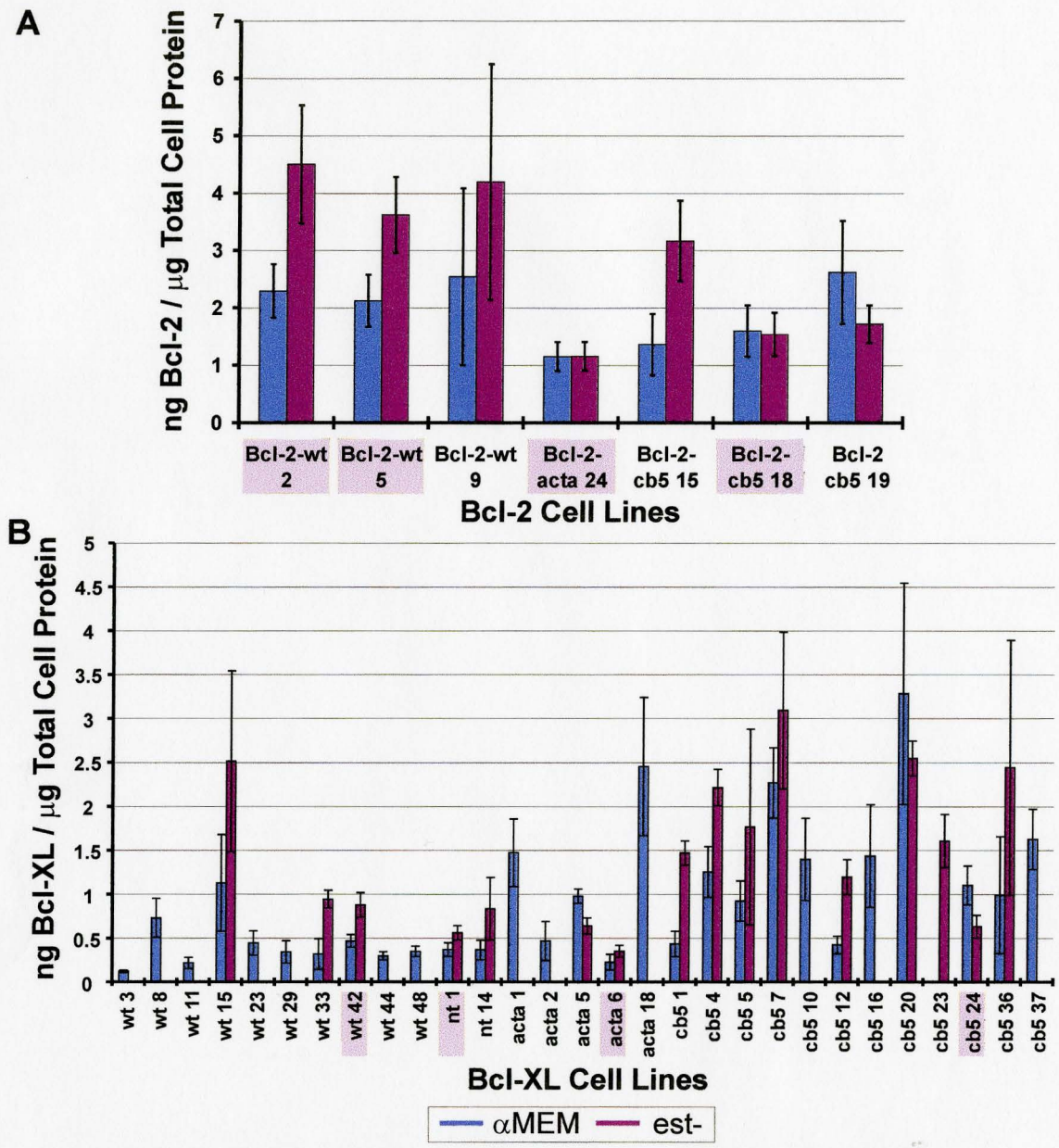

Figure 8: Amounts of A) Bcl-2 and B) Bcl-XL expressed in MCF-7 cell lines. The amount of Bcl-2 or Bcl-XL was evaluated as described in section 2.10. From these samples the cell lines expressing the lowest amounts of Bcl-2 were chosen (Bcl-2-wt 5, Bcl-2-acta 24 and Bcl-2-cb5 18) as well as an additional Bcl-2-wt cell line (Bcl-2-wt 2) as a duplicate control. Results are derived from at least one sample grown in αMEM for 3 days (blue) or 6 days in estrogen depleted conditions (est-) (mauve). Cell lines enclosed in pink boxes were selected for experiments to measure Bcl-2 or Bcl-XL function. See table 5 for the number of independent experiments and total number of measurements for each cell line. Error bars (where the number of independent samples is greater than 1) are standard error of the mean and standard deviation where there is only 1 independent sample.

Table 5: The number of independent experiments and total number of measurements of expression levels of Bcl-2, Bcl-XL and mutant cell lines.

Cell Line	Number of Individual Experiments		Total Number of Measurements	
	αMEM	est-	αMEM	est-
Bcl-2-wt 2 *	6	6	43	43
Bcl-2-wt 5 *	9	8	81	59
Bcl-2-wt 9	1	1	9	7
Bcl-2-acta 24 *	7	7	49	56
Bcl-2-cb5 15	1	1	9	5
Bcl-2-cb5 18 *	5	6	34	36
Bcl-2-cb5 19	1	1	6	7
Bcl-XL-wt 3	1		2	
Bcl-XL-wt 8	4		42	
Bcl-XL-wt 11	1		6	
Bcl-XL-wt 15	1	1	5	11
Bcl-XL wt 23	1		7	
Bcl-XL-wt 29	1		4	
Bcl-XL-wt 33	1	1	8	4
Bcl-XL-wt 42 *	7	7	65	50
Bcl-XL-wt 44	1		4	
Bcl-XL-wt 48	1		4	
Bcl-XL-nt 1 *	5	6	39	39
Bcl-XL-nt 14	1	1	4	4
Bcl-XL-acta 1	1		14	
Bcl-XL-acta 2	1		4	
Bcl-XL-acta 5	2	1	13	4
Bcl-XL-acta 6	4	5	34	33
Bcl-XL-cb5 1	1	1	4	4
Bcl-XL-cb5 4	1	1	7	4
Bcl-XL-cb5 5	2	2	11	15
Bcl-XL-cb5 7	1	1	12	9
Bcl-XL-cb5 10	1		10	
Bcl-XL-cb5 12	1	1	6	4
Bcl-XL-cb5 16	1		3	
Bcl-XL-cb5 20	3	2	25	15
Bcl-XL-cb5 23		1		4
Bcl-XL-cb5 24 *	6	6	52	47
Bcl-XL-cb5 36	1	1	12	7
Bcl-XL-cb5 37	1		5	

Cell lines denoted by * selected for experiments to measure Bcl-2 and Bcl-XL function; αMEM and est- denote cells grown in regular αMEM medium for 3 days and in estrogen depleted conditions of 6 days, respectively. For the amounts of Bcl-2 and Bcl-XL expressed in these cell lines see Figure 8.

Pilot studies of Bcl-XL and Bcl-2 inhibition of doxorubicin-induced apoptosis, performed by Dr. Weijia Zhu and myself, demonstrated that Bcl-XL is more effective at inhibiting cell death when compared in MCF-7 cells to a similar amount of Bcl-2 (W. Zhu, personal communication). Therefore cell lines with approximately half the amount of Bcl-XL compared to Bcl-2 in the other cell lines were selected to measure the functional differences between Bcl-2 and Bcl-XL within the limits of our assay system (see below). The following Bcl-XL cell lines were used: Bcl-XL-wt 42, Bcl-XL-nt 1, Bcl-XL-acta 6 and Bcl-XL-cb5 24. These Bcl-XL cell lines express roughly equal amounts of exogenous protein after growth in estrogen free medium (see Figure 8B).

3.2 PARP Cleavage and Degradation Following Induction of Apoptosis

The data in Figure 8 demonstrate that the expression levels of both Bcl-2 and Bcl-XL change following estrogen depletion. In all experiments, cells grown for 6 days in estrogen free conditions were harvested and lysed. However, cells treated with doxorubicin were grown for an additional two days. Therefore, it is necessary to monitor what changes occur in PARP expression following growth in estrogen free conditions for 8 days. MCF-7 cells were maintained in estrogen free media for a period of 6 - 8 days, after which the amount of PARP cleavage and degradation was assayed (see Figure 9). There is no significant difference between PARP expression in Neo, Bcl-2-wt 5 or Bcl-XL-wt 42 following 6 - 8 days in estrogen free conditions.

PARP cleavage and degradation were used to measure apoptosis following doxorubicin treatment (see Materials and Methods sections 2.11.1 to 2.11.3 and

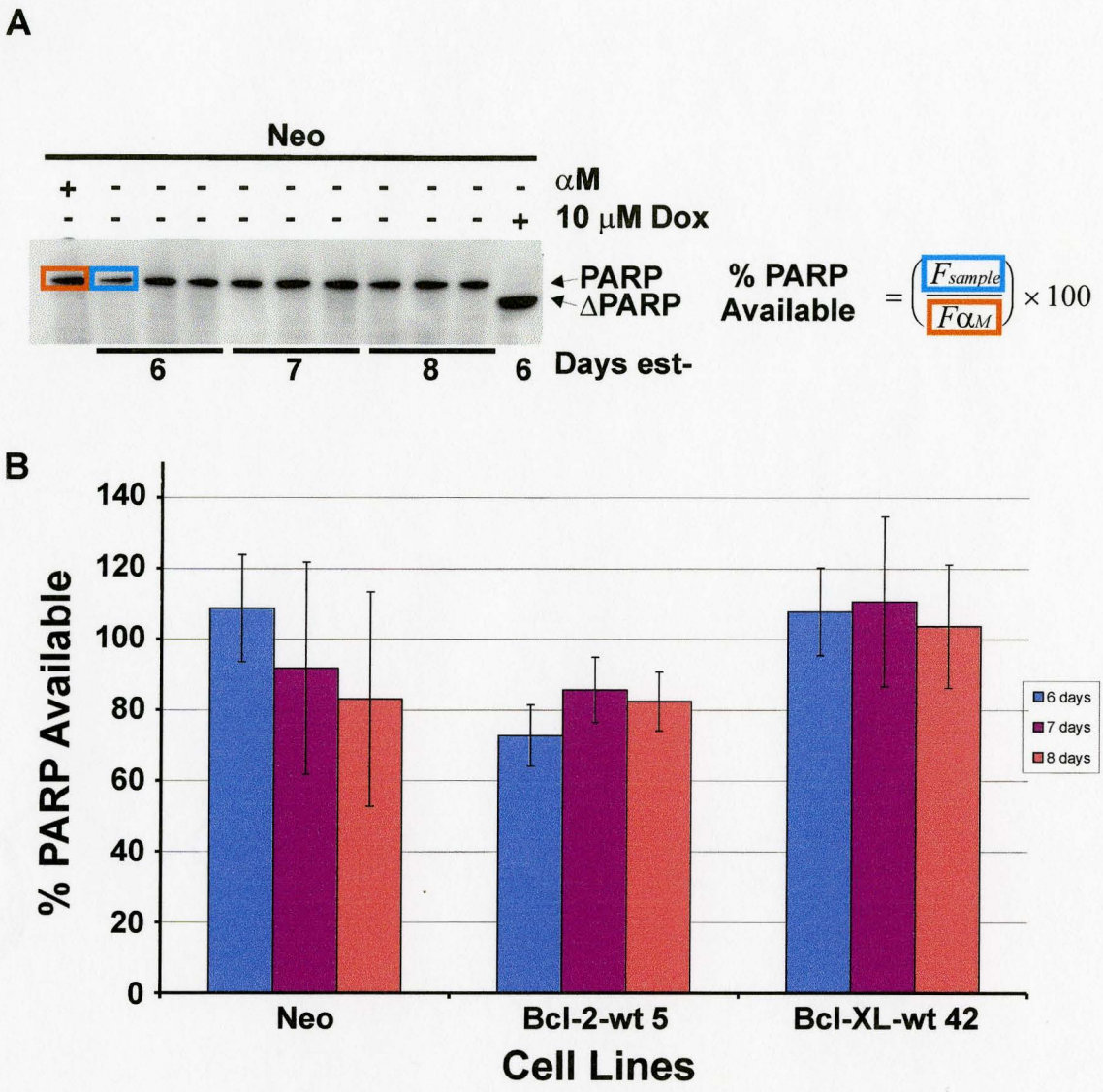

Figure 9: Effect on % PARP cleavage and degradation following growth for 6 - 8 days in estrogen depleted conditions (est-). A) Lysates from MCF-7 cells grown in estrogen depleted conditions for 6 - 8 days were resolved by SDS-PAGE and measured using the Kodak Image station. Lysates from three separate dishes of cells is shown. The positive control for PARP cleavage consists of MCF-7 Neo cells treated with 10 μM doxorubicin for 48 hours. B) The amount of 116 kDa PARP available does not differ in Bcl-2-wt 5 or Bcl-XL-wt 42 cell lines following growth in estrogen free conditions for 6 - 8 days (Sample 6 = 6 days growth in estrogen-free conditions; etc.). Results are derived from 6 separate samples. Error bars are standard error of the mean.

Figure 5). The apparent cleavage of PARP decreases if, due to a non-caspase-7 dependent mechanism, the rate of loss of the upper band (116 kDa) exceeds that for the lower band (89 kDa). For simplicity, all of the possible non-caspase-7 mechanisms leading to a decrease in the amount of PARP detected by the C-2-10 monoclonal PARP antibody are referred to here collectively as degradation.

The first drug assayed for the induction of apoptosis in MCF-7 cells was etoposide. Etoposide was chosen because its effect is inhibited by Bcl-2-acta but not Bcl-2-cb5 in Rat-1 cells (Annis et al., 2001; Soucie et al., 2001). Therefore use of this drug may demonstrate differences between the activities of Bcl-2 and Bcl-XL at different organelles in MCF-7 cells. At the beginning of this project the only other drug displaying specificity for inhibition by mitochondria localized Bcl-2 was doxorubicin. As doxorubicin is highly fluorescent and future assays may use a fluorescent read-out as a measure of apoptosis, etoposide was initially the drug of choice. To determine the range of drug concentrations MCF-7 Neo cells (empty neomycin pRcCMV vector) transfected cells were treated for up to 3 days with various doses of etoposide and PARP cleavage was assayed (see Figure 10A). However, the 89 kDa PARP cleavage product was not detected. This is in agreement with results previously published by Wilson *et al.* and Yang *et al.* (Wilson et al., 1995; Yang et al., 2001). It is possible that etoposide in MCF-7 cells might induce apoptosis via a caspase-3 dependent pathway. Therefore, MCF-7 cells expressing exogenous procaspase-3 were treated with 100 μM etoposide for up to three days (see Figure 10B). However, PARP cleavage was still not observed, although

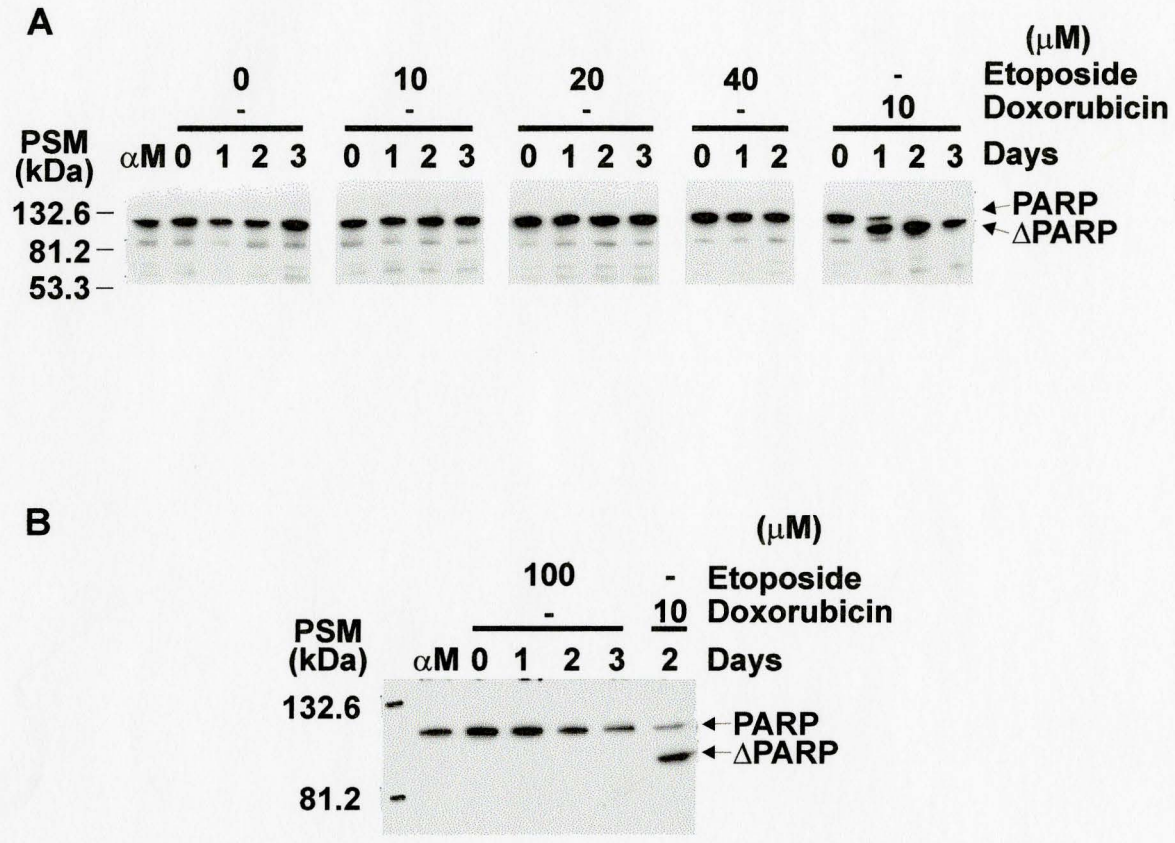

Figure 10: Etoposide does not induce PARP cleavage in MCF-7 cells. A) MCF-7 cells transfected with pRcCMV vector only, Neo, were treated with 10 - 40 μM etoposide or 10 μM doxorubicin for up to 3 days. PARP cleavage was not observed in any of the etoposide treated cells (compare to the doxorubicin control). B) MCF-7 cells, stably transfected with procaspase-3, were treated with 100 μM etoposide for up to 3 days. Full length PARP appears to be degraded as treatment times increase.

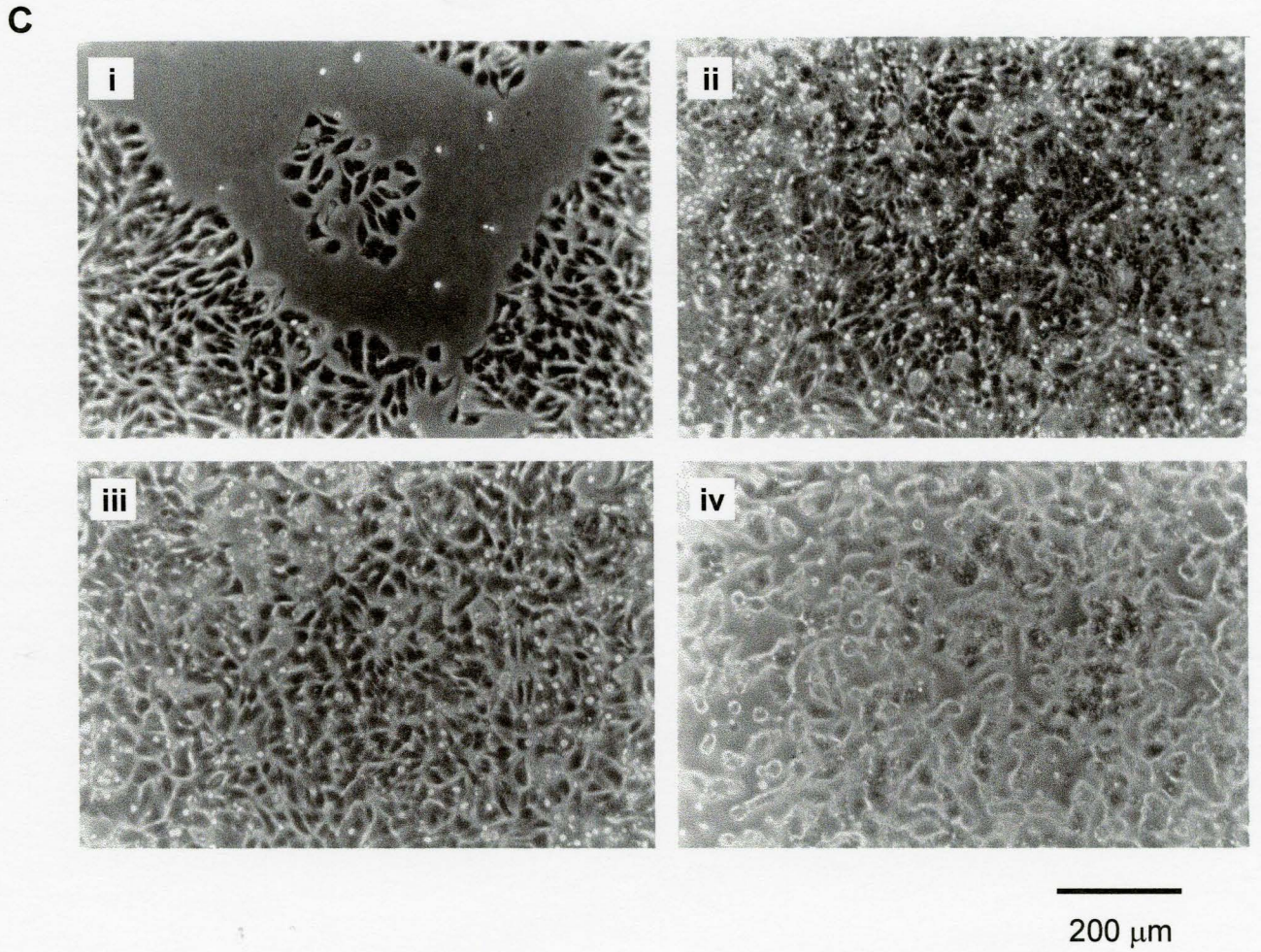

Figure 10 (con't): C) MCF-7 cells, Neo, were photographed using an inverted microscope at i) 6 days and ii) 8 days growth in estrogen-depleted conditions, and 6 days growth in estrogen-depleted conditions including 2 days of iii) 50 μM and iv) 400 μM etoposide.

116 kDa PARP did partially disappear as treatment times increased. Previous studies had demonstrated that MCF-7 cells expressing caspase-3 exogenously do undergo apoptosis as measured by PARP cleavage following 18 hours of treatment with 100 μM etoposide (Yang et al., 2001). However, Yang *et al.* treated the cells 6 hours after seeding whereas cells in the present study were treated following one and 6 days of maintenance in αMEM and estrogen depleted media, respectively. Growth conditions and extent of adhesion are both known to effect induction of apoptosis and may explain the difference in the two sets of results. It is also possible that the MCF-7 cells that were used previously were different from the ones used in the present investigation, as there is evidence that genotypic differences exist in MCF-7 cell lines grown in different laboratories (Bahia et al., 2002). Photographs of etoposide treated MCF-7 Neo cells for exposures of etoposide less than 50 μM reveal that the cells have a normal morphology, with a few scattered round cells (see Figure 10C; panel iii). At higher doses of etoposide (> 400 μM) the cells show an abnormal morphology that is not consistent with classical apoptosis (see Figure 10C; panel iv).

Both etoposide and doxorubicin inhibit topoisomerase II and generate reactive oxygen species (ROS) (Burden and Osheroff, 1998). DNA topoisomerases convert DNA from one conformation to another. Topoisomerase II is an enzyme that binds to double stranded DNA and introduces double strand breaks in the DNA and covalently binds the ends to form a gap through which another DNA helix can pass. This results in a relaxed form of DNA, essential during DNA synthesis and transcription (reviewed in Walker and Nitiss, 2002). Etoposide and doxorubicin can stabilize the DNA-topoisomerase II

complex, resulting in a stable protein-linked DNA strand break (reviewed in Burden and Osheroff, 1998). Nevertheless, different targets of the neoplastic drugs to the topoisomerase II-DNA complex may explain differential resistance to etoposide and doxorubicin in our cell line (Burden and Osheroff, 1998).

Therefore, because doxorubicin gives useful, reproducible results in our assay system, further experiments were performed with doxorubicin alone.

3.3 The Effect of Bcl-2 Wildtype and Mutant Location on Doxorubicin Induced PARP Cleavage

Because our MCF-7 cells lack caspase-3, PARP cleavage is a measure of caspase-7 activity. When two Bcl-2-wt cell lines expressing similar amounts of Bcl-2 wt were compared, (see Figure 11A) there appeared to be no significant difference in the amount of PARP cleavage throughout the range of drug concentrations tested. However, there were minor differences in the amount of PARP degradation between Bcl-2-wt 2 and -wt 5 (see Figure 11C) that results in an increased level of combined PARP cleavage and degradation at lower doses of doxorubicin (see Figure 11B). However, the EC_{50} values for Bcl-2-wt 2 (23 μM doxorubicin) and -wt 5 (30 μM doxorubicin) are roughly similar. As well, the amount of Bcl-2 expressed in the Bcl-2-wt 2 cell line is higher at lower doses of doxorubicin than in the Bcl-2-wt 5 cell line (see Figure 11D). Due to small differences in Bcl-2 expression and the responses to doxorubicin at lower doses, data from both the Bcl-2-wt 2 and -wt 5 cell lines are represented by the Bcl-2-wt 5 cell line and presented for comparisons with the other cell lines expressing mutants of Bcl-2. Together these results demonstrate the variability between independent cell lines when doxorubicin

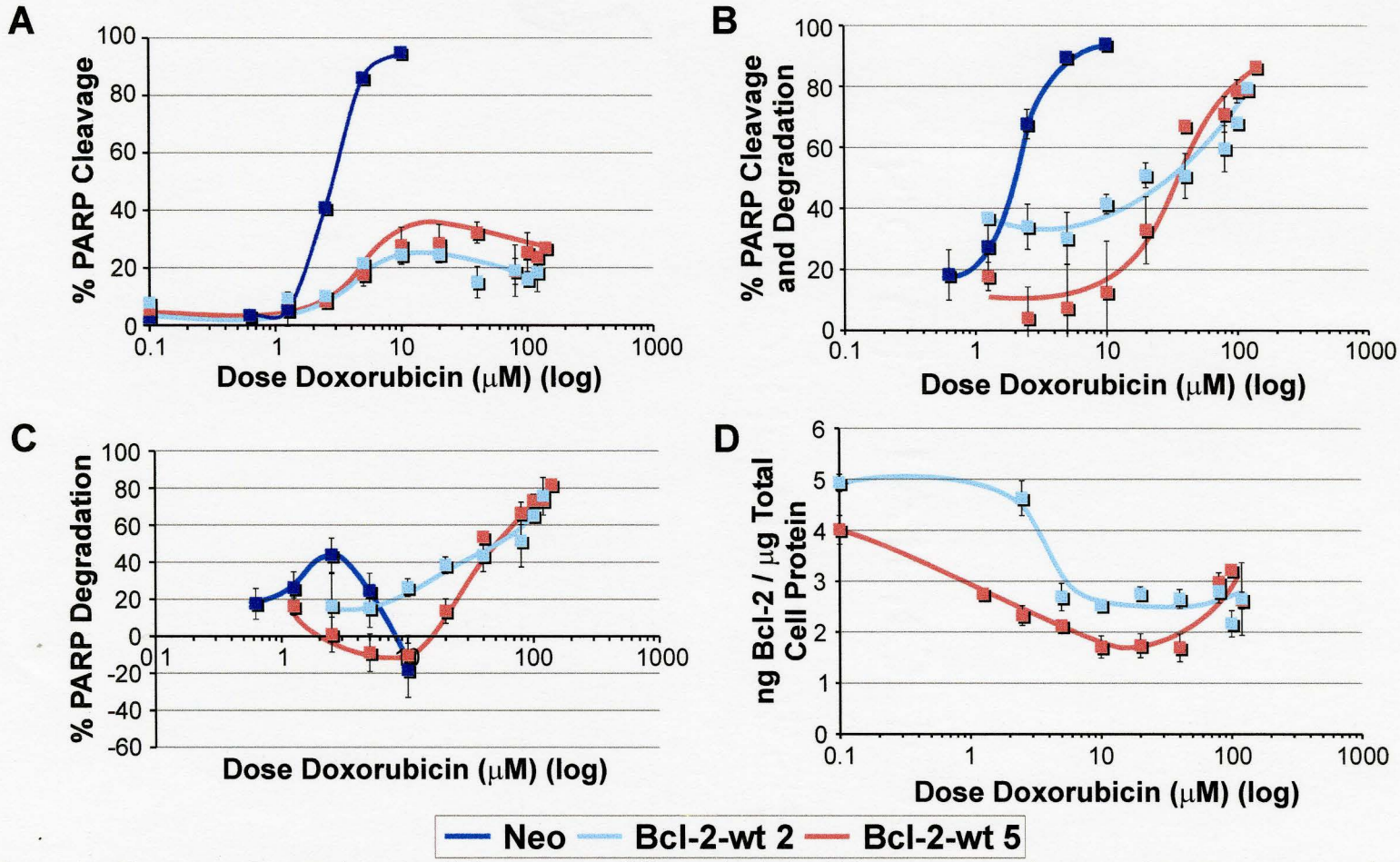

Figure 11: The two MCF-7 Bcl-2-wt cell lines are not different in their ability to prevent cleavage of PARP. A) Both Bcl-2-wt cell lines maintain approximately 20 % PARP cleavage over all doxorubicin doses tested. Due to the similarity of the two cell lines in % PARP cleavage, B) % PARP cleavage and degradation, C) % PARP degradation, and D) Bcl-2 expression, the Bcl-2-wt 5 cell line was used in all future experiments. All results are derived from the number of samples given in Table 6. All samples were treated with the dose of doxorubicin indicated following growth for 6 days in estrogen depleted conditions. Error bars are standard error of the mean.

induced apoptosis is measured by PARP cleavage. In this study samples are defined as independent if they come from different dishes of cells. The exact number of independent samples for each experiment is outlined in Table 6. The calculations of PARP cleavage or degradation involve the comparison of full length and cleaved bands of PARP using Western blots (see Figure 5). One would expect there to be no PARP cleavage in healthy cells (C_{est-} to equal zero). In most cases the value of C_{est-} is < 5 %. This error could be due to the difficulty in establishing an appropriate background value using the Image Station or it might result from the number of cells, < 10 % undergoing apoptosis in a tissue culture dish at any one time (unpublished data). The mean value of C_{est-} is < 5 % in all cell lines except Bcl-2-wt 5 (5.12 %) and Bcl-2-wt 2 (9.35 %).

When the Bcl-2 mutants were compared, Bcl-2-wt is the most effective at inhibiting doxorubicin-induced apoptosis (see Figure 12A). Bcl-2-acta was less effective than Bcl-2-wt, but more effective than Bcl-2-cb5. Bcl-2-cb5 provided no protection against doxorubicin induced apoptosis. These results are in agreement with qualitative assessments made previously by Dr. Weijia Zhu in MCF-7 cells (W. Zhu, unpublished data). However, since the goal of this project is to accurately measure and compare the protective ability of Bcl-2 and Bcl-XL at the ER and mitochondria using dose response curves and EC_{50} determinations, any cell lines that do not show a significant degree of PARP cleavage will not be comparable. After exposure of MCF-7 cells to concentrations of 40 μM or higher doxorubicin for 48 hours the apparent percent cleavage of PARP decreased. This was due to further cleavage or degradation of both the full length (116 kDa) and the 89 kDa fragment of PARP. However, the morphology of these cells is still

Table 6: Number of independent samples used to assay PARP for each cell line and dose of doxorubicin in the assays of PARP cleavage and degradation.

	Dose Doxorubicin (μM)												
	est-	**0.6**	**1.3**	**2.5**	**5**	**10**	**20**	**40**	**80**	**100**	**120**	**140**	**160**
Neo	3	6	6	6	6	4							
Bcl-2-wt 2	6		2	4	4	6	6	4	3	4	3		
Bcl-2-wt 5	7		6	6	6	6	6	6	6	6	6	3	
Bcl-2-acta 24	6		2	2	6	5	5	4	4	4	4		
Bcl-2-cb5 18	5	5	6	6	6	6	5						
Bcl-XL-wt 42	6					5	5	6	5	6	4	6	6
Bcl-XL-nt 1	5	2	4	4	5	5	5	4	4	2	2		
Bcl-XL-acta 6	5					2	4	4	4	4	4	4	
Bcl-XL-cb5 24	6	2	6	6	5	4	4	4	3	6	6		

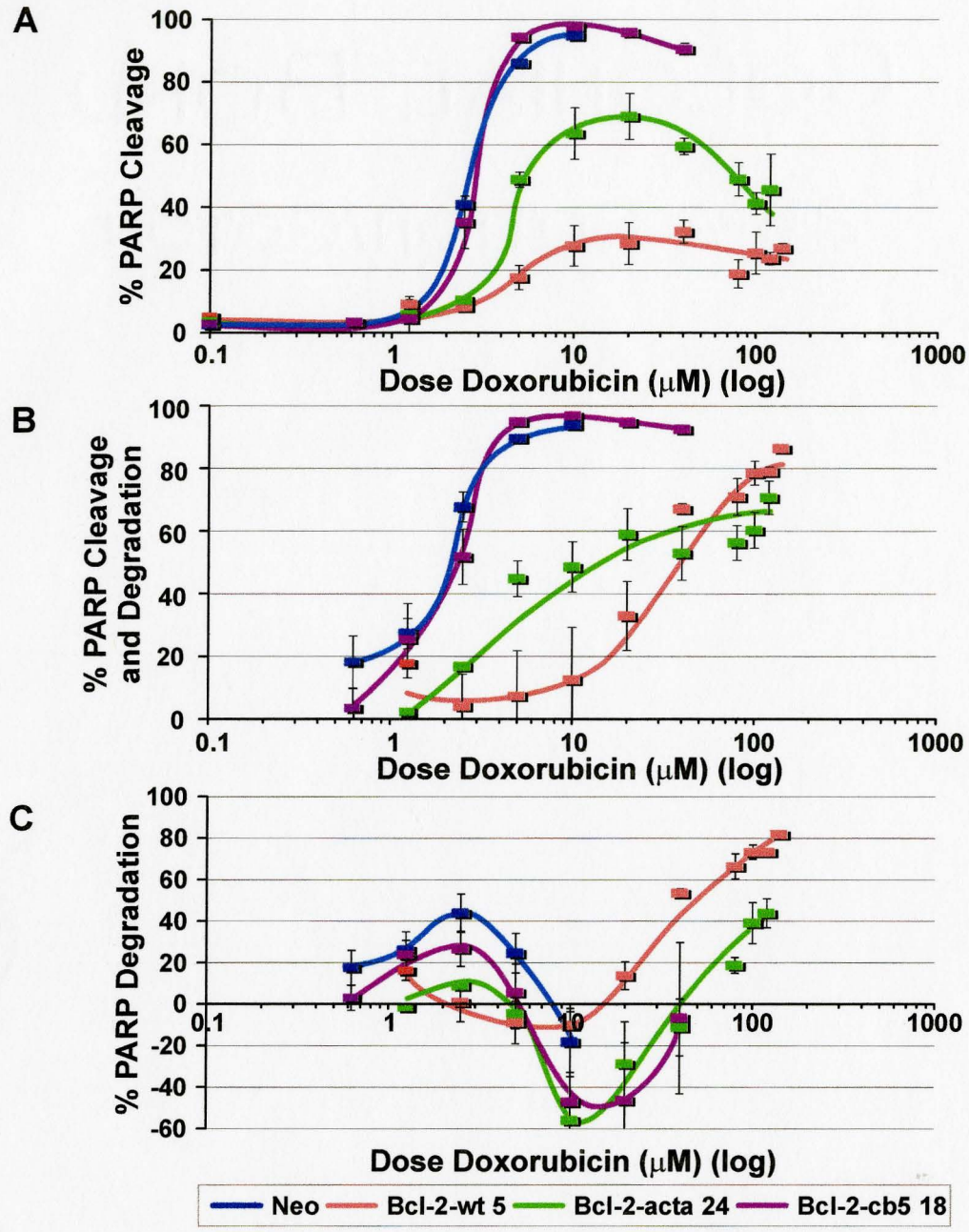

Figure 12: Combined PARP cleavage and degradation is the best method by which to determine EC_{50} values between cell lines. A) PARP cleavage data indicates that the Bcl-2-wt followed by the Bcl-2-acta cell lines offer some protection from doxorubicin-induced apoptosis. B) When Both PARP cleavage and degradation are considered, a similar pattern of protection by both Bcl-2 mutant cell lines is evident, except now all cell lines can be assigned EC_{50} values. C) Degradation of PARP is similar for all cell lines. Following an apparent synthesis of PARP at ~3 μM doxorubicin, the amount of PARP degradation increases at doses higher than 10 μM. All results are derived from the number of samples indicated in Table 6. Error bars are standard error of the mean.

typical of apoptosis at higher doxorubicin doses. During apoptosis caspases are not the only active proteases; calpains and catherines are also active (reviewed in Johnson, 2000). By measuring for PARP cleavage and degradation (see Figure 5), EC_{50} values were obtained (the effective concentration of doxorubicin required to elicit 50 % PARP cleavage and degradation combined). Images representative of observed morphological changes in the cells following doxorubicin treatment are shown in the appendix (see Figures A9 and A10 in the Appendix). In addition, PARP cleavage by caspase-7 was examined separately from PARP degradation in doxorubicin-treated cells (see results graphed in Figure 12A and C as per Figure 5). The amount of PARP cleavage in Bcl-2-cb5 cells is the same as that in Neo cells (compare the purple and blue lines in Figure 12A). Therefore, Bcl-2-cb5 is no more effective than vector control at inhibiting PARP cleavage. Bcl-2-acta demonstrates an intermediate level of apoptosis inhibition, with Bcl-2-wt being most effective. When the PARP cleavage and degradation are combined and analysed in cell lines expressing the various forms of Bcl-2, Bcl-2-wt is more effective than Bcl-2-acta. At doses ≤ 20 μM doxorubicin the results are similar to those obtained when assaying for PARP cleavage only (see Figure 12B). The EC_{50} values obtained for PARP degradation and combined PARP cleavage and degradation are similar for Neo and Bcl-2-cb5. Therefore, there is no protection from Bcl-2-cb5 (see Table 7). Cell lines that do not have an EC_{50} for PARP cleavage have an EC_{50} for PARP degradation (see Figure 12C and Table 7). This suggests that when the cells are exposed to $\geq 40 - 80$ μM doxorubicin PARP degradation occurs. The pattern of PARP degradation is similar for all

Table 7: EC_{50} values for doxorubicin induced PARP cleavage and degradation and expression levels of exogenous protein in each cell line. Stable transfections of MCF-7 cells with Bcl-2 and Bcl-XL mutants were treated with a range of doses of doxorubicin following 6 days growth in estrogen-free conditions. Quantification of the Western blots for PARP yields a dose response curve as described previously (see Figure 13). EC_{50} values were determined by graphical extrapolation of the dose at which 50 % PARP cleavage or degradation occurs. Results are averages of 4 separate EC_{50} determinations ± standard deviation or averages of several independent samples of Bcl-2 or Bcl-XL expression after six days growth in estrogen depleted conditions ± standard error of the mean. N/A indicates that the dose response curves did not reach 50 % PARP cleavage or degradation.

					EC_{50} Values (µM doxorubicin)			PARP Cleavage and Degradation	
	Number of Independent Experiments	Expression of Bcl-2 or Bcl-XL (ng / µg total protein) (EC_{50})	PARP Remaining (at 20 µM Dox)	% Protected / ng (at 20 µM Dox)	PARP Cleavage	PARP Degradation	PARP Cleavage and Degradation	EC_{50} / ng	Normalized (EC_{50} / ng)
Neo	N/A	N/A	N/A	N/A	2.9 ± 0.1	N/A	1.9 ± 0	N/A	N/A
Bcl-2-wt 2	6	2.5 ± 0.1	49.2 ± 4.1	10.0 ± 1.0	N/A	69.8 ± 5.8	22.8 ± 3.3	9.0 ± 1.4	1.5 ± 0.3
Bcl-2-wt 5	7	1.6 ± 0.1	67.1 ± 11.0	16.8 ± 2.9	N/A	37.7 ± 0.9	30.6 ± 1.0	19.4 ± 1.2	3.2 ± 0.5
Bcl-2-acta 24	7	0.2 ± 0.02	41.1 ± 8.2	34.3 ± 8.9	5.2 ± 0.4	N/A	13.2 ± 1.7	74.4 ± 14.2	12.3 ± 2.8
Bcl-2-cb5 18	5	1.3 ± 0.02	2.3 ± 0.4	1.4 ± 0.4	3.0 ± 0.1	N/A	2.3 ± 0.1	1.8 ± 0.08	0.3 ± 0.04
Bcl-XL-wt 42	6	0.7 ± 0.05	83.2 ± 14.6	91.3 ± 19.2	N/A	91.3 ± 2.6	85.4 ± 0.6	120.5 ± 9.1	19.9 ± 3.0
Bcl-XL-nt 1	5	0.5 ± 0.01	39.2 ± 9.9	78.4 ± 20.8	9.4 ± 0.9	72.9 ± 2.3	8.7 ± 1.7	17.0 ± 3.3	2.8 ± 0.7
Bcl-XL-acta 6	4	0.2 ± 0.02	91.1 ± 12.6	303.7 ± 58.3	N/A	108.0 ± 0.6	97.8 ± 1.5	606.5 ± 80.7	100.0 ± 18.8
Bcl-XL-cb5 24	5	0.6 ± 0.1	59.9 ± 7.1	99.8 ± 20.4	N/A	91.9 ± 1.0	32.3 ± 1.8	50.4 ± 9.3	8.3 ± 1.9

Bcl-2 expressing cell lines assayed (see Figures 12C and 13C). There appears to be an increase in the amount of total PARP after ~ 3 μM doxorubicin in all cell lines except the Bcl-2-wt 2 cell line, possibly as a stress response to DNA damage (Germain et al., 1999).

3.4 The Effect of Bcl-XL Wildtype and Mutants on Doxorubicin Induced PARP Cleavage

Representative cell lines expressing targeted mutants of Bcl-XL were compared. Among the Bcl-XL mutants, Bcl-XL-wt and -acta are most effective at inhibiting PARP cleavage, followed by Bcl-XL-nt and -cb5 (see Figure 13A and Table 7). Neither the wild type nor mitochondrial forms of Bcl-XL demonstrate PARP cleavage greater than 20 % at any dose of doxorubicin tested (see Figure 13A).

Therefore, Bcl-XL-wt and Bcl-XL-acta inhibit doxorubicin induced PARP cleavage to a greater degree than the Bcl-2 cell lines (see Figure 12A). Furthermore, the majority of death in the Bcl-XL-wt and -acta cell lines is due to a pathway that results in PARP degradation (see Figure 13C). An intermediate level of protection is observed in the Bcl-XL-cb5 and -nt cell lines (see Figure 13 B). This latter result is in contrast to targeted Bcl-2, where Bcl-XL-nt is significantly less effective at preventing PARP cleavage than Bcl-XL-cb5 at doses > 10 μM. This suggests that Bcl-XL functions by inhibiting a pathway that activates caspase-7. This pathway is preferentially inhibited at mitochondria, since Bcl-XL-acta completely inhibits PARP cleavage (see Figure 13A), while Bcl-XL-cb5 is only partially effective. However, Bcl-XL has an additional function that inhibits PARP degradation at lower doxorubicin doses compared to Bcl-2 (see

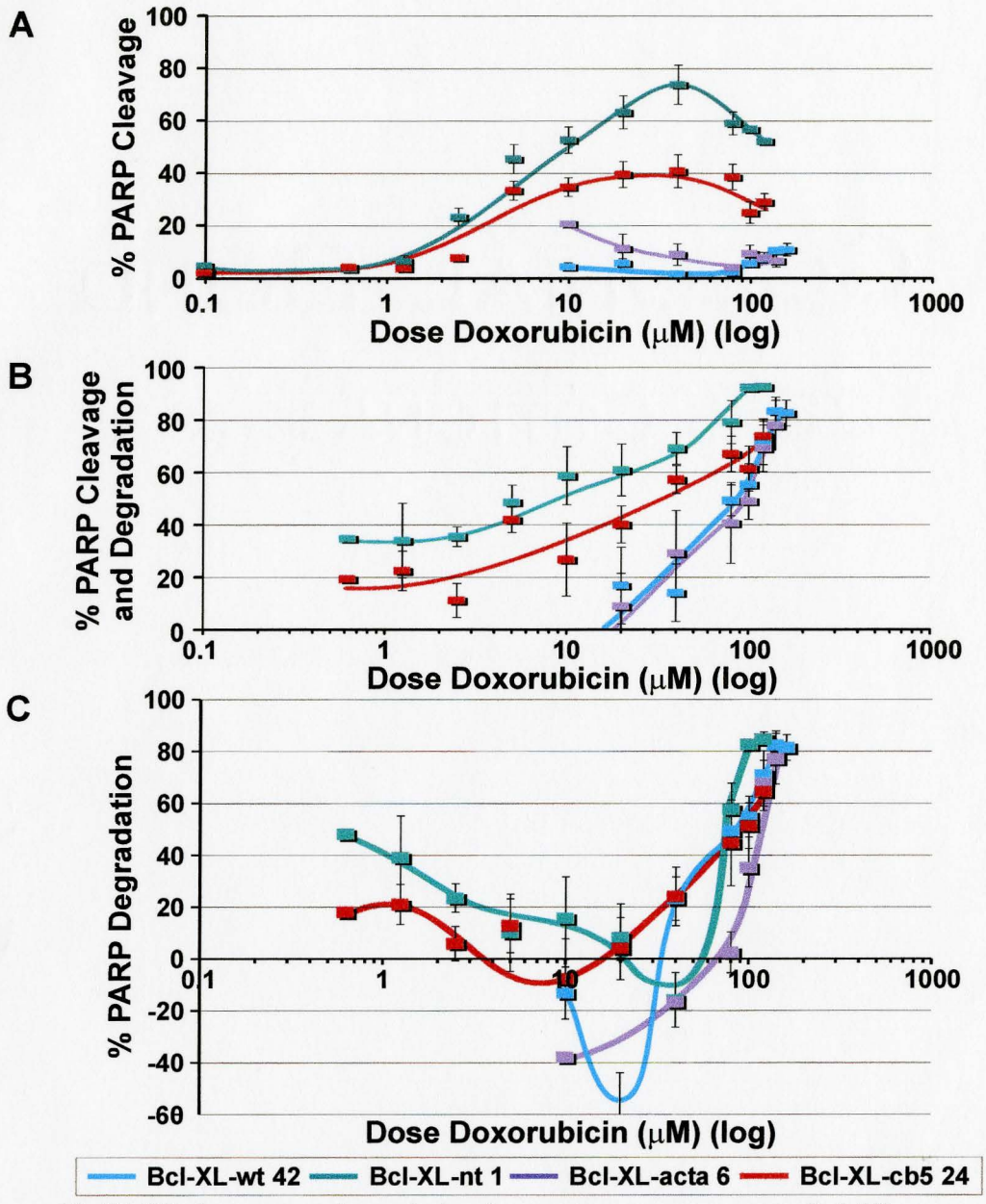

Figure 13: PARP cleavage or degradation in response to exogenous Bcl-XL expression. Bcl-XL-acta is similarly effective to Bcl-XL wt at inhibition of doxorubicin induced apoptosis. Cytosolic Bcl-XL (nt) and Bcl-XL-cb5 display an intermediate protective ability. A) Bcl-XL-nt and -cb5 offer similar degrees of protection from caspase-7 cleavage. Neither Bcl-XL-wt nor Bcl-XL-acta show PARP cleavage above 20 % over the range of doxorubicin doses. B) Among the Bcl-XL mutants, Bcl-XL-nt and -cb5 have a greater amount of PARP cleavage and degradation than Bcl-XL-wt or -acta. C) Degradation of PARP is similar for all cell lines except Bcl-XL-wt, which shows a large apparent synthesis of PARP at 20 μM doxorubicin. All results are derived from the number of samples indicated in Table 6. Error bars are standard error of the mean.

Figures 12C and 13C). This activity of Bcl-XL is seen only at doses of doxorubicin > 40 μM and results in an EC_{50} for degradation of 90 μM for Bcl-XL-wt compared to 40 – 70 μM for Bcl-2-wt.This additional activity possessed by Bcl-XL is also noted in Bcl-XL targeted to the ER and to a lesser degree in the cytosol.

The difference between Bcl-XL-cb5 and Bcl-XL-nt may be due to a small amount of Bcl-XL-cb5 mis-targeting its sole function site at the mitochondria. However, I believe this is unlikely for the following reason. In Figure 7 the targeting of Bcl-XL-cb5 was assessed both low and high expressing cell lines (Bcl-XL-cb5 24 and Bcl-XL-cb5 20, respectively). Bcl-XL-cb5 20 contains roughly three fold as much Bcl-XL as Bcl-XL-cb5 24. When compared to the Bcl-XL-acta cell line, the Bcl-XL-cb5 20 cell line expresses 10 times as much Bcl-XL (0.3 and 26 ng Bcl-XL protein / μg total cell protein, respectively) (see Figure 8). There was no co-localization of Bcl-XL-cb5 20 with Mitotracker Red (see Figure 7). There is a margin of error in visualizing fluorescent structures in immunofluorescence is 10 % (Wilhelm et al., 2000), so less than 10 % of the Bcl-XL-cb5 24 would be mistargeting to mitochondria, or 0.06 ng Bcl-XL (see Table 7). The EC_{50} obtained for Bcl-XL-cb5 is 50.4 μM doxorubicin. This is 12 times less than the EC_{50} of Bcl-XL-acta. Assuming that there is a linear relationship between the amount of Bcl-XL expressed and the degree of inhibition of PARP cleavage and degradation at any site, 1/12 the amount of Bcl-XL protein would be required to target the mitochondrion to achieve a similar level of protection (0.2 ng Bcl-XL-acta). This amount of Bcl-XL is more than the amount of Bcl-XL-cb5 24 that could be detected as mis-targeting by immunofluorescence (0.06 ng Bcl-XL-cb5 24). Therefore, even if less than 0.06 ng of

Bcl-XL-cb5 24 mis-targeted to the mitochondria, this mis-targeted fraction is not completely responsible for the EC_{50} observed for Bcl-XL-cb5 24. To verify the accuracy of the EC_{50} of Bcl-XL-nt in a high expressing cell line should be analysed by a similar immunofluorescence study.

As Bcl-XL is more potent than Bcl-2, it is possible that Bcl-2 is being degraded, while Bcl-XL protein was not. To test this hypothesis, we measured PARP cleavage and degradation along with the levels of Bcl-2 and Bcl-XL at each dose of doxorubicin. Indeed, Bcl-2-cb5 levels decrease, but only after the EC_{50} has been reached (see Figure 14). The Bcl-XL-nt cell line is similar to the Bcl-XL-cb5 cell line. Neo cells had undetectable amounts of Bcl-2 present following growth in estrogen depletion conditions. The amount of Bcl-2 or Bcl-XL decreases as the dose of doxorubicin increases, except for Bcl-2-acta, Bcl-XL-nt and Bcl-XL-cb5. The amount of Bcl-2 protein decreases below control levels (without doxorubicin treatment) at doses higher than the EC_{50} for the Bcl-2-acta cell line. The amount of protein decreases by approximately half from control values by 10 μM doxorubicin in all cell lines, except the Bcl-XL-nt, Bcl-XL-acta and Bcl-XL-cb5 cell lines. The disappearance of exogenous Bcl-2 and Bcl-XL levels could be due to caspase cleavage of these proteins (Cheng et al., 1997; Clem et al., 1998). These changes in Bcl-2 and Bcl-XL represent specific loss of these proteins, since the levels of actin remain constant up to 80 μM doxorubicin (see Figure 15A and 15B, respectively). Actin is cleaved by caspase-3 (Mashima et al., 1997) that is not present in MCF-7 cells, so actin cleavage would not be expected (Janicke et al., 1998) (It is not known if actin is a substrate for caspase-7). Therefore, use of an EC_{50} as a reference point

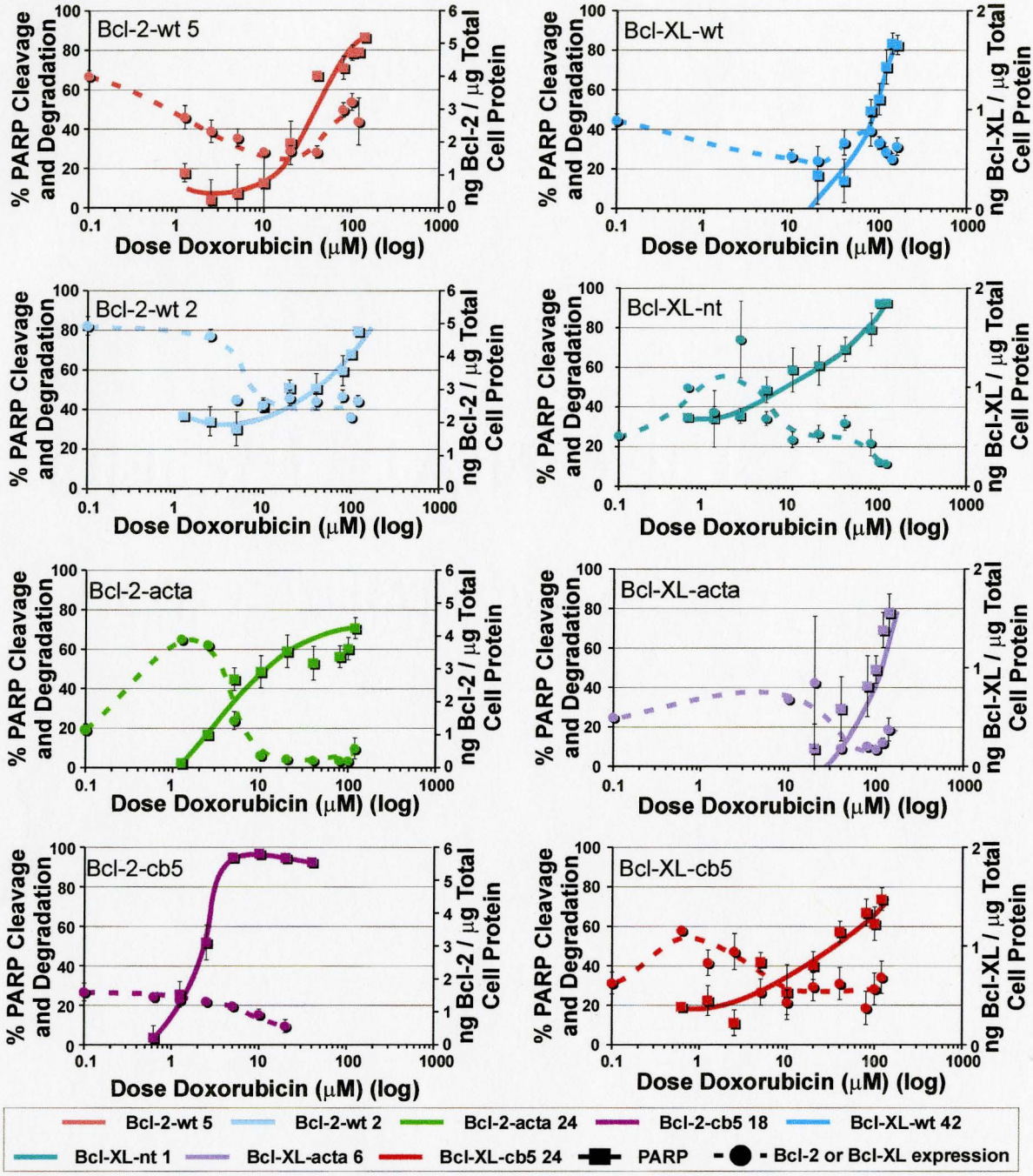

Figure 14: Expression of exogenous Bcl-2 or Bcl-XL prevents doxorubicin induced PARP cleavage and degradation. MCF-7 cells expressing Bcl-2-wt 5, Bcl-2-acta 24, Bcl-2-cb5 18, Bcl-XL-wt 42, Bcl-XL-nt 1, Bcl-XL-acta 6 and Bcl-XL-cb5 24 were treated for 2 days with the dose of doxorubicin indicated following 6 days of growth in estrogen depletion conditions. Western blots of PARP and Bcl-2 or Bcl-XL expression were quantified and results plotted to determine effective concentrations (EC_{50}). Error bars are standard error of the mean.

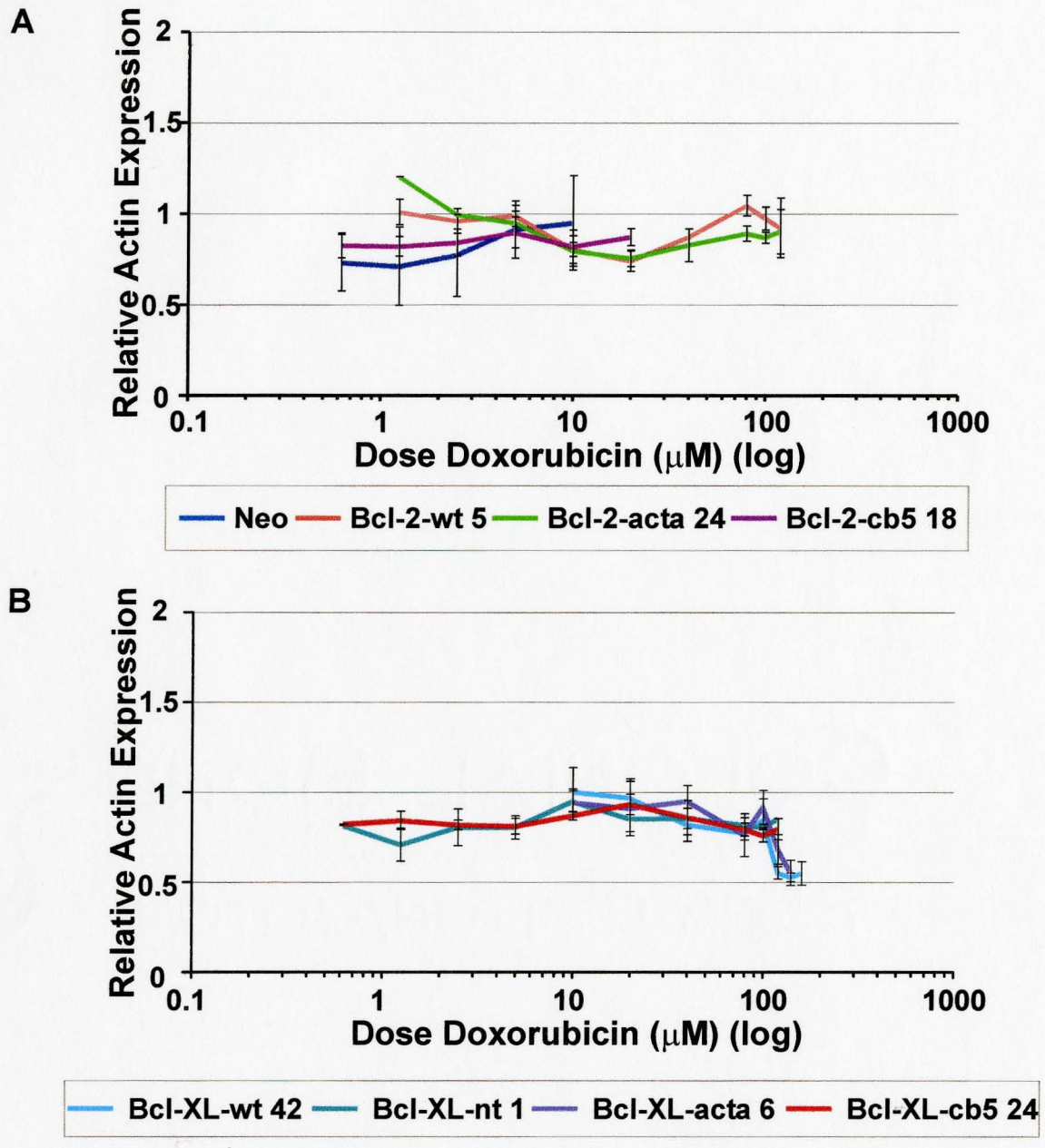

Figure 15: Quantification of actin ratios over a range of doxorubicin doses demonstrates that actin levels do not change significantly. The relative expression of actin in A) Bcl-2-wt 5, Bcl-2-acta and Bcl-2-cb5 and B) the Bcl-XL mutants (Bcl-XL- wt, Bcl-XL-nt, Bcl-XL-acta and Bcl-XL-cb5) remains at roughly the same levels as compared to when grown in estrogen-depleted conditions. Some cell lines, Bcl-XL-wt and Bcl-XL-acta, show a slight decrease in actin levels beyond 80 μM. All results are derived from at least 2 separate samples following two days of doxorubicin treatment at the doses indicated. Error bars are standard error of the mean.

is problematic because the amount of Bcl-XL determines the degree of apoptosis inhibition (Gottschalk et al., 1994).

However, assuming that the inhibition of PARP cleavage and degradation is linearly proportional to the amount of Bcl protein, the change in EC_{50} per unit exogenous protein present at that concentration of doxorubicin, we can compare the efficacy of wt and mutant Bcl-2 and Bcl-XL as shown in figure 16. The EC_{50} for Neo was subtracted from the EC_{50} of the Bcl-2 and Bcl-XL normalized EC_{50} values. By this analysis, the Bcl-XL is 8 - 27 times more protective than Bcl-2 at different subcellular locations. Although Bcl-2 affords less protection than the Bcl-XL in these cell lines, the mitochondrial targeted mutants offer better protection than the wild type version for both proteins. A striking difference exists for the ER targeted versions of these two molecules: while Bcl-XL-cb5 is effective, Bcl-2-cb5 is not. Furthermore, Bcl-XL-nt affords some protection, while the Bcl-2-nt does not (W. Zhu, unpublished data).

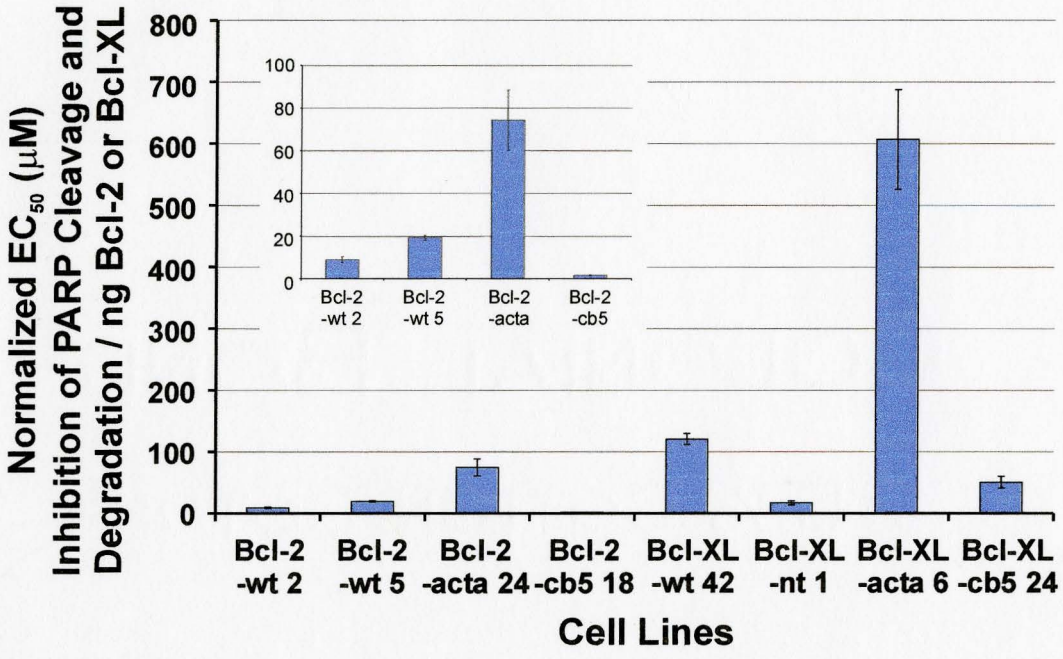

Figure 16: Histogram of the % PARP cleavage and degradation at the EC_{50} normalized for the amount of exogenous Bcl-2 or Bcl-XL present (see Table 7). The Bcl-XL cell lines are at least 8 times as potent as their Bcl-2 counterparts (eg. Bcl-2 vs. Bcl-XL). Of the Bcl-XL cell lines, the Bcl-XL-acta followed by Bcl-XL-wt are most effective at inhibiting doxorubicin-induced apoptosis. The insert graph is an expanded view of the Bcl-2 cell lines. The amount of PARP cleavage and degradation from Neo cells was subtracted from other cell lines to account for effects on PARP not due to exogenous protein.

4 Discussion

4.1 Robustness of the Assay

One of the aims of this study is to analyze the difference between of two anti-apoptotic proteins using PARP cleavage as an indication of caspase activity. Monitoring PARP cleavage by immunoblotting following doxorubicin treatment was used to measure the activity of caspase-7 in MCF-7 cells. PARP cleavage is a specific indicator of caspase-7, as our line of MCF-7 cells contains a gene deletion in *procaspase-3* that results in the synthesis of a non-functional protein (Janicke et al., 1998). By monitoring PARP degradation not due to caspase-7, we can measure the effect of other proteases activated during apoptosis.

This study demonstrates that quantitative immunoblotting of PARP and measuring its cleavage product following doxorubicin treatment is an effective method to determine differences between Bcl-2-wt and Bcl-XL-wt, Bcl-2-cb5 and Bcl-2-acta, and Bcl-2-cb5 and Bcl-XL-cb5. Furthermore, the assay yeilds reproducible measures of band intensities within a blot, between different blots resolved at different times and within a 6 – 8 day range of pre-treatment in estrogen depleted media. All of this complementary data is provided in the appendix.

To achieve this level of accuracy, good antibodies are essential. What determines the quality of an antibody for Western blotting? The antibody must have high

affinity for the protein target with minimal cross-reactivity to other proteins. It is possible to determine the strength of binding between a monoclonal Fab fragment and an epitope by equilibrium dialysis (Abbas et al., 2000). In this method the monoclonal antibody is placed inside a dialysis bag and a small antigen outside the bag. Any excess antigen inside the bag after equilibrium is reached is due to the formation of antibody-antigen complexes. However, two different polyclonal antibodies directed against different antigens would contain antibodies to a different number and set of epitopes. Polyclonal antibodies bind antigen epitopes with a certain range of affinities. Therefore, a problem in comparing different antigens by Western blotting is the use of alternative antibodies for detection. It is necessary to normalize for the affinity of two polycolonal antibodies in quantitative immunoblotting. This can be accomplished using an internal standard: a dilution series of a known amount of antigen in included in the blot to compare expression levels of exogenous protein in a test sample (cell lysate). Thus, differing antibody affinity from does not preclude quantitative analysis by Western blot.

The assay explored in this study requires an abundant supply of purified protein to determine amounts of protein expression in a cell line (Bcl-2 and Bcl-XL). The stability of the protein in the sample is also important, as both the purity and stability of the protein affect the dynamic range of the assay. For both Bcl-2 and Bcl-XL the dynamic range in this study was between 1 – 30 ng of protein.

Even if the technique outlined in this study is reproducible, the question of accuracy arises. In general, statistics dictates that the more samples one assays, the more one approaches the actual value. It is for this reason that at least four samples for each

dose of doxorubicin were assayed to determine Bcl protein expression. Using this number of independent samples, the standard error associated with a particular result would be the amount of standard deviation associated with that result divided by the square root of the number of samples assayed. As the number of samples assayed increases, one will be more assured of the accuracy of a result, but this must also be weighed with the determination of the number of samples to assay to make the process more efficient. Therefore, a limitation is the number of independent samples available to analyze.

Two Bcl-2-wt cell lines were assayed that express similar amounts of Bcl-2 (Bcl-2-wt 2 and Bcl-2-wt 5). The two cell lines show similar responses to doxorubicin treatment when PARP degradation and Bcl-2 expression are assayed (see Figure 11 and Table 7), indicating that measurement of PARP cleavage by Western blotting is highly reproducible between two independent cell lines. This result assumes a linear relationship between the amount of Bcl expression and the level of protection afforded by that expression. However, the cell lines expressing mutants of Bcl-XL offered complete protection against doxorubicin induced apoptosis when a similar amount of Bcl-XL protein was expressed compared to the amount of Bcl-2 expressed in Bcl-2-wt 2 or -wt 5 cell lines. Therefore, cell lines expressing similar amounts of Bcl-XL mutants were selected with which an EC_{50} (i.e. where 50 % of 116 kDa PARP remains following doxorubicin treatment) could be obtained. These cell lines expressed less exogenous protein than the cell lines expressing the Bcl-2 mutants.

It is important to verify that there is a linear relationship between exogenous protein expression and the degree of inhibition of doxorubicin induced apoptosis by

caspase-7 at higher doxorubicin doses (up to 20 μM for Bcl-2 and up to 40 μM for Bcl-XL). Therefore, Bcl-XL inhibits caspase-7 cleavage of PARP preferentially at the mitochondrion, but also at the ER; while Bcl-2 must be located at the mitochondrion to inhibit caspase-7 cleavage of PARP. The data obtained on the cells expressing accurately measured amounts of Bcl-2 mutants in this study are in good agreement with qualitative observations made previously by Dr. Weijia Zhu in MCF-7 cells (W. Zhu, personal communication). Both Bcl-2 and Bcl-XL fail to prevent PARP degradation by other proteases above 10 – 40 μM doxorubicin as we observed a decrease in total PARP protein not due to a caspase-7 cleavage at these doses. In all cell lines at doses of doxorubicin between 5 – 40 μM there is an increase in the amount of total PARP protein, possibly as a response to DNA damage caused by doxorubicin. This increase may be due to *de novo* synthesis of PARP, or alternatively, as a result of caspase-7 cleavage of another protease that is involved in normal PARP turnover.

The method used in this study directly compares the efficacy of Bcl-2 and Bcl-XL. We have found that Bcl-XL is at least 8 fold more effective at inhibition doxorubicin induced apoptosis than Bcl-2 when activity is determined per ng protein: Bcl-2 and Bcl-XL expression at the EC_{50} in the Bcl-XL-wt 42 and Bcl-2-wt cell lines (average of Bcl-2-wt 2 and Bcl-2-wt 5) are 0.7 and 2.1 ng / μg total cell protein, respectively. The EC_{50} for combined PARP cleavage and degradation is 85.4 μM and 26 μM doxorubicin for Bcl-XL-wt and Bcl-2-wt, respectively. Previous crude estimates have suggested that half the Bcl-2-wt or Bcl-XL-wt is found at the mitochondrion as determined by cellular fractionation followed by immunoprecipitation and immunostaining, respectively

assaying cell lines expressing three different amounts of Bcl-XL (Bcl-XL-wt 3, Bcl-XL-wt 42 and Bcl-XL-wt 11) at ~ 80 μM doxorubicin. As the level of exogenous Bcl-XL increases at this single dose ([Bcl-XL-wt 3] < [Bcl-XL-wt 42] < [Bcl-XL-wt 11]) (see Figure 8), so should the degree of protection.

Western blot detection of the caspase-induced cleavage of PARP is a good assay to determine the degree of inhibition of apoptosis elicited by Bcl-2 and Bcl-XL expressing cell lines. This assay allows one to separate the role of different proteases activated during apoptosis by measuring the amounts of full length (116 kDa) and cleaved (89 kDa) PARP. Other assays would not allow for independent analysis of both caspase-7 induced cleavage and non-caspase-7 degradation of PARP. For example, the use of an ELISA assay would not distinguish between the full length and 89 kDa PARP with our present antibody. The same would be true for use of a radioactive ATP assay whereby auto-ADP ribosylation of active PARP could be monitored. By using this assay, we can measure an EC_{50} for doxorubicin for both PARP cleavage and degradation. The EC_{50} for each Bcl-2 and Bcl-XL expressing cell line can then be normalized for the amount of Bcl-2 or Bcl-XL expressed to allow a direct comparison of functional activity per ng of protein.

4.2 Functional Comparison of Bcl-2 and Bcl-XL

The results from this project show that PARP undergoes caspase-7 cleavage at doxorubicin doses less than 40 μM in the Bcl-XL-nt and -cb5 cell lines and less than 20 μM in all the Bcl-2 cell lines regardless of cellular location (see Figures 13 and 12, respectively). Bcl-2-wt, Bcl-2-acta and all Bcl-XL cell lines prevent PARP cleavage by

(Krajewski et al., 1993; Gonzalez-Garcia et al., 1994). If we assume that half the exogenous Bcl-XL and Bcl-2 is located at the mitochondrion (0.35 and 1.1 ng / μg total protein, respectively), then the protective ability normalized per ng at the mitochondrion indicates that Bcl-XL-wt is10 times more effective than Bcl-2. However, this is likely an underestimate: Bcl-XL-wt is as effective as Bcl-XL-acta, yet there is 75 % less protein expressed in the Bcl-XL-acta cell line compared to the Bcl-XL-wt cell line (see Table 7). This suggests that the amount of Bcl-XL-wt exceeds what is required for maximal Bcl-XL activity.

Since Bcl-2-cb5 does not prevent doxorubicin induced apoptosis at any dose (see Figure 12), then only the Bcl-2-wt located at the mitochondrion, (1.1 ng Bcl-2 / μg total cell protein) is inhibiting apoptosis. Assuming that the amount of Bcl-2 expressed is linearly proportional to the level of protection at an EC_{50} of 26 μM, then 0.5 ng of Bcl-2 would have an EC_{50} of 13 μM doxorubicin. Indeed, this is roughly equal to the EC_{50} of Bcl-2-acta. However, at 0.2 ng Bcl-2-acta / μg total cell protein, the EC_{50} is13.2 μM doxorubicin (see Table 7). Therefore, as the amount of Bcl-2-wt present exceeds the concentration that offers maximal protection, Bcl-XL-wt is more effective than Bcl-2-wt by a factor slightly less than 10. Another estimate is that Bcl-XL-wt is 8 fold more than Bcl-2-wt, as this is the amount of increased protection Bcl-XL-acta affords over Bcl-2-acta. Similarly there is an excess of Bcl-XL-acta and Bcl-XL-cb5 protein present for maximal protection. Bcl-XL-acta offers slightly better protection than Bcl-XL-wt and Bcl-XL-cb5 is roughly 2.5 times less effective than Bcl-XL-wt. If the same comparisons are made with Bcl-XL as with Bcl-2 we find that only 0.3 ng of Bcl-XL is necessary at

the ER and only 0.2 ng of Bcl-XL is necessary at the mitochondrion for maximal protection. In both cases, this is in excess of the amount of Bcl-XL protein in the assayed cell lines.

The increased efficacy of Bcl-XL compared to Bcl-2 is consistent with observations of some (Gottschalk et al., 1994; Boise et al., 1993), but not all previous studies (Chao et al., 1995). Gottschalk *et al.* studied WEHI-231 cells, a murine B lymphoma line transfected with Bcl-2 or Bcl-XL, then treated with cyclosporin A (CsA). The cells expressing Bcl-XL were less susceptible to CsA induced apoptosis than the Bcl-2 expressing cells. However, Bcl-2 protein expression was not assessed, and Bcl-XL expression was assessed by non-quantitative immunoblots. Of the two Bcl-XL expressing cell lines, the one expressing roughly three fold more Bcl-XL was more effective (Gottschalk et al., 1994). Similar results were obtained by Boise *et al.*, who compared the protective ability of pooled Bcl-2 and Bcl-XL expressing FL5.12 cells. When deprived of IL-3, cells expressing Bcl-XL survived longer than Bcl-2 expressing cells. However, these authors did not evaluate Bcl-2 or Bcl-XL protein levels. Chao *et al.* generated transgenic mice expressing either Bcl-2 or Bcl-XL. Single cell thymus suspensions were treated with 100 nM dexamethasone or 225 rad of γ radiation. After 100 hours of treatment there was no significant difference in cell viability between the Bcl-2 or Bcl-XL expressing cells. Separate Western blots show expression of Bcl-2 and Bcl-XL in the two thymus suspensions (Chao et al., 1995). In these studies the Bcl-2 and Bcl-XL expression was assessed by immunoblotting using different antibodies. Differences in antibody affinities preclude the ability to compare the relative expression levels of two

different antigens. Only by using known amounts of protein as an internal standard can one quantitatively compare expression levels of two different proteins.

4.3 Function of Bcl-2 and Bcl-XL at the Mitochondrion or the ER

Previous studies have shown that Bcl-2 functions at the mitochondrion in an epithelial cell line (Zhu et al., 1996). These results are consistent with data obtained here. In Rat-1 fibroblasts treated with etoposide, Bcl-2 located at mitochondria inhibits Bax translocation from the cytosol to mitochondria. Under these conditions, Bax translocation and cytochrome c release occur prior to mitochondrial membrane potential ($\Delta\Psi m$) loss and cytochrome c release in control cells (Annis et al., 2001). In the absence of the proto-oncogene myc, Bax is still targeted to the mitochondrion and integrates into the outer membrane, but it is not activated and cytochrome c release does not occur (Soucie et al., 2001). Therefore, Bax must be in an active conformation and not just located at mitochondria for cytochrome c release to occur. These studies showed that Bcl-2 prevents Bax translocation, but not whether Bcl-2 inhibits Bax activation when myc is present. These issues need to be addressed in MCF-7 cells. The antibody used to determine Bax activation cross-reacts with human Bax (Hsu and Youle, 1997b), therefore studies with MCF-7 cells could determine if targeted Bcl-2 or Bcl-XL mutants inhibit either Bax translocation or activation.

How do Bcl-2 or Bcl-XL function at mitochondria? One possibility is that these anti-apoptotic proteins inhibit Bax-induced cytochrome c release. There are currently two models: Bax combines with the voltage dependent anion channel (VDAC) to form a pore in the outer mitochondrial membrane, or Bax alone could form homo-

oligomers to form a pore within the membrane. VDAC is an outer mitochondrial membrane channel that allows movement of substances in and out of the mitochondrion (reviewed in Colombini, 1989). Both models predict that activated Bax would release cytochrome c from the inter-membrane space. Consistent with the first model Bax (Shimizu et al., 2001), Bak (Shimizu et al., 1999) and Bim (Sugiyama et al., 2002) directly interact with VDAC to induce cytochrome c release, and an anti-VDAC antibody prevents cytochrome c release (Shimizu et al., 2001; Sugiyama et al., 2002). Bcl-XL inhibits Bax induced cytochrome c release through VDAC in detergent solublized membranes, and both Bak and Bax induce changes in mitochondrial membrane potential ($\Delta\Psi m$) in yeast mitochondria (Shimizu et al., 1999). By contrast, Vander Heiden *et al.* suggest that Bcl-XL keeps VDAC open, thereby maintaining metabolite exchange between the cytosol and mitochondria under conditions where the channel would normally be closed (Vander Heiden et al., 2001), such as during the early stages of growth factor withdrawal induced apoptosis. The authors point out that the pore is not large enough for cytochrome c release. Therefore, during the early stages of apoptosis Bcl-2 or Bcl-XL may facilitate oxidative respiration until Bax is activated, possibly via myc or tBid (Soucie et al., 2001; Desagher et al., 1999). In Hela cells treated with staurosporine or UV radiation, Bax inserts into and forms large molecular weight oligomers in mitochondrial membranes, a process that is inhibited by Bcl-2 (Antonsson et al., 2001). In contrast to other studies, Bax oligomers in Hela cells are not bound to VDAC (Antonsson et al., 2001; Kuwana et al., 2002). Whatever the architecture of the Bax complex that causes cytochrome c release, Bcl-2 and Bcl-XL prevent these

mitochondrial changes (loss of $\Delta\Psi m$ and cytochrome c) by inhibiting the pro-apoptotic family members.

To date, there is no direct comparison of the function of Bcl-XL localized exclusively at either the ER or mitochondria. The present results suggest that Bcl-XL has (at least) two activities, as Bcl-XL is a very potent inhibitor of apoptosis when located at the mitochondrion, but less effective when at the ER or in the cytoplasm. Thus, even though there is twice as much Bcl-XL-cb5 at the ER than Bcl-XL-acta at mitochondria, the EC_{50}s are 32 and 98 μM doxorubicin, respectively. The observation that cytosolic Bcl-XL has an anti-apoptotic function has been previously noted (Fang et al., 1994).

We confirm that Bcl-XL-nt is only moderately effective as expression levels of 0.5 ng / μg total cell protein yields an EC_{50} of 9 μM, compared to an EC_{50} of 98 μM for 0.2 ng Bcl-XL-acta / μg total cell protein (see Table 7). Comparison of the EC_{50} for Bcl-XL-nt with a similar expression to Bcl-XL-cb5 reveals that binding the ER membrane confers significantly more anti-apoptotic activity. Thus, unlike Bcl-2, the present data shows that Bcl-XL is still functional at sites other than the mitochondria suggesting that Bcl-XL protects cells by an additional mechanism not shared by Bcl-2. Bcl-2-nt is non-functional in our hands using different apoptotic stimuli (Zhu et al., 1996). However it is important to accurately measure Bcl-2-nt levels and to assess apoptosis quantitatively to verify this.

Previous results from our laboratory indicate that Bcl-2 located at the ER can inhibit certain apoptotic stimuli, demonstrating that the lack of Bcl-2-cb5 function in the present study is not due to mis-folding of the hybrid protein (Zhu et al., 1996).

Several studies have been performed to determine how Bcl-2 might inhibit apoptosis at sites other than the mitochondrion. Several potential mechanisms have been investigated, including Ca^{2+} signals, activation of caspases, pH signals, sequestration of Bax and regulation of ROS.

Ca^{2+} is usually found in the ER lumen in either a free state or bound to calreticulin or calnexin. Fluxes or acute release of ER Ca^{2+} can induce apoptosis (reviewed in Ferri and Kroemer, 2001). However, when Rat-1/myc fibroblast cells were treated with etoposide, cytosolic calcium levels did not change and did not differ between vector control cells and those overexpressing Bcl-2 (Lee et al., 1999). Over-expression of Bcl-XL prevents ER calcium depletion and apoptosis in CHO cells treated with ryanodine (which depletes ER calcium by maintaining an open state of the ryanodine receptor) (Pan et al., 2000). A similar effect occurs when expression of the ER calcium pump, SERCA, (which causes an increase in ER uptake of calcium), increases due to Bcl-2 over-expression in MCF-10A cells (Kuo et al., 1998). Therefore control of calcium efflux from the ER by Bcl-XL following doxorubicin treatment may explain Bcl-XL located at the ER, but not of Bcl-2.

Both caspase-8 and -12 are located at the ER (Ng et al., 1997; Nakagawa and Yuan, 2000). Procaspase-8 is present at the ER in a complex containing Bcl-2 (or Bcl-XL) and p28 Bap31. Active caspase-8 can cleave p28 Bap31 to p20 Bap31, which is pro-apoptotic. Bcl-2 inhibits p20 Bap31 induced apoptosis and cleavage at p28 Bap31 (Ng et al., 1997). However, a broad range caspase inhibitor, z-VAD-fmk, did not prevent loss of $\Delta\Psi m$ in doxorubicin treated MTLn3 cells, so it is unlikely that caspase-8 is involved in

doxorubicin induced apoptosis (Huigsloot et al., 2002). Similarly, Bcl-2-cb5 inhibits steps in apoptosis that are not susceptible to using z-VAD-fmk (Annis et al., 2001). Procaspase-12 is located on the cytoplasmic side of the ER and becomes activated by m-calpain in response to an ER stress and calcium release (Nakagawa and Yuan, 2000). Caspase-12 activates the caspase cascade via direct procaspase-9 cleavage (without cytochrome c release), followed by activation of procaspase-3 (Morishima et al., 2002) and procaspase-7 (Gil-Parrado et al., 2002). However, no genes encoding caspase-12 have been found in the human genome (Fischer et al., 2002).

Treatment of MCF-7 cells with somatostatin triggers acidification of the cytosol and apoptosis. The mechanism of somatostatin-induced intracellular acidification is a phosphatase-dependent process, mediated by SHP-1 that decreases the functional activity of the Na^+/H^+ exchanger and the H^+-ATPase. Bcl-2 over-expression maintains the activity of these pumps (Thangaraju et al., 1999). Inhibition of caspase-8, but not caspase-3 or -7, prevents cellular acidification after somatostatin treatment and allowed MCF-7 cells to maintain $\Delta\Psi m$ and retain cytochrome c within mitochondria. This suggests that active caspase-8 is necessary for intracellular acidification to occur, and that loss of $\Delta\Psi m$ and cytochrome c release are a consequence of intracellular acidification following somatostatin treatment (Liu et al., 2000). To determine if Bcl-XL can inhibit intracellular acidification from the ER, it would be necessary to assay caspase-8 activation following somatostatin treatment on Bcl-XL-cb5 expressing MCF-7 cells. However, procaspase-8 is not activated following doxorubicin treatment of MCF-7 cells

(W. Zhu, personal communication), so this is not a suitable model system to address this question.

In some circumstances, Bcl-2 or Bcl-XL may bind Bax when both are located at the ER. Consistent with this, pro-apoptotic proteins are located at, and can be functional by altering ER mechanisms (Scorrano et al., 2003). Consistent with this, in murine thymocytes and splenocyte lysates (Hsu and Youle, 1997b), Bax antibody can co-immunoprecipitate Bcl-2 and Bcl-XL, the latter with greater efficiency (Hsu and Youle, 1997b). However, these co-immunoprecipitations are not quantitative in that the total amount of Bcl-2 and Bcl-XL in the cells was not evaluated, and therefore the results were not normalized for Bcl-2 and Bcl-XL expression levels. To determine if Bcl-XL can bind and sequester (and inactivate) Bax at the ER, MCF-7 cells expressing Bcl-XL mutants that retain their anti-apoptotic activity but fail to bind Bax could be assayed (Cheng et al., 1996).

Another theory postulates that Bcl-2 might function by regulation of ROS production (Hockenbery et al., 1993). However, Bcl-2 still functions in hypoxic conditions where generation of ROS is limited (Shimizu et al., 1995; Jacobson and Raff, 1995). However, this does not preclude the fact that in some circumstances Bcl-2 is effective by inhibiting ROS generation. Indeed, in Rat-1 cells exposed to low serum, ROS generation is inhibited by Bcl-2 located at the ER (Annis et al., 2001).

Furthermore, our studies show that etoposide fails to induce apoptosis in MCF-7 cells, while treatment with doxorubicin leads to cell death. Both drugs kill cells by inhibiting topoisomerase II; however at doses higher than 2 – 5 μM, doxorubicin has the

additional function of generating ROS (Harris et al., 1998; reviewed in Gewirtz, 1999). Our studies used doses of doxorubicin that included the possibility of ROS generation as an additional mechanism of cytotoxicity. Previous studies confirm that etoposide does not induce apoptosis in MCF-7 cells while doxorubicin does (Yang et al., 2001). As Bcl-2 and Bcl-XL inhibit apoptosis at these higher doses, organelle-specific regulation of ROS production is a testable hypothesis in our system.

4.4 Potential Differences between the Bcl-2 and Bcl-XL Mutants

The present study also addresses whether Bcl-2 and Bcl-XL expression changes during apoptosis, and looks for the functional effect of these changes. The expression of Bcl-XL is lower in the cell lines assayed than that of Bcl-2, and yet Bcl-2 is less effective at than Bcl-XL. Bcl-2 or Bcl-XL expression decreased two fold over the range of doses of doxorubicin treatment investigated, except in the Bcl-2-acta 24 cell line, which increases expression at low doses of doxorubicin and is then rapidly degraded as it approaches the EC_{50}. The decrease of Bcl-2 and Bcl-XL expression correlates with the degree of PARP cleavage (see Figure 14). In the cell lines where the Bcl-2 or Bcl-XL inhibits apoptosis, the expression levels decrease with dose until a critical level is reached, at which point PARP cleavage or degradation increases. Due to fluctuations in the expression levels of Bcl-2 and Bcl-XL after doxorubicin treatment, the EC_{50} can not be used as a reference point to compare the functions of the cell lines, if we assume that the amount of Bcl-2 or Bcl-XL expression affects PARP cleavage and therefore the determination of EC_{50}. As a result, the EC_{50} values have been normalized for the amount of Bcl-2 or Bcl-XL expression (see Figure 16 and Table 7).

Why do Bcl-2 and Bcl-XL levels decrease? It has been previously shown that the loop regions of Bcl-2 and Bcl-XL contain a regulatory domain, cleavage of which results in the formation of a C-terminal pro-apoptotic Bcl-2 or Bcl-XL fragment (Cheng et al., 1997; Clem et al., 1998). Caspase-3, but not caspase-7, cleaves Bcl-2 *in vitro*, and both caspases-3 and -7 cleave Bcl-2 *in vivo* (Cheng et al., 1997; Kirsch et al., 1999). Bcl-XL is cleaved by caspase-1 and -3 *in vitro* (Clem et al., 1998), but only caspase-3 *in vivo* (Fujita et al., 1998). The involvement of caspase-7 in Bcl-XL cleavage has not been investigated. Mutation of asp31 to ala abolished cleavage of Bcl-2 *in vitro* and enhanced Ba/F3 cell viability *in vivo* following puromycin treatment (Cheng et al., 1997). A similar mutation at asp61 (to ala) of Bcl-XL reduced cleavage of Bcl-XL D61A *in vitro* and *in vivo* (Clem et al., 1998). The full range of caspases have not been tested for Bcl-2 or Bcl-XL cleavage. MCF-7 cells do not contain functional caspase-3 and do not cleave Bcl-2 *in vitro* (Kirsch et al., 1999); however, other caspases may be active at it would be interesting to assay Bcl-2 D34A and Bcl-XL D61A point mutants in our system to determine if cleavage is organelle specific (Fadeel et al., 1999).

M-calpain also cleaves Bcl-2 and Bcl-XL in the regulatory loop region (Gil-Parrado et al., 2002), and this reaction is more complete for Bcl-2 than Bcl-XL as assessed by qualitative Western blots (Gil-Parrado et al., 2002). Note that for each antibody the protein acts as its own internal standard for cleavage providing that the antibodies recongized both the full length and cleaved products equally. Therefore, non-caspase proteases may be responsible for the decrease in Bcl-2 and Bcl-XL. To examine

this possibility, cells could be treated with the selective calpain inhibitor, AC27P (Gil-Parrado et al., 2002).

Another explanation for loss of Bcl-2 or Bcl-XL expression is due to accelerated physiologic turnover of the proteins, indeed TNFα treatment results in the dephosphorylation of ser87 in Bcl-2 mutants (Breitschopf et al., 2000) with increased ubiquitin-dependent degradation (Dimmeler et al., 1999). This is verifiable using a pulse chase assay.

4.5 Summary and Future Work

In the present study we have shown that quantitative immunoblotting is a good method to determine the efficiency of anti-apoptotic proteins, as measured by PARP cleavage. Expression levels of Bcl-2 and Bcl-XL decrease during doxorubicin treatment. Bcl-XL is 8 to 27 times more potent than Bcl-2 inhibiting doxorubicin induced apoptosis when activity is determined on a per ng basis. Although both Bcl-2 and Bcl-XL are most effective when located at mitochondria, Bcl-XL is also effective when located at the ER, and to a lesser extent, in the cytoplasm.

Several issues still need to be addressed. Dual immunofluorescence with staining for Bcl-XL and ER or mitochondrial markers needs to be performed to confirm correct localization and to verify the absence of mis-targeting due to over-expression of the Bcl-XL mutants.

An underlying assumption for this study is that as the amount of Bcl-2 or Bcl-XL expressed increases, the level of protection from treatment increases linearly. To test this assumption, it would be necessary to measure the level of protection of three cell

lines expressing increasing amounts of Bcl-XL protein at a constant dose and time of doxorubicin treatment and to ascertain that the level of Bcl-XL does not change over time.

Our previous work indicated that Bcl-2 is functional at the mitochondria but not ER following doxorubicin treatment in Rat-1 fibroblasts, and this information was used to guide the present study (Soucie et al., 2001). Both Bcl-2-acta and Bcl-2-cb5 protect epithelial cells from serum starvation, ceramide and taxol (Annis et al., 2001; Soucie et al., 2001). Treatment of MCF-7 cells expressing Bcl-2 mutants with either ceramide or taxol may demonstrate a difference between the mitochondrial targeted and wild type Bcl-2. The only known apoptosis stimulus not inhibitable from the mitochondria is somatostatin (Liu et al., 2000), however this effect has yet to be verified. However, MCF-7 cells require an extended period of time to die from apoptosis following serum withdrawal (W. Zhu, personal communication), making this an impractical experiment; ceramide and taxol may be more promising. The effect of targeted Bcl-XL mutants to these stimuli would also be of interest.

Apoptosis can be induced via either an intrinsic or extrinsic death receptor pathway. These two pathways can be distinguished by assaying the activities of caspase-8 and caspase-9, using fluorescent caspase substrates or by monitoring caspase cleavage. Recently W. Zhu has shown that neither caspase-8 nor caspase-9 is cleaved in vector control MCF-7 cells treated with doxorubicin (W. Zhu, personal communication). Fluorescent caspase substrates are problematic in these cells (Kottke et al., 2002). Other

techniques such as the use of inhibitors or dominant negative caspases could be investigated.

5 Appendix

5.1 Bcl-XL Polyclonal Antibody Characterization

In this study, expression of Bcl-2 and Bcl-XL was assayed by quantitative western blotting. Antibodies were also needed for immunofluorescence experiments. An antibody was already available for Bcl-2 (Zhu et al., 1996); however, an antibody to Bcl-XL was not available. To obtain protein for immunization, recombinant full length Bcl-XL was purified using the Intein Mediated Purification with an Affinity Chitin-binding Tag (IMPACT) system as described in section 2.5. Coomassie stained SDS-PAGE gels were used to document the purification steps. Most of the Bcl-XL was purified from the intein column, however, some Bcl-XL protein was present in the flow through (Figure A1). Therefore, a greater amount of chitin beads should have been used during the purification to improve the yield. By using DTT to initiate intein cleavage, conventional colourimetric tests to determine protein concentrations are not feasible. Instead, known amounts of BSA protein were loaded as standards on the same gel as the elution fractions (see Figure A2). These SDS-PAGE gels were stained with Coomassie blue and visualized on the Kodak Image Station. Net band densities were obtained and Bcl-XL protein concentrations were determined by using a BSA standard curve (see section 2.5). A total of 1.7 mg of Bcl-XL protein (> 95 % pure) was obtained from the purification procedure. Bcl-XL eluted from the chitin column (fractions from figure A1) was injected subcutaneously into SPF rabbits as described in section 2.3. Test bleeds (TB) were

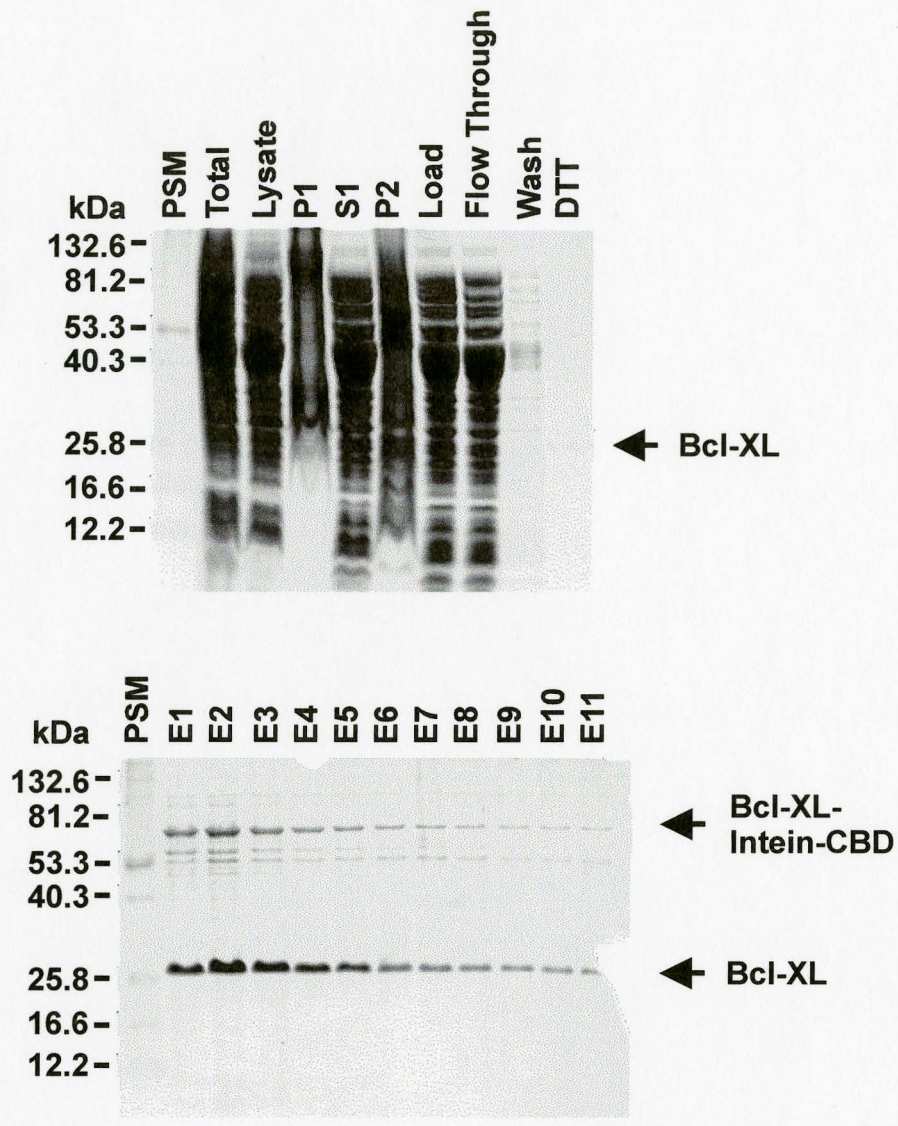

Figure A1:Full length human Bcl-XL was purified as a fusion protein using the IMPACT system. Proteins were separated by SDS-PAGE on a 10 % gel, and visualized by staining with Coomassie brilliant blue R-250. The lanes contain the following: total- total bacterial pellet lysed in 1 % SDS buffer; lysate - cell pellet was resuspended in column buffer and cells were lysed using a french press; P1 - pellet following low speed spin; S1- solubilized extract following low speed spin; P2 - pellet following high speed spin; load - solubilized extract following high speed spin; flow through - flow through from chitin column; wash - wash of chitin column with column buffer; DTT - eluate following addition of cleavage buffer; E1 to E11 - elution fractions following intein cleavage. 5.4 g of total bacterial pellet was used for the purification. Equal volumes (7.5 µl) of each fraction were loaded on each lane. The Bcl-XL-intein fusion protein is ~ 81 kDa. The sizes (in kDa) of the pre-stained markers (PSM) are indicated on the left.

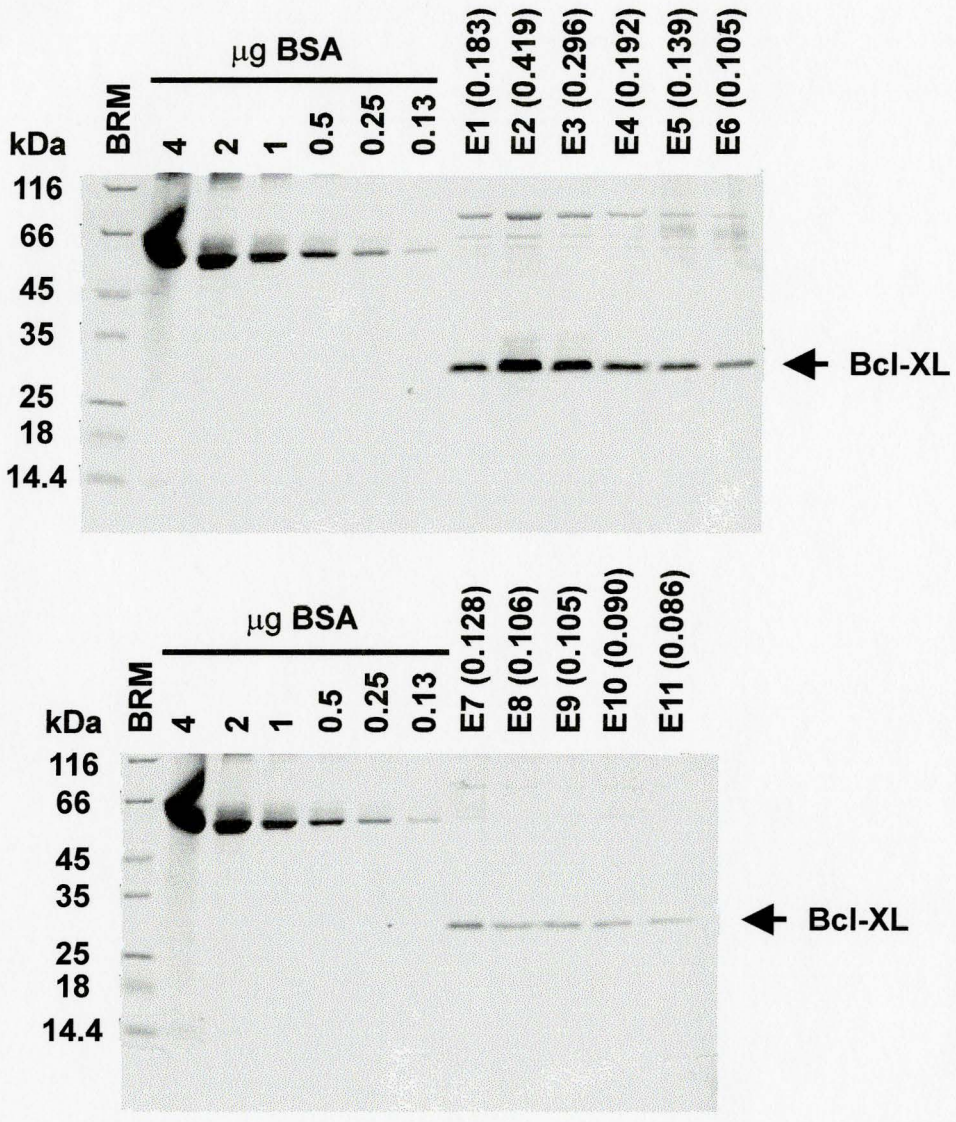

Figure A2: Measurement of Bcl-XL in elution fractions. Serial dilutions of BSA standard were loaded on the same gel as an unknown amount of Bcl-XL from an IMPACT purification (5µl each lane). The proteins were separated on a 10 % SDS-PAGE gel then stained with Coomassie blue R-250. The band densities were obtained using the Kodak Image Station and associated software. Using a standard curve from the BSA data, the amount of Bcl-XL in each elution fraction was calculated and is indicated in µg / µl above each lane. The sizes (in kDa) of the broad range markers (BRM) are indicated on the left.

taken every two weeks and assayed for Bcl-XL detection by Western blotting. The second test bleed of the rabbit named Yosemite Sam (YS TB2) was used for further Western blot experiments. Figure A3A shows the detection by Western blotting of endogenous Bcl-XL in lysates of HepG2 cells. No endogenous Bcl-XL was detected in MCF-7 cells. These results are in agreement with those previously (Takehara et al., 2001; Hsu et al., 1997a). Bcl-XL protein has also been reported in Jurkat cells (Cuvillier et al., 2000); however the detection of endogenous Bcl-XL is hampered by the large number of background bands in this lane. The16 kDa band in Figure A3A may be Bcl-XS (Boise et al., 1993), or the product of an internal initiation of Bcl-XL at met45 (Clem et al., 1998). However, since an appropriate size marker was not available the identity of this faster migrating species is uncertain. YS TB2 is also suitable for the detection endogenous Bcl-XL in rat and mouse kidney tissues (see Figure A3C). However, due to low signal, this is not an ideal antibody to detect mouse or rat Bcl-XL. The protein results are consistent with Northern blots of mouse tissues (Gonzalez-Garcia et al., 1994). Takahashi *et al.* have also found significant amounts of Bcl-XL protein in adult mouse germinal centres (Takehara et al., 2001), however, a band corresponding to the correct size of Bcl-XL was not found in rat spleen (see Figure A3C). Interspecies differences could account for differences in Bcl-XL expression. YS TB8 was also tested for detection of Bcl-XL protein on Western blots, and does detect Bcl-XL protein exogenously expressed

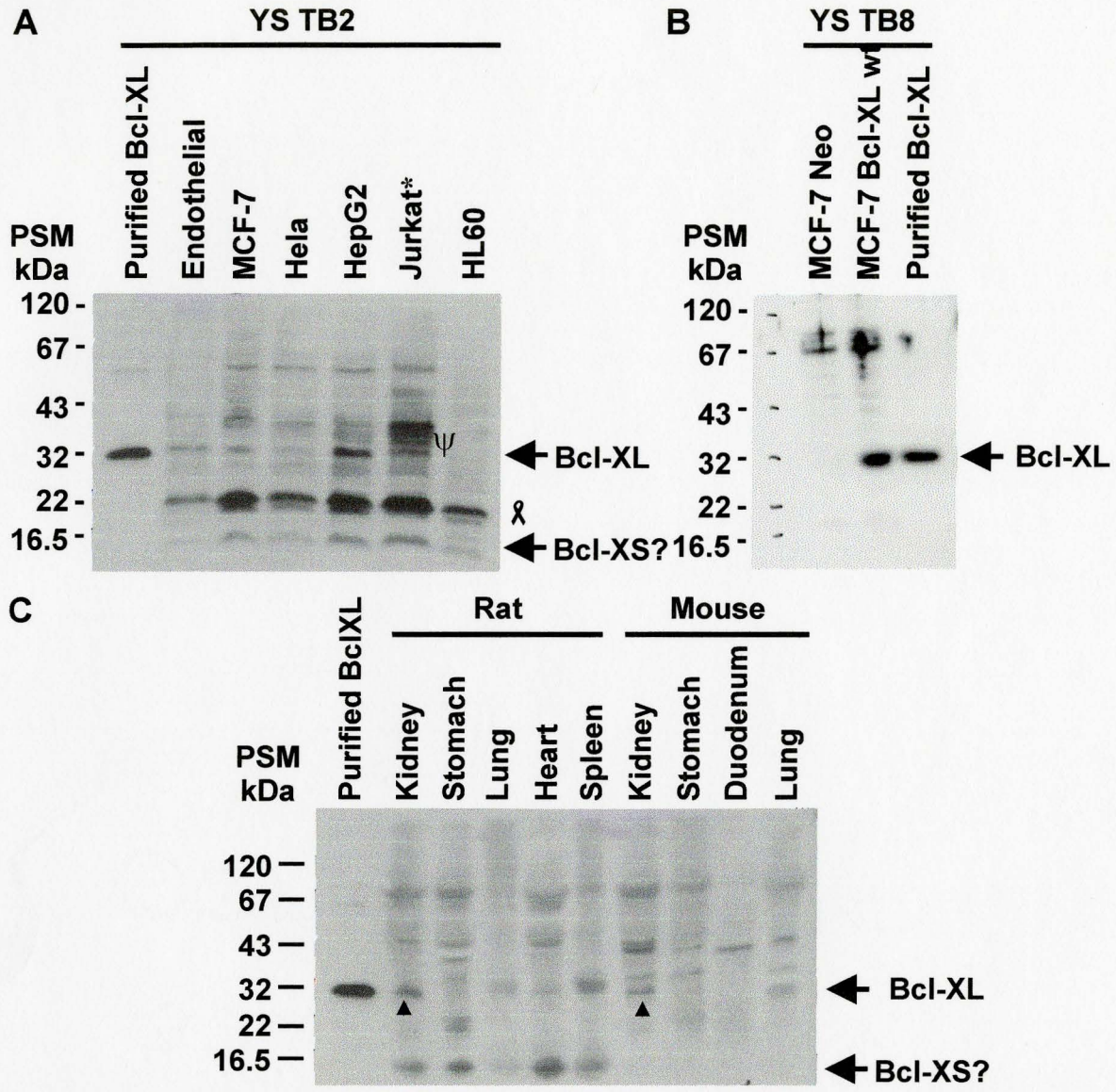

Figure A3: Detection of endogenous Bcl-XL. A) Cultured cells. 40 µg of total cell protein of each tissue cell culture lysate was loaded per lane, except Jurkat cells (*) where only 30 µg total cell protein was loaded, and assayed for Bcl-XL protein expression using the YS TB2 antibody. Only HepG2 cells contain significant amounts of Bcl-XL protein. The identity of the band from Jurkat cells is unknown (ψ). The identity of the 20 kDa band is unknown ( ). B) Cultured Cells. 5 µg of total cell protein was loaded per lane and assayed using the YS TB8 Bcl-XL antibody. No Bcl-XL was detected in the MCF-7 Neo cells. The antibody does detect Bcl-XL in the MCF-7 Bcl-XL wt cell line as well as purified Bcl-XL. C) Adult rat and mouse tissues. An aliquot containing 50 µg of total cell protein of the rat and mouse tissue lysates was loaded per lane and Bcl-XL expression monitored using the YS TB2 Bcl-XL antibody. Among the lysates from rat and mouse tissues, Bcl-XL was only detected in significant amounts in rat and mouse kidney tissues (▲). Purified Bcl-XL was used as a size marker for comparisons with the lysates.

in MCF-7 cells (see Figure A3B). No endogenous Bcl-XL protein was detected in MCF-7 Neo cells; and no 16 kDa band was seen (see Figure A3A). As these antibodies are derived from different bleeds of the same rabbit, it is possible that the later bleed (TB8) has an increased specificity for Bcl-XL and therefore could display less cross-reactivity.

Immunoprecipitation was used as a rapid screen for the suitability of the antibodies for use in immunofluorescence. While efficient immunoprecipitation does not ensure an antibody will work for immunofluorescence, it is very rare for an antibody that dose not work well for immunoprecipitation to work in immunofluorescence. YS TB2 and YS TB8 were tested for immunoprecipitation of Bcl-XL synthesized in the reticulocyte lysate system (see Figure A4). Both antibodies bound ^{35}S methionine labelled Bcl-XL protein. The decreased intensity of the Bcl-XL band obtained when 1 µl of the antibody added to 9 µl of reticulocyte lysate (when compared to 0.5 µl of antibody added to 9.5 µl of reticulocyte lysate) is most likely due to an increased amount of total protein in the 0.5 µl sample. The decreased intensity obtained from using 1µl of antibody was repeatable. No bands were visible when pre-immune serum was used. Both antibodies detected a minor amount of another species at approximately 20 kDa. It is likely that both antibodies could still be further optimized for use in immunoprecipitations. YS TB8 was chosen for use in immunofluorescence since there appeared to be negligible differences between the antibodies in the amount of background bands in the immunoprecipitations. The YS TB2 antibody could therefore be spared for Western blotting.

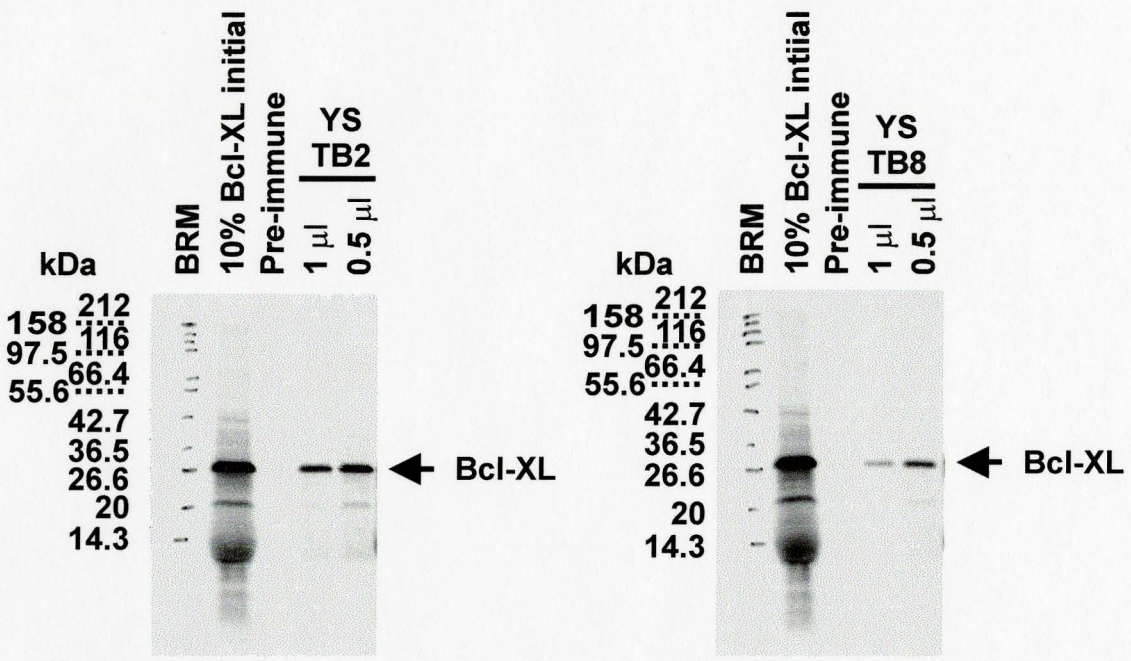

Figure A4: Bcl-XL polyclonal antibodies bind to Bcl-XL translated *in vitro*. Plasmid 1175 (pSPUTK Bcl-XL-wt) was transcribed and translated *in vitro* in a rabbit reticulocyte transcription/translation system using ^{35}S methionine as a radioactive label. Bcl-XL protein was immunoprecipitated using YS TB2, YS TB8 and pre-immune serum.

5.2 Validation of the Quantitative Western Blotting Procedure

Prior to analysing doxorubicin treated lysates for PARP cleavage and degradation, the assay had to be tested to ensure that measurements were reproducible within a gel as well as between gels (see Figure A5). Sample lysates from Bcl-XL nt cells treated with either 2.5 or 80 μM doxorubicin were loaded on three different positions on an SDS-PAGE gel and resolved (a, b and c) (see Figure A5A). There is at most a 10 % difference in PARP cleavage and degradation between measurements of the same sample loaded on different areas of a gel. To determine the amount of variability of the amount of Bcl-XL protein in a gel, sample lysates were compared to the lysates of cells grown in estrogen-free medium for Bcl-XL expression on the same gel (positions a, b and c) (see Figure A5B). Having previously determined the amount of Bcl-XL in cells grown in estrogen-free medium, determination of Bcl-XL in the doxorubicin-treated samples is a ratio of doxorubicin sample: estrogen free sample (see section 2.11.4). Due to an error associated with measurements of Bcl-XL in the estrogen-free sample, each separate sample (a, b and c) also has an error. The error bars in the average accounts for this and are therefore the sums of the errors in each sample (propagation of error). There is a small degree of variability in Bcl-XL-nt expression on a blot (0.4 ± 0.2 ng Bcl-XL protein or ± 50 %) (see Figure A5B, compare figure A5A with A5C and figure A5B with A5D). As expected, the amount of variability between gels is higher than within a gel (see Figure A5C and D). The reproducibility of PARP degradation and cleavage is better at higher than lower doxorubicin doses (see Figure A5C). This is reflected in the error

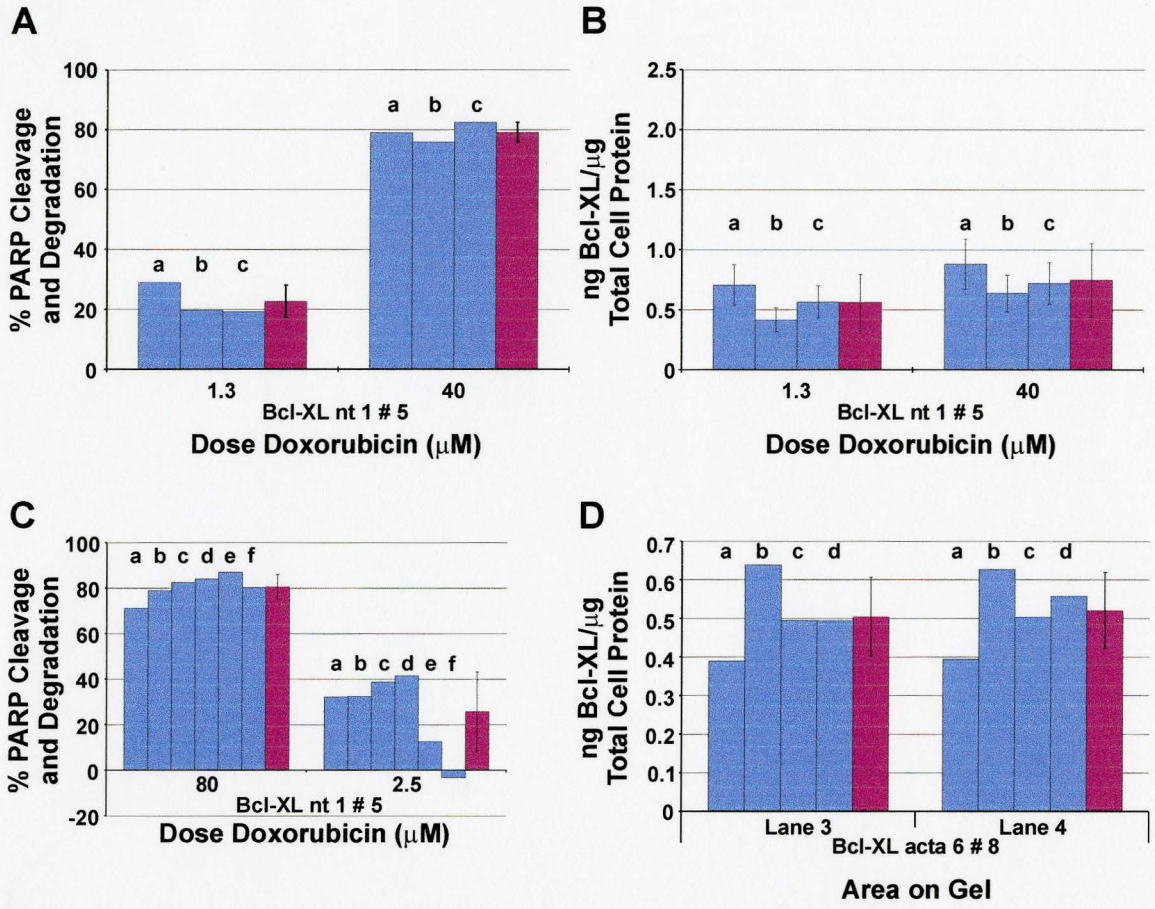

Figure A5: Reproducibility of % PARP cleavage and degradation, and exogenous Bcl-XL expression within and between SDS-PAGE gels. Blots were prepared as described in section 2.10 and optical density measurements obtained using the Kodak Image Station and software. Percent PARP cleavage and degradation and absolute Bcl-XL expression were calculated as described in section 2.11. A) Within a gel there is approximately a 10 % variation in % PARP cleavage and degradation and a B) 0.4 ± 0.2 ng difference in absolute Bcl-XL measurements. Both samples, MCF-7 cells expressing Bcl-XL nt treated with either 1.4 and 40 μM of doxorubicin were loaded on the same gel in three different areas (a, b and c). The final bar indicates the average of the three samples. In both graphs, error bars are standard deviation. The error bar on the averaged sample has been corrected for propagation of error. C) Between gels there is a very high degree of reproducibility in the higher doses of doxorubicin for % PARP cleavage and degradation. There is less reproducibility at lower doxorubicin doses. All bars represent the same sample resolved on the same position of 6 different gels (a, b, c, d, e and f). The following samples were resolved at the same time: a/b, c/d and e/f. D) For Bcl-XL expression reproducibility between four gels, the amount of Bcl-XL expression is 0.50 ± 0.1 and 0.51 ± 0.1 ng Bcl-XL for lanes 3 and 4 respectively. The bars represent the same sample resolved on the same position of 4 different gels (a, b, c, and d). Lanes 3 and 4 described above are adjacent to one another.

bars of the sample lysates in Figures 11 - 14. The variability of Bcl-XL measurements is low, 0.5 ± 0.1 ng Bcl-XL protein / μg total cell protein (or ± 20 %), between the same sample loaded on 4 different gels at the same position (see Figure A5D). Bcl-XL-acta is the lowest expressing cell line and therefore ± 0.1 ng difference is just outside of the error associated with the average expression in most cell lines (see Table 7). Since ± 0.1 ng is the standard deviation of one sample, the error will be larger when many independent samples are assayed.

Another possible source of variation is the operation of the Kodak Image Station used to acquire net intensity readings. Sample lysates of vector control cells were resolved by SDS-PAGE and probed for either PARP or actin. The same gel was then analysed using the Kodak Image Station and a net intensity reading taken three times (see Figure A6). The percent variability is 5 - 10 % for PARP cleavage and degradation, and a 0.2 band intensity unit difference in the ratio of actin readings.

5.3 Western Blots and Cellular Morphology

Sample western blots are provided of both the Bcl-2 mutant cell lines (see Figure A7) and the Bcl-XL mutant cell lines (see Figure A8). The notation "A10" indicates that the cells from which the lysate was made were treated with 10 μM doxorubicin. The "A" or "B" preceding the dose of doxorubicin denotes two different samples for the same experiment.

Sample micrographs are provided of the differentially targeted Bcl-2 (see

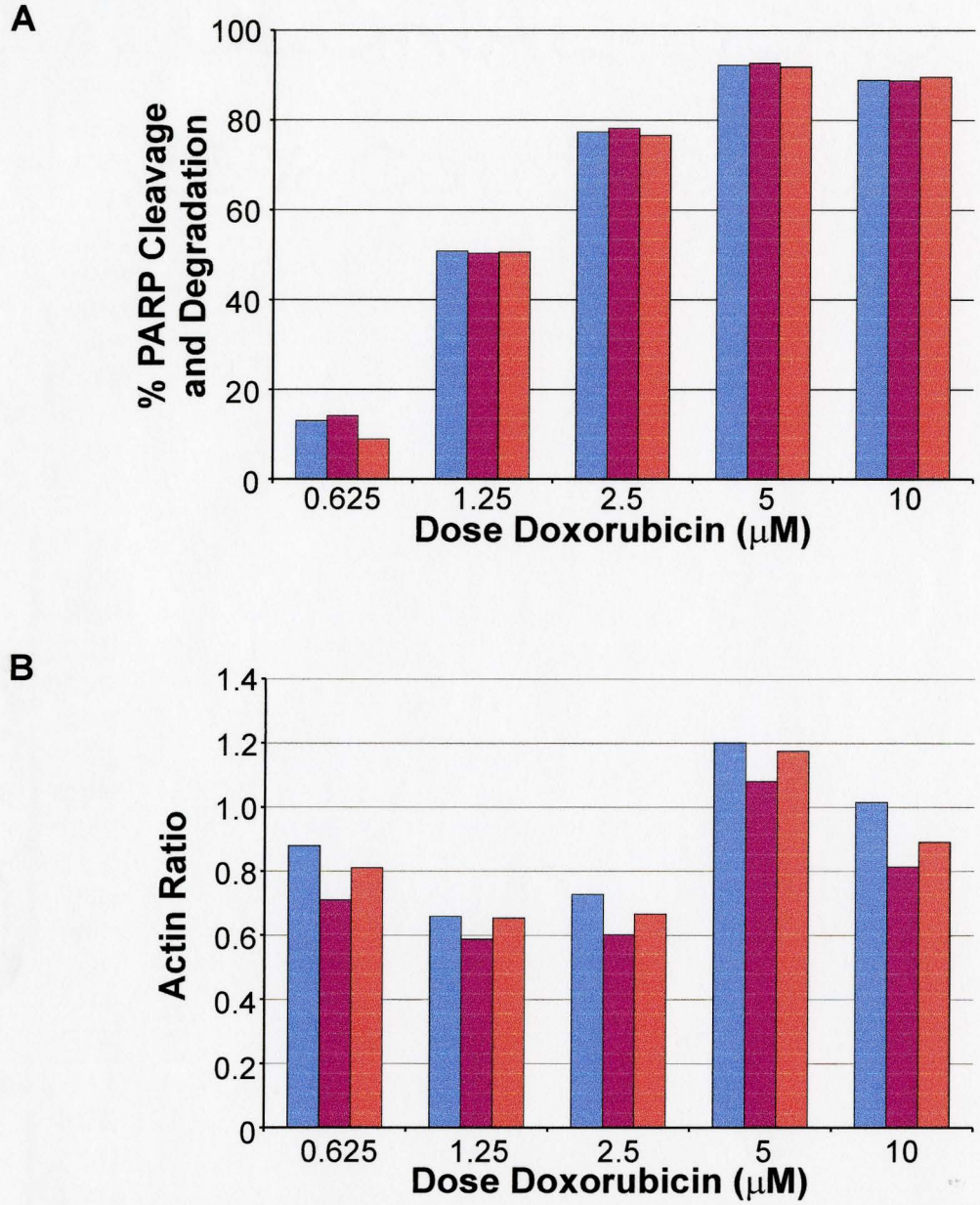

Figure A6: Reproducibility (by Kodak Image Station software analysis) A) PARP cleavage and degradation and B) determination of actin ratio in vector control cells. A total of 5 μg (PARP) or 1 μg (actin) total cell protein was separated on a 10 % tricine SDS-PAGE gel and transferred to either a PVDF or nitrocellulose membrane, respectively. Blots were prepared as described in section 2.10 and optical density measurements obtained using the Kodak Image Station system and software. Each colour bar represents different band intensity measurements taken of three separate Western blots at three separate occasions of the same sample resolved on the same SDS-PAGE gel. PARP cleavage and degradation and actin ratios were calculated as described in section 2.11.

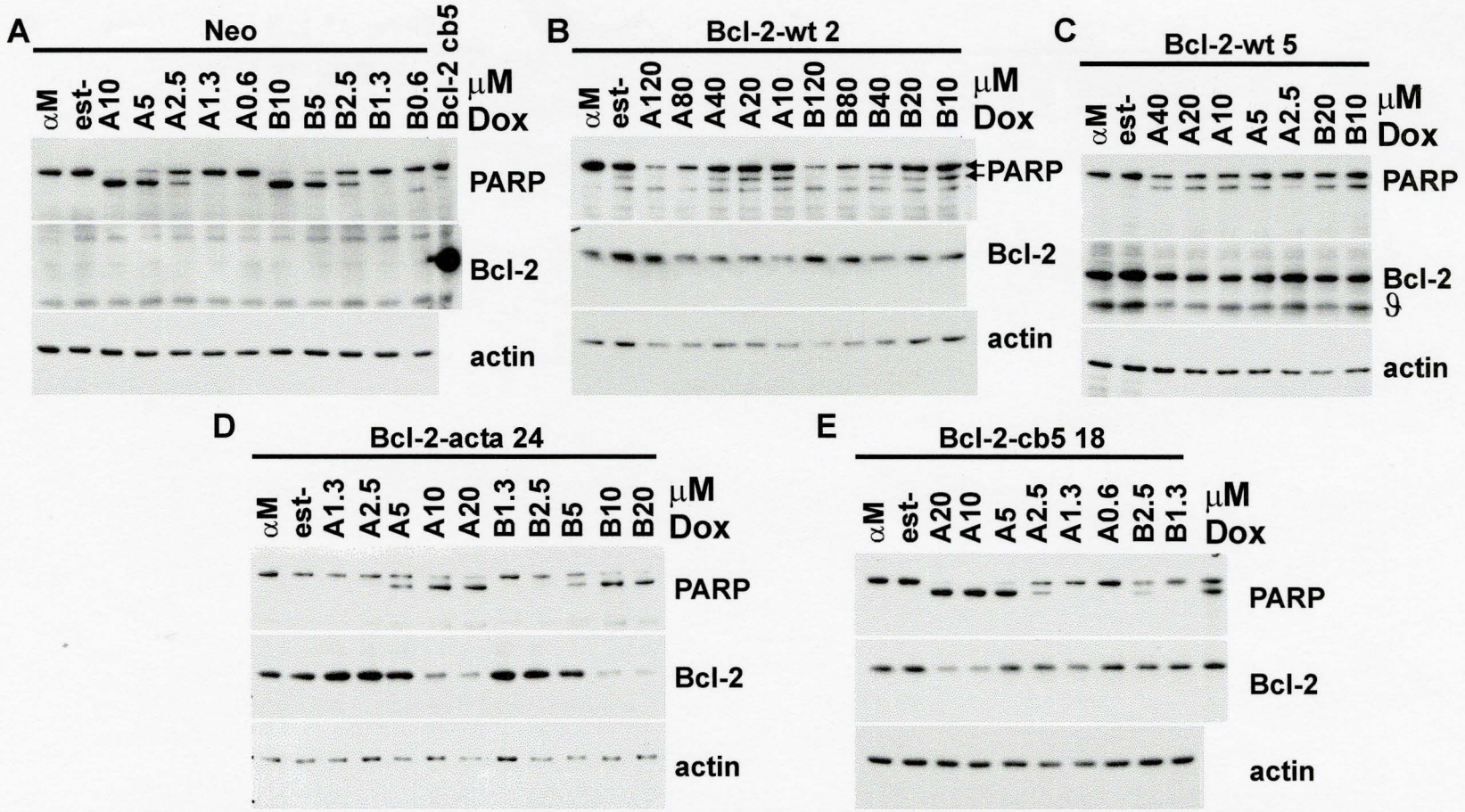

Figure A7: Sample Western blots detecting PARP, Bcl-2 and actin in the Bcl-2 cell lines used in this study following 6 days of growth in estrogen free media. Cells were treated with the dose of doxorubicin indicated for 48 hours. The letters "A" and "B" preceding the dose denotes two identical samples treated with the same dose of doxorubicin in the same experiment. Bcl-2-cb5 18 cells treated with 2.5 μM doxorubicin for 48 hours represent a positive control for PARP cleavage and the presence of Bcl-2. A) Neo (pRcCMV vector), B) Bcl-2-wt 2, C) Bcl-2-wt 5, D) Bcl-2-acta 24 and E) Bcl-2-cb5 18 cell lines. The specificity of the antibody used to develop the blot is shown on the right. An unknown cross-reacting band (ϑ) was sometimes visible on Bcl-2 blots, however, the presence of this band was not always reproducible.

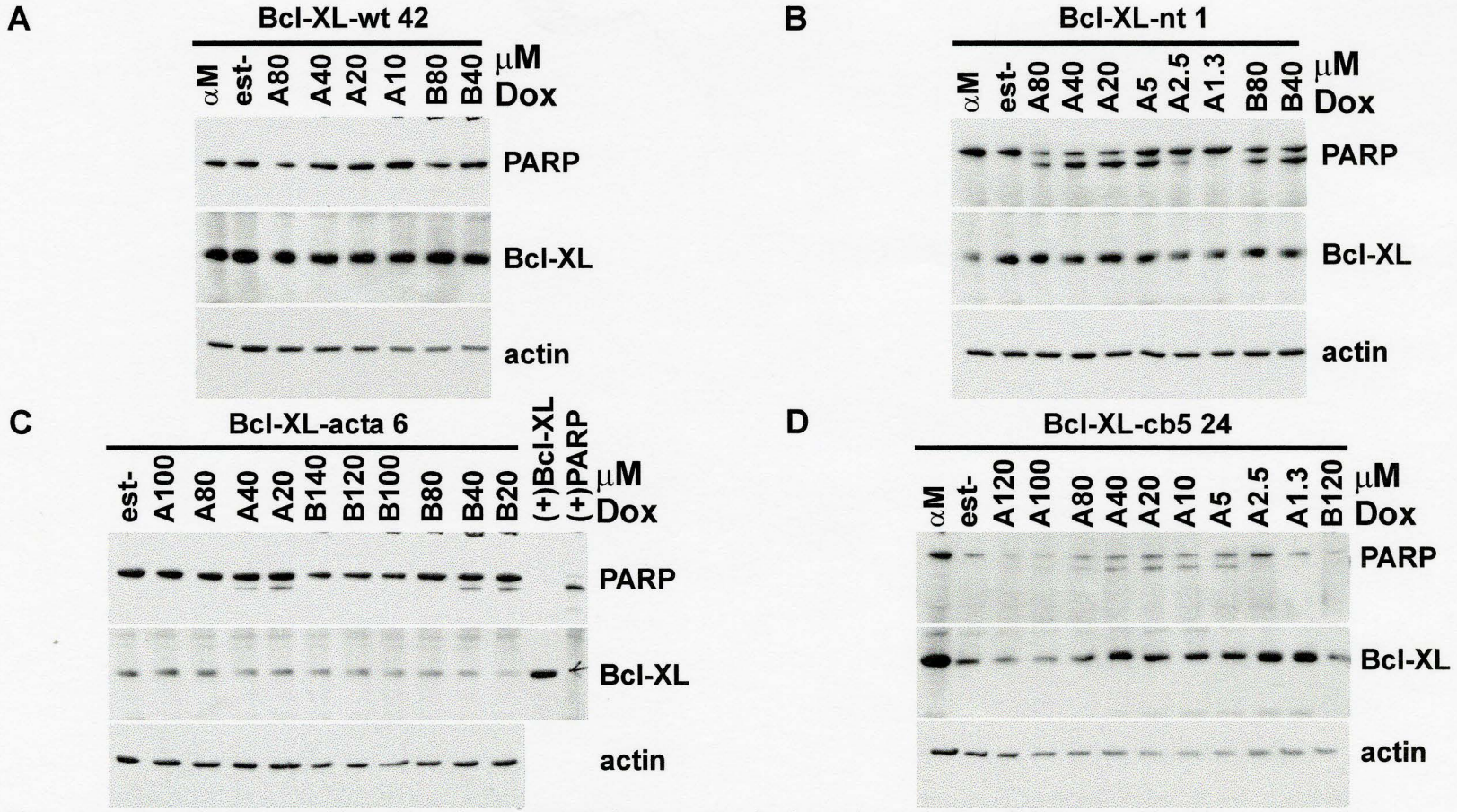

Figure A8: Sample Western blots detecting PARP, Bcl-XL and actin from the Bcl-XL cell lines used in this study. Cells were treated with the dose of doxorubicin indicated for 48 hours following 6 days of growth in estrogen free media. The letters "A" and "B" preceding the dose denote two identical samples treated with the same dose of doxorubicin in the same experiment. The (+)PARP sample are Neo cells treated with 2.5 μM doxorubicin for 48 hours, and represents a positive control for PARP cleavage. The presence of Bcl-XL was compared to purified Bcl-XL protein resolved on the same gel ((+)Bcl-XL). A) Bcl-XL-wt 42, B) Bcl-XL-nt 1, C) Bcl-XL-acta 6 and D) Bcl-XL-cb5 24 cell lines. The specificity of the antibody used to develop the blot is shown on the right.

Figure A9) and Bcl-XL (see Figure A10) cell lines treated with doses of doxorubicin at and above the EC_{50}. These show the changes in cellular morphology that accompanies doxorubicin treatment at doses below, at and above the EC_{50}.

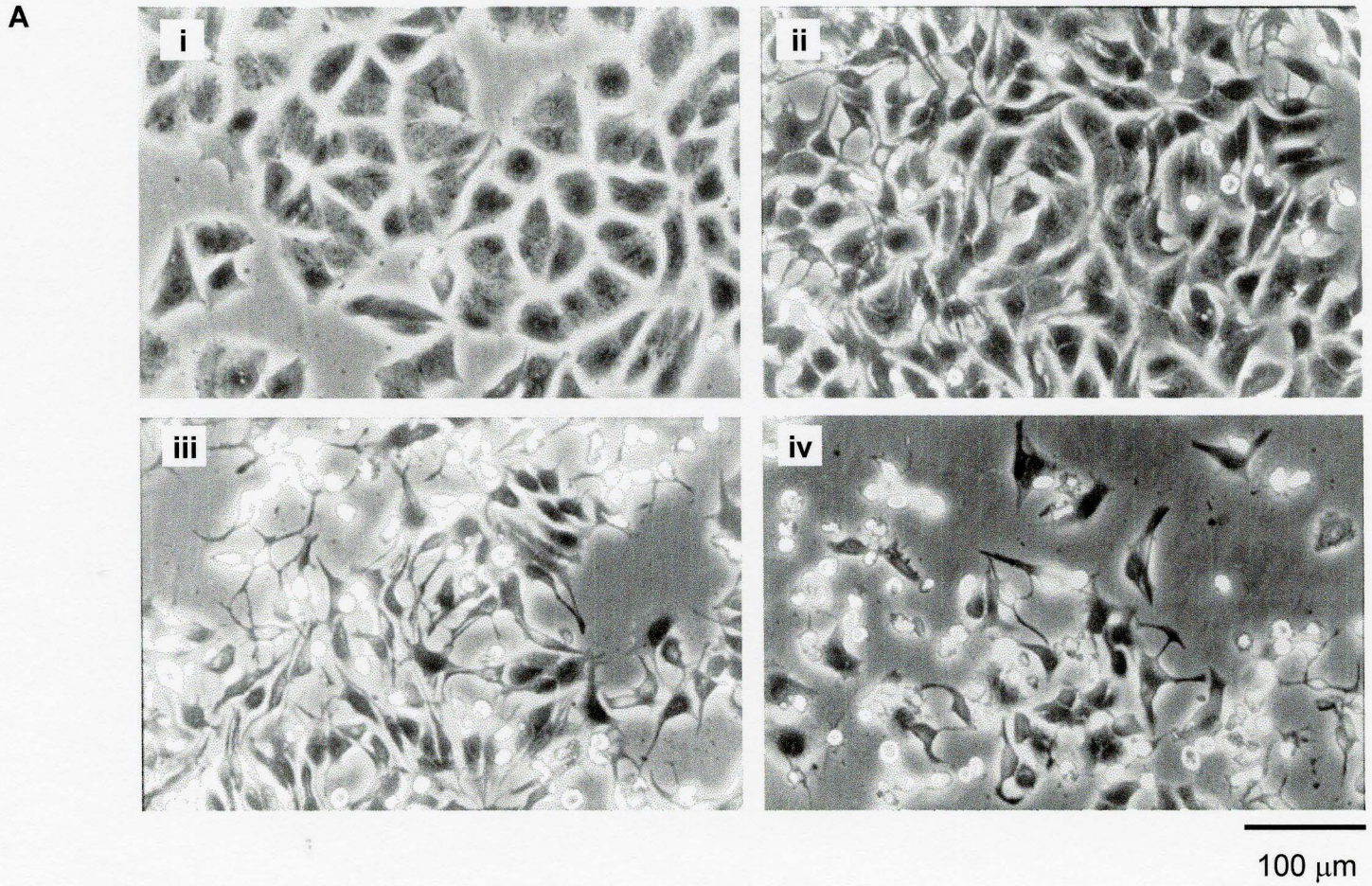

Figure A9: Micrographs of MCF-7 cell lines. A) MCF-7 cells, Neo, i) untreated, ii) 0.6 μM, iii) 1.3 μM and iv) 2.5 μM doxorubicin for 48 hours. Photos were taken on an inverted microscope.

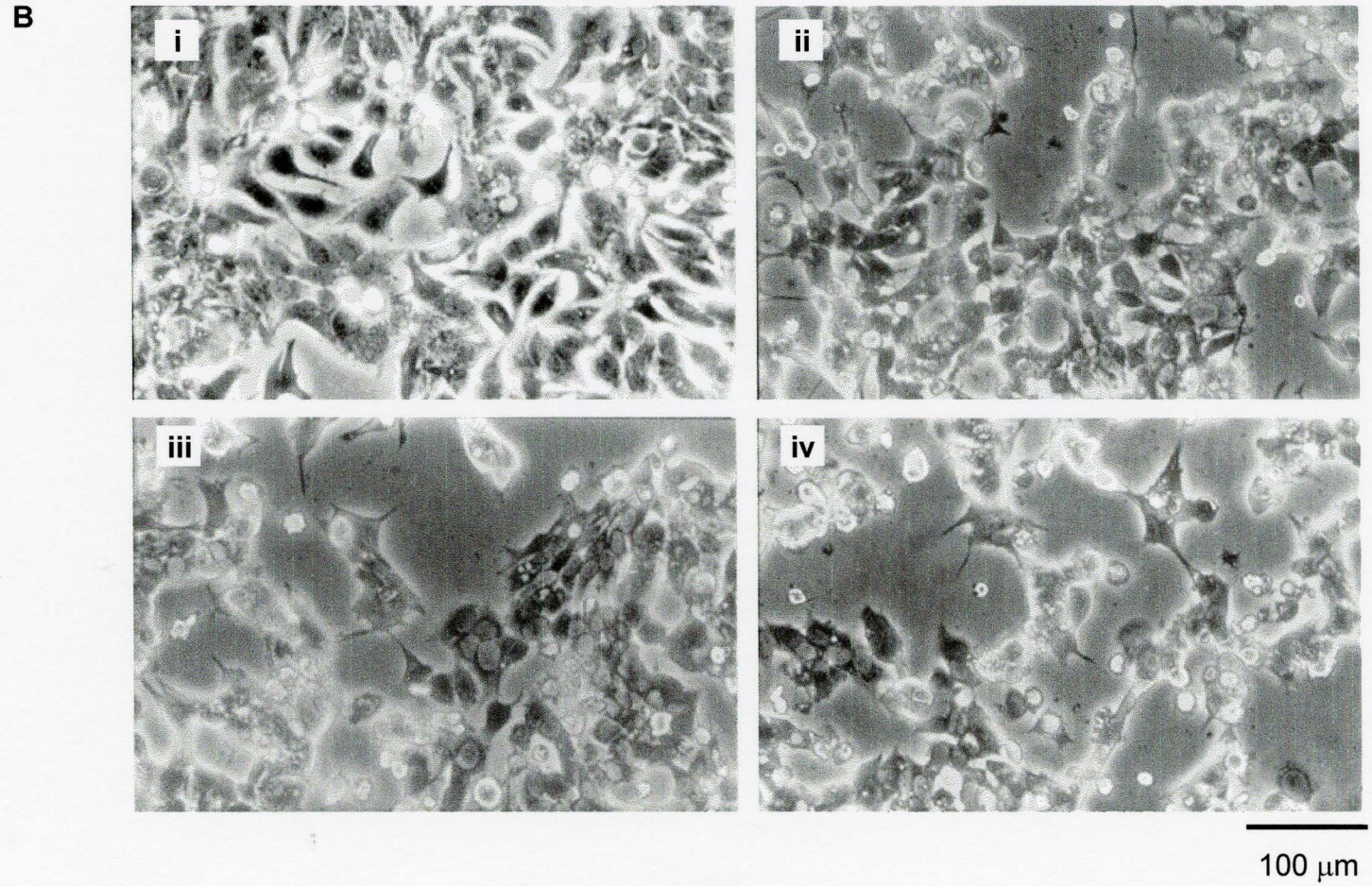

Figure A9 (con't): Micrographs of MCF-7 cell lines. B) MCF-7 cells, Bcl-2-wt 2, i) untreated, ii) 10 μM, iii) 20 μM and iv) 40 μM doxorubicin for 48 hours. Photos were taken on an inverted microscope.

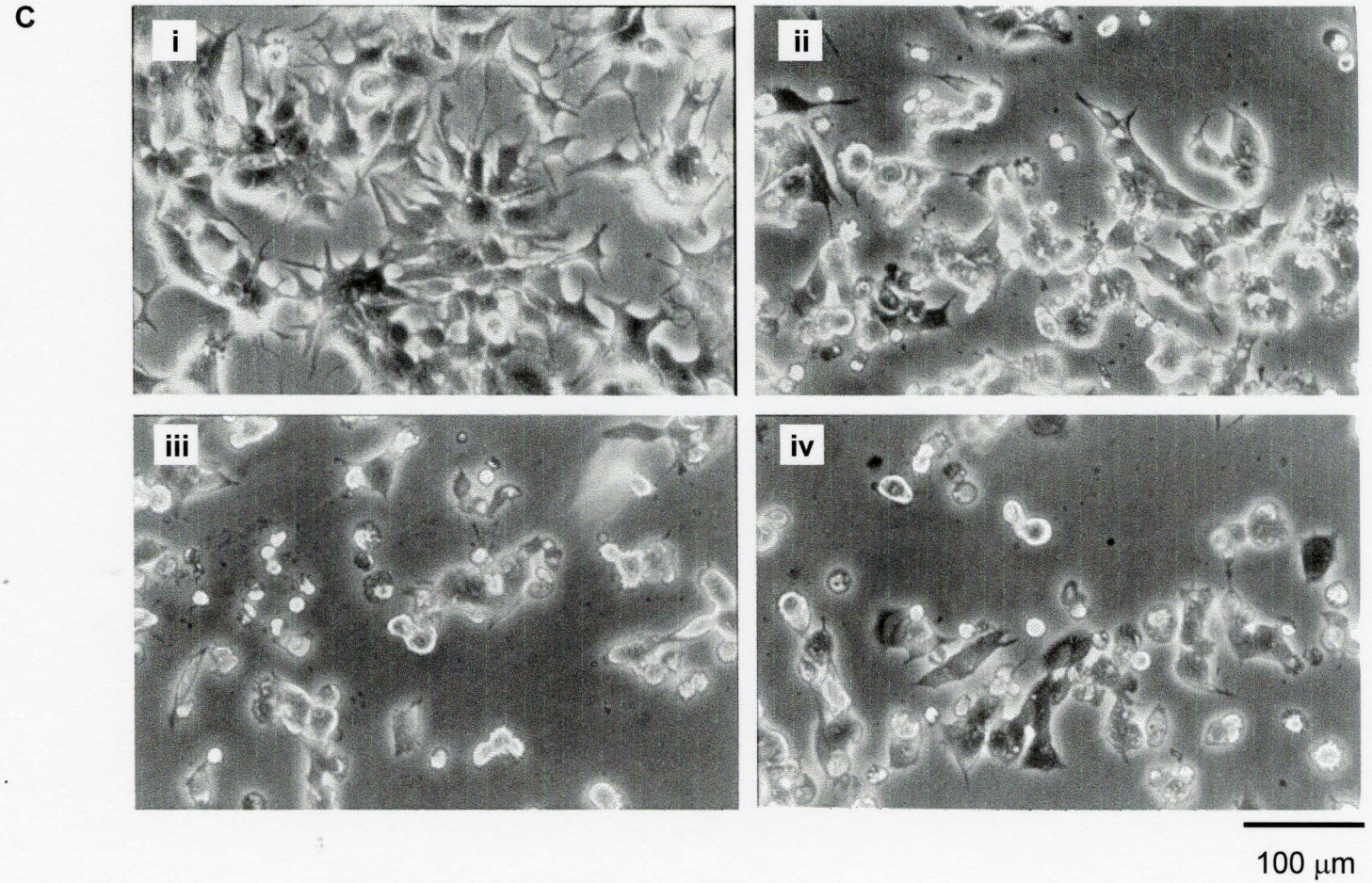

Figure A9 (con't): Micrographs of MCF-7 cell lines. C) MCF-7 cells, Bcl-2-wt 5, i) untreated, ii) 10 μM, iii) 20 μM and iv) 40 μM doxorubicin for 48 hours. Photos were taken on an inverted microscope.

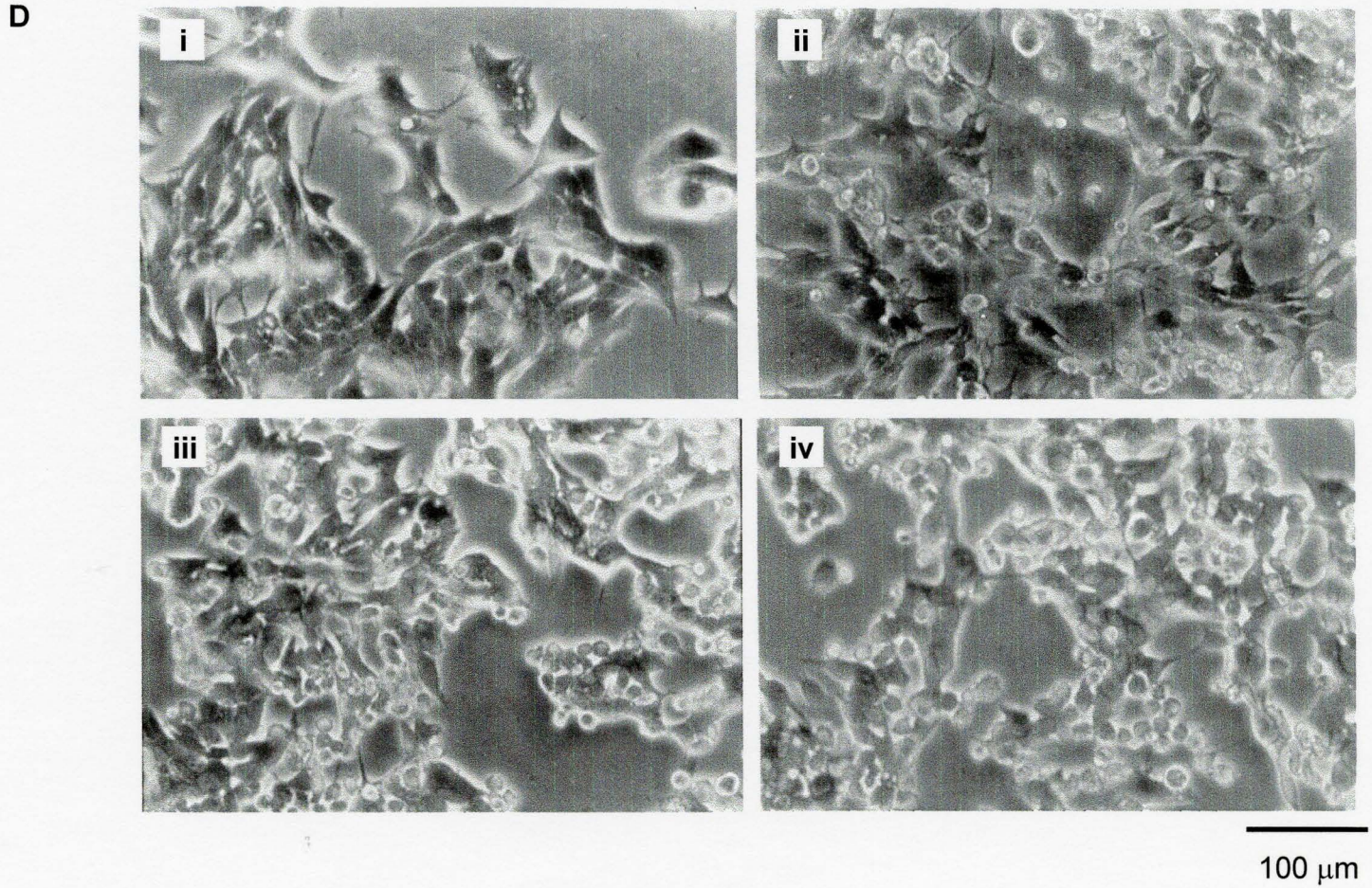

Figure A9 (con't): Micrographs of MCF-7 cell lines. D) MCF-7 cells, Bcl-2-acta 24, i) untreated, ii) 5 μM, iii) 10 μM and iv) 20 μM doxorubicin for 48 hours. Photos were taken on an inverted microscope.

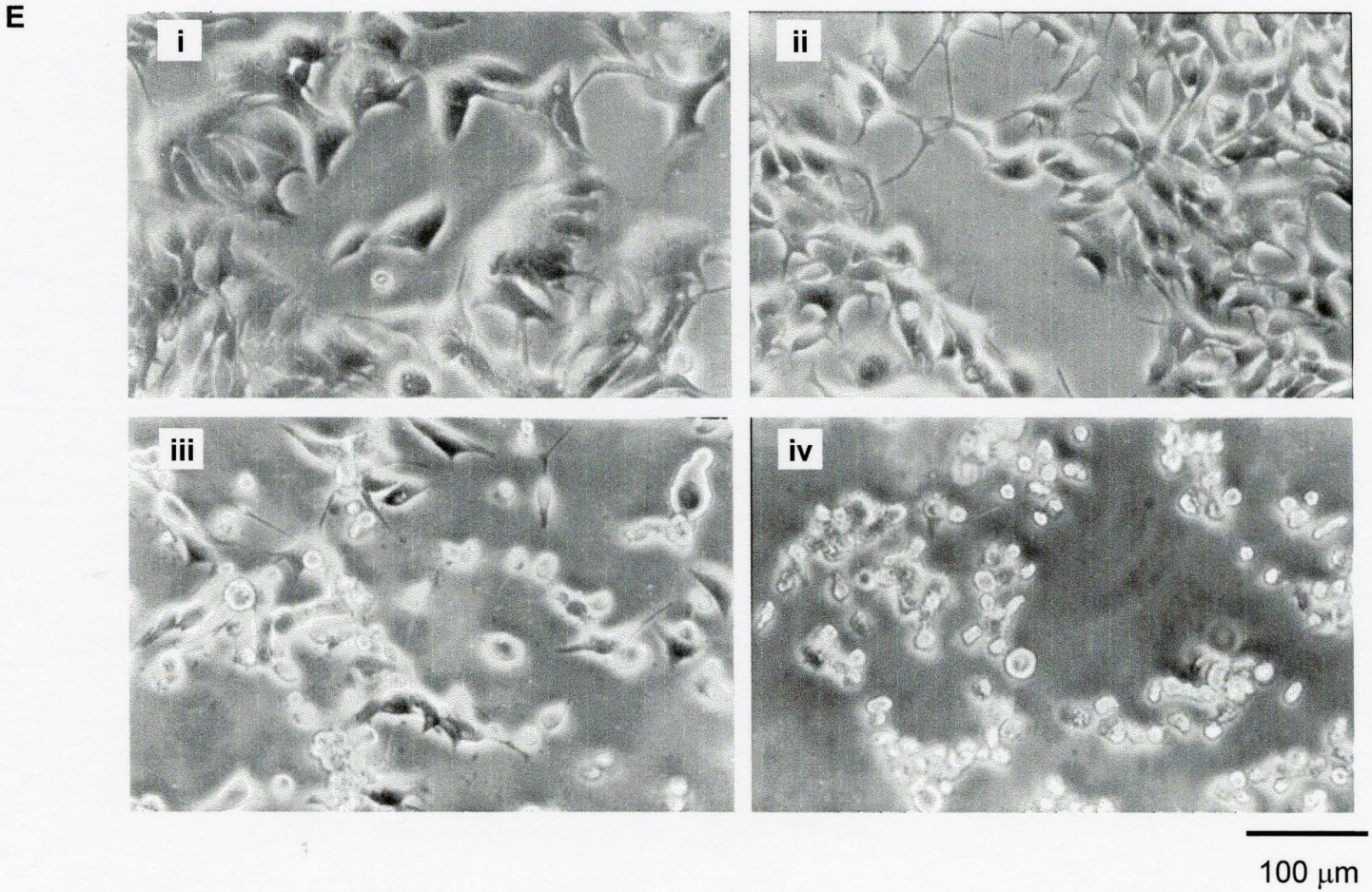

Figure A9 (con't): Micrographs of MCF-7 cell lines. E) MCF-7 cells, Bcl-2-cb5 18, i) untreated, ii) 1.3 μM, iii) 2.5 μM and iv) 5 μM doxorubicin for 48 hours. Photos were taken on an inverted microscope.

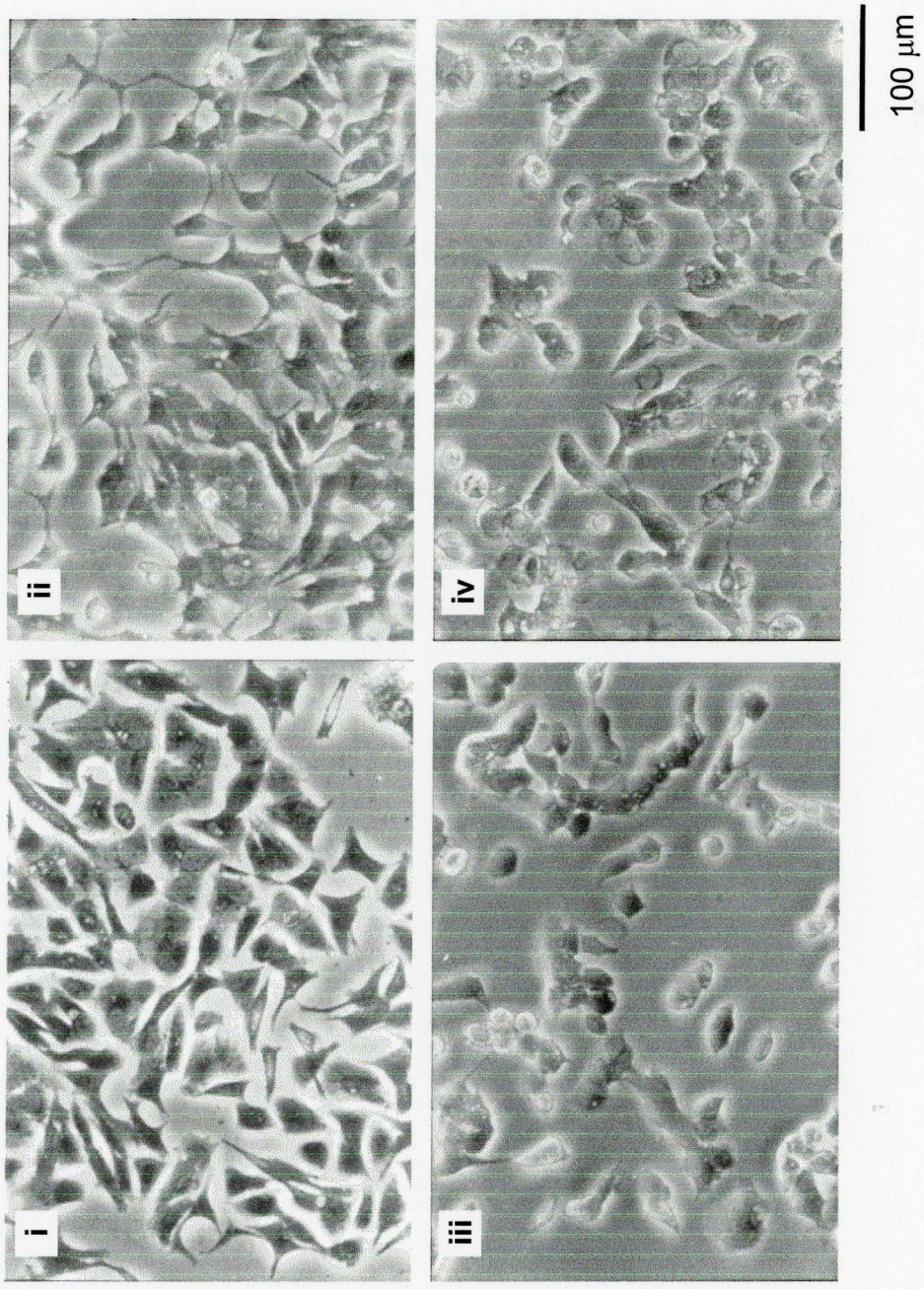

Figure A10: Micrographs of MCF-7 cell lines. A) MCF-7 cells, Bcl-XL-wt 42, i) untreated, ii) 20 µM, iii) 80 µM and iv) 100 µM doxorubicin for 48 hours. Photos were taken on an inverted microscope.

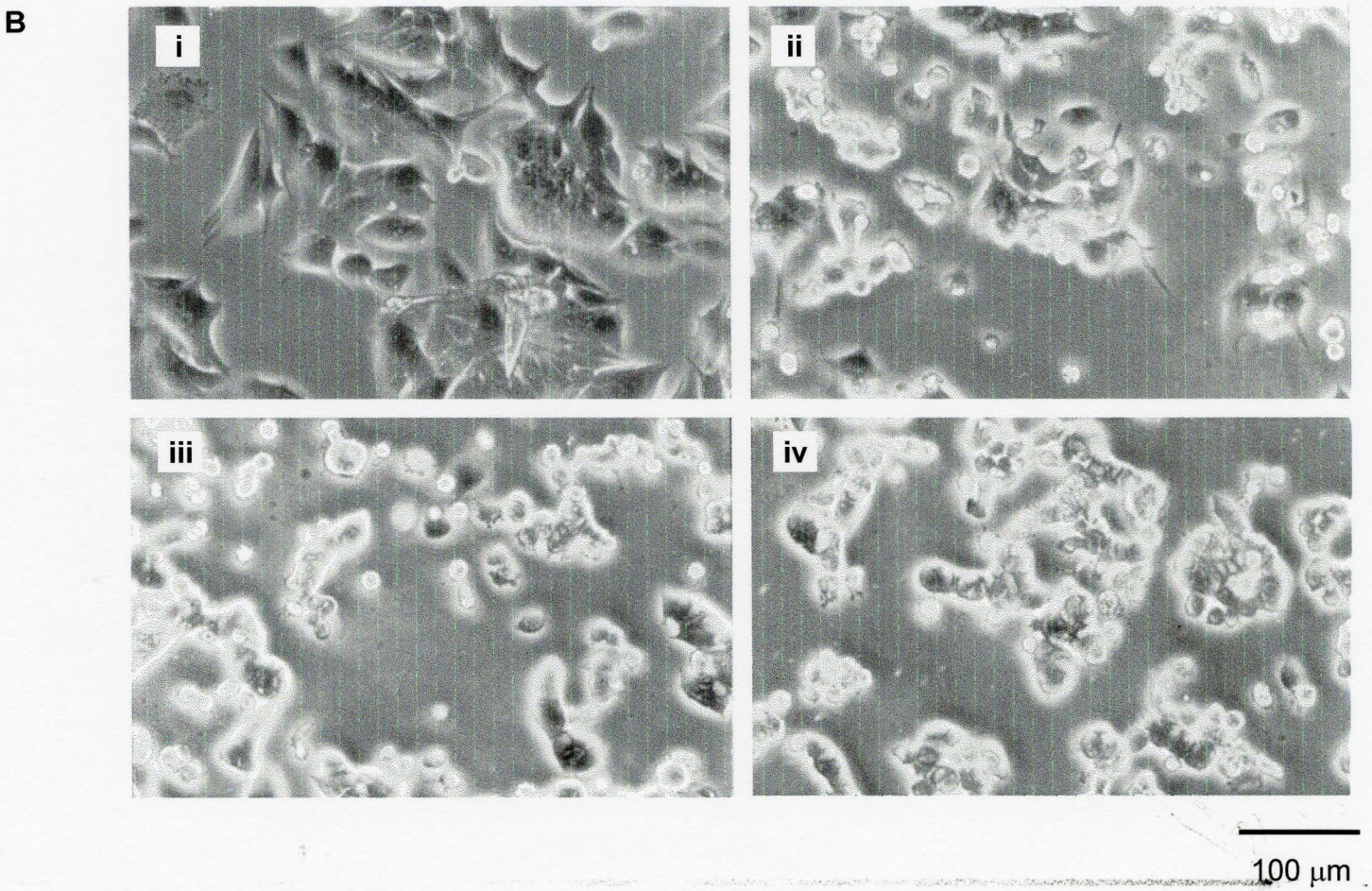

Figure A10 (con't): Micrographs of MCF-7 cell lines. B) MCF-7 cells, Bcl-XL-nt 1, i) untreated, ii) 5 µM, iii) 10 µM and iv) 20 µM doxorubicin for 48 hours. Photos were taken on an inverted microscope.

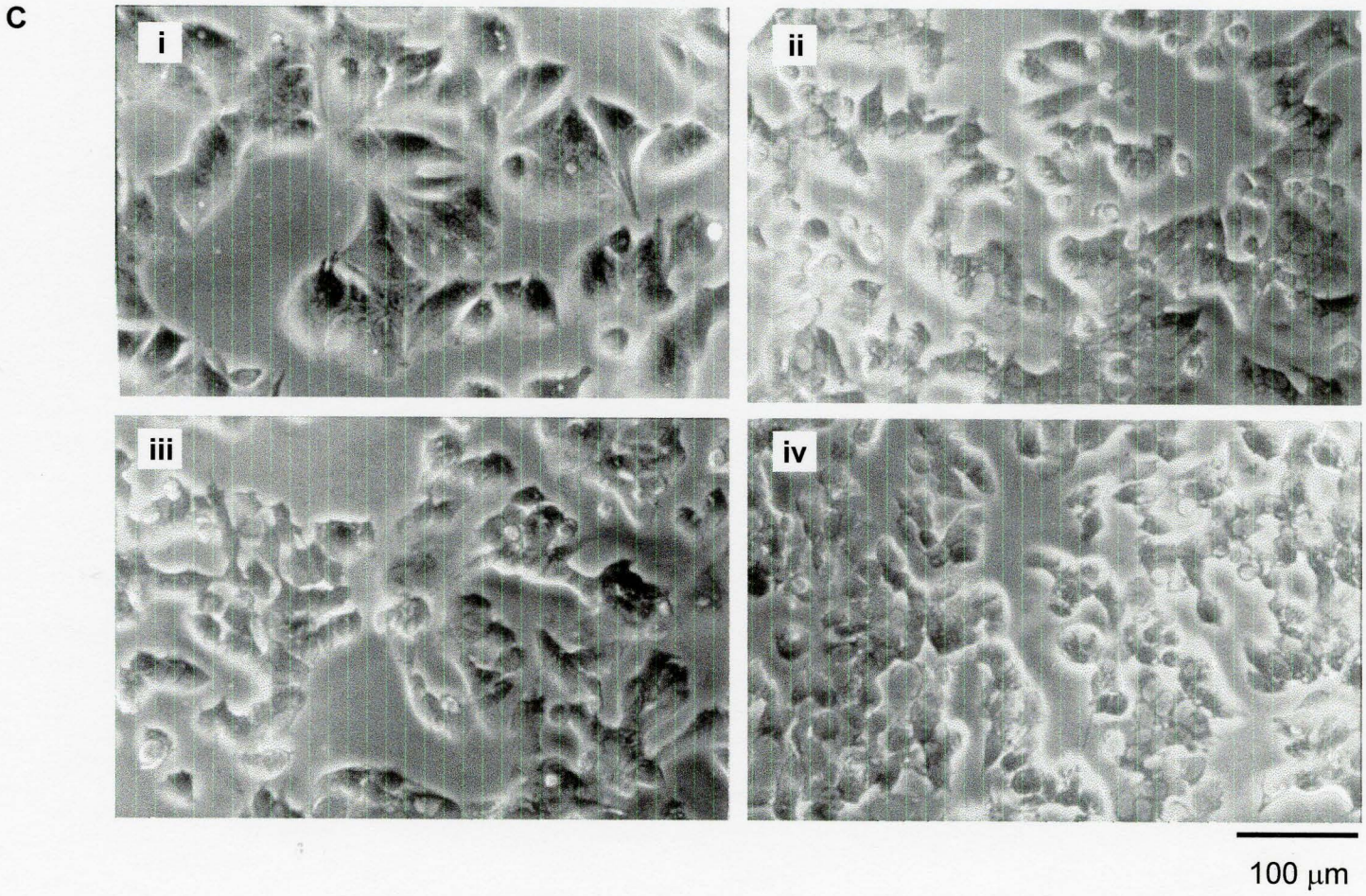

Figure A10 (con't): Micrographs of MCF-7 cell lines. C) MCF-7 cells, Bcl-XL-acta 6, i) untreated, ii) 40 μM, iii) 80 μM and iv) 100 μM doxorubicin for 48 hours. Photos were taken on an inverted microscope.

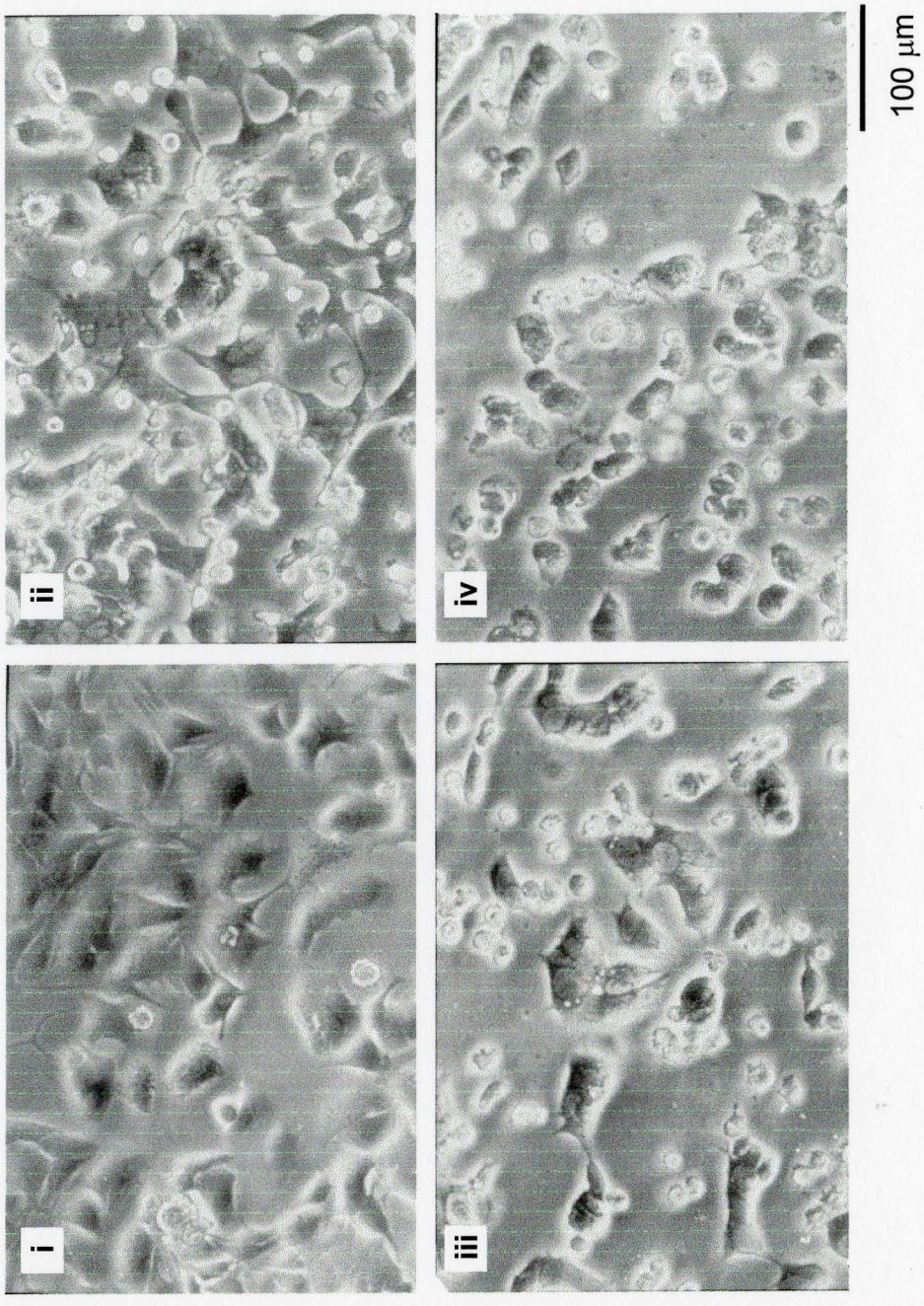

Figure A10 (con't): Micrographs of MCF-7 cell lines. D) MCF-7 cells, Bcl-XL-cb5 24, i) untreated, ii) 20 µM, iii) 40 µM and iv) 80 µM doxorubicin for 48 hours. Photos were taken on an inverted microscope.

6 Reference List

Abbas, A.K., Lichtman, A.H., and Pober, J.S. **Cellular and Molecular Immunology: Fourth Edition**. Toronto: W.B. Saunders Company, 2000.

Adams, J.M. and Cory, S. (1998). The Bcl-2 protein family: arbiters of cell survival. Science *281*, 1322-1326.

Annis, M.G., Zamzami, N., Zhu, W., Penn, L.Z., Kroemer, G., Leber, B., and Andrews, D.W. (2001). Endoplasmic reticulum localized Bcl-2 prevents apoptosis when redistribution of cytochrome c is a late event. Oncogene *20*, 1939-1952.

Antonsson, B., Montessuit, S., Sanchez, B., and Martinou, J.C. (2001). Bax is present as a high molecular weight oligomer/complex in the mitochondrial membrane of apoptotic cells. J.Biol.Chem. *276*, 11615-11623.

Aritomi, M., Kunishima, N., Inohara, N., Ishibashi, Y., Ohta, S., and Morikawa, K. (1997). Crystal structure of rat Bcl-xL. Implications for the function of the Bcl-2 protein family. J.Biol.Chem. *272*, 27886-27892.

Atkinson, H. M. (2001) A Fluorescence-Based Method for Studying the Membrane Topology of the Anti-Apoptotic Protein Bcl-XL. McMaster University. Ref Type: Thesis/Dissertation

Bahia, H., Ashman, J.N., Cawkwell, L., Lind, M., Monson, J.R., Drew, P.J., and Greenman, J. (2002). Karyotypic variation between independently cultured strains of the cell line MCF-7 identified by multicolour fluorescence in situ hybridization. Int.J.Oncol. *20*, 489-494.

Boise, L.H., Gonzalez-Garcia, M., Postema, C.E., Ding, L., Lindsten, T., Turka, L.A., Mao, X., Nunez, G., and Thompson, C.B. (1993). bcl-x, a bcl-2-related gene that functions as a dominant regulator of apoptotic cell death. Cell *74*, 597-608.

Bovia, F., Nabili-Tehrani, A.C., Werner-Favre, C., Barnet, M., Kindler, V., and Zubler, R.H. (1998). Quiescent memory B cells in human peripheral blood co-express bcl-2 and bcl-x(L) anti-apoptotic proteins at high levels. Eur.J.Immunol. *28*, 4418-4423.

Breitschopf, K., Haendeler, J., Malchow, P., Zeiher, A.M., and Dimmeler, S. (2000). Posttranslational modification of Bcl-2 facilitates its proteasome-dependent degradation: molecular characterization of the involved signaling pathway. Mol.Cell Biol. *20*, 1886-1896.

Brown, S.B., Bailey, K., and Savill, J. (1997). Actin is cleaved during constitutive apoptosis. Biochem.J. *323*, 233-237.

Burden, D.A. and Osheroff, N. (1998). Mechanism of action of eukaryotic topoisomerase II and drugs targeted to the enzyme. Biochim.Biophys.Acta *1400*, 139-154.

Chao, D.T., Linette, G.P., Boise, L.H., White, L.S., Thompson, C.B., and Korsmeyer, S.J. (1995). Bcl-XL and Bcl-2 repress a common pathway of cell death. J.Exp.Med. *182*, 821-828.

Cheng, E.H., Kirsch, D.G., Clem, R.J., Ravi, R., Kastan, M.B., Bedi, A., Ueno, K., and Hardwick, J.M. (1997). Conversion of Bcl-2 to a Bax-like death effector by caspases. Science *278*, 1966-1968.

Cheng, E.H., Levine, B., Boise, L.H., Thompson, C.B., and Hardwick, J.M. (1996). Bax-independent inhibition of apoptosis by Bcl-XL. Nature *379*, 554-556.

Clem, R.J., Cheng, E.H., Karp, C.L., Kirsch, D.G., Ueno, K., Takahashi, A., Kastan, M.B., Griffin, D.E., Earnshaw, W.C., Veliuona, M.A., and Hardwick, J.M. (1998). Modulation of cell death by Bcl-XL through caspase interaction. Proc.Natl.Acad.Sci.U.S.A *20; 95*, 554-559.

Colombini, M. (1989). Voltage gating in the mitochondrial channel, VDAC. J.Membr.Biol. *111*, 103-111.

Cuvillier, O., Edsall, L., and Spiegel, S. (2000). Involvement of sphingosine in mitochondria-dependent Fas-induced apoptosis of type II Jurkat T cells. J.Biol.Chem. *275*, 15691-15700.

Desagher, S., Osen-Sand, A., Nichols, A., Eskes, R., Montessuit, S., Lauper, S., Maundrell, K., Antonsson, B., and Martinou, J.C. (1999). Bid-induced conformational change of Bax is responsible for mitochondrial cytochrome c release during apoptosis. J.Cell Biol. *144*, 891-901.

Dimmeler, S., Breitschopf, K., Haendeler, J., and Zeiher, A.M. (1999). Dephosphorylation targets Bcl-2 for ubiquitin-dependent degradation: a link between the apoptosome and the proteasome pathway. J.Exp.Med. *189*, 1815-1822.

Fadeel, B., Hassan, Z., Hellstrom-Lindberg, E., Henter, J.I., Orrenius, S., and Zhivotovsky, B. (1999). Cleavage of Bcl-2 is an early event in chemotherapy-induced apoptosis of human myeloid leukemia cells. Leukemia *13*, 719-728.

Falcone, D. and Andrews, D.W. (1991). Both the 5' untranslated region and the sequences surrounding the start site contribute to efficient initiation of translation in vitro. Mol.Cell Biol. *11*, 2656-2664.

Fang, W., Rivard, J.J., Mueller, D.L., and Behrens, T.W. (1994). Cloning and molecular characterization of mouse bcl-x in B and T lymphocytes. J.Immunol. *153*, 4388-4398.

Ferri, K.F. and Kroemer, G. (2001). Organelle-specific initiation of cell death pathways. Nat.Cell Biol. *3*, E255-E263

Fischer, H., Koenig, U., Eckhart, L., and Tschachler, E. (2002). Human caspase 12 has acquired deleterious mutations. Biochem.Biophys.Res.Commun. *293*, 722-726.

Fujita, N., Nagahashi, A., Nagashima, K., Rokudai, S., and Tsuruo, T. (1998). Acceleration of apoptotic cell death after the cleavage of Bcl-XL protein by caspase-3-like proteases. Oncogene *17*, 1295-1304.

Germain, M., Affar, E.B., D'Amours, D., Dixit, V.M., Salvesen, G.S., and Poirier, G.G. (1999). Cleavage of automodified poly(ADP-ribose) polymerase during apoptosis. Evidence for involvement of caspase-7. J.Biol.Chem. *274*, 28379-28384.

Gewirtz, D.A. (1999). A critical evaluation of the mechanisms of action proposed for the antitumor effects of the anthracycline antibiotics adriamycin and daunorubicin. Biochem.Pharmacol. *57*, 727-741.

Gil-Parrado, S., Fernandez-Montalvan, A., Assfalg-Machleidt, I., Popp, O., Bestvater, F., Holloschi, A., Knoch, T.A., Auerswald, E.A., Welsh, K., Reed, J.C., Fritz, H., Fuentes-Prior, P., Spiess, E., Salvesen, G.S., and Machleidt, W. (2002). Ionomycin-activated calpain triggers apoptosis. A probable role for Bcl-2 family members. J.Biol.Chem. *277*, 27217-27226.

Gobeil, S., Boucher, C.C., Nadeau, D., and Poirier, G.G. (2001). Characterization of the necrotic cleavage of poly(ADP-ribose) polymerase (PARP-1): implication of lysosomal proteases. Cell Death.Differ. *8*, 588-594.

Gonzalez-Garcia, M., Perez-Ballestero, R., Ding, L., Duan, L., Boise, L.H., Thompson, C.B., and Nunez, G. (1994). bcl-XL is the major bcl-x mRNA form expressed during murine development and its product localizes to mitochondria. Development *120*, 3033-3042.

Gottschalk, A.R., Boise, L.H., Thompson, C.B., and Quintans, J. (1994). Identification of immunosuppressant-induced apoptosis in a murine B-cell line and its prevention by bcl-x but not bcl-2. Proc.Natl.Acad.Sci.U.S.A *19;91*, 7350-7354.

Gross, A., McDonnell, J.M., and Korsmeyer, S.J. (1999a). BCL-2 family members and the mitochondria in apoptosis. Genes Dev. *13*, 1899-1911.

Gross, A., Yin, X.M., Wang, K., Wei, M.C., Jockel, J., Milliman, C., Erdjument-Bromage, H., Tempst, P., and Korsmeyer, S.J. (1999b). Caspase cleaved BID targets mitochondria and is required for cytochrome c release, while BCL-XL prevents this release but not tumor necrosis factor-R1/Fas death. J.Biol.Chem. *274*, 1156-1163.

Harris, L.N., Yang, L., Tang, C., Yang, D., and Lupu, R. (1998). Induction of sensitivity to doxorubicin and etoposide by transfection of MCF-7 breast cancer cells with heregulin beta-2. Clin.Cancer Res. *4*, 1005-1012.

Hockenbery, D.M., Oltvai, Z.N., Yin, X.M., Milliman, C.L., and Korsmeyer, S.J. (1993). Bcl-2 functions in an antioxidant pathway to prevent apoptosis. Cell *75*, 241-251.

Hsu, Y.T., Wolter, K.G., and Youle, R.J. (1997a). Cytosol-to-membrane redistribution of Bax and Bcl-X(L) during apoptosis. Proc.Natl.Acad.Sci.U.S.A *94*, 3668-3672.

Hsu, Y.T. and Youle, R.J. (1997b). Nonionic detergents induce dimerization among members of the Bcl-2 family. J.Biol.Chem. *272*, 13829-13834.

Huigsloot, M., Tijdens, I.B., Mulder, G.J., and van de, W.B. (2002). Differential regulation of doxorubicin-induced mitochondrial dysfunction and apoptosis by Bcl-2 in mammary adenocarcinoma (MTLn3) cells. J.Biol.Chem. *277*, 35869-35879.

Jackson, R.J., Campbell, E.A., Herbert, P., and Hunt, T. (1983). The preparation and properties of gel-filtered rabbit-reticulocyte lysate protein-synthesis systems. Eur.J.Biochem. *131*, 289-301.

Jacobson, M.D. and Raff, M.C. (1995). Programmed cell death and Bcl-2 protection in very low oxygen. Nature *374*, 814-816.

Janiak, F., Glover, J.R., Leber, B., Rachubinski, R.A., and Andrews, D.W. (1994a). Targeting of passenger protein domains to multiple intracellular membranes. Biochem.J. *300*, 191-199.

Janiak, F., Leber, B., and Andrews, D.W. (1994b). Assembly of Bcl-2 into microsomal and outer mitochondrial membranes. J.Biol.Chem. *269*, 9842-9849.

Janicke, R.U., Sprengart, M.L., Wati, M.R., and Porter, A.G. (1998). Caspase-3 is required for DNA fragmentation and morphological changes associated with apoptosis. J.Biol.Chem. *273*, 9357-9360.

Johnson, D.E. (2000). Noncaspase proteases in apoptosis. Leukemia *14*, 1695-1703.

Johnstone, R.W., Ruefli, A.A., and Lowe, S.W. (2002). Apoptosis: a link between cancer genetics and chemotherapy. Cell *108*, 153-164.

Kamada, S., Shimono, A., Shinto, Y., Tsujimura, T., Takahashi, T., Noda, T., Kitamura, Y., Kondoh, H., and Tsujimoto, Y. (1995). bcl-2 deficiency in mice leads to pleiotropic abnormalities: accelerated lymphoid cell death in thymus and spleen, polycystic kidney, hair hypopigmentation, and distorted small intestine. Cancer Res. *55*, 354-359.

Kiefer, M.C., Brauer, M.J., Powers, V.C., Wu, J.J., Umansky, S.R., Tomei, L.D., and Barr, P.J. (1995). Modulation of apoptosis by the widely distributed Bcl-2 homologue Bak. Nature *20;374*, 736-739.

Kirsch, D.G., Doseff, A., Chau, B.N., Lim, D.S., Souza-Pinto, N.C., Hansford, R., Kastan, M.B., Lazebnik, Y.A., and Hardwick, J.M. (1999). Caspase-3-dependent cleavage of Bcl-2 promotes release of cytochrome c. J.Biol.Chem. *274*, 21155-21161.

Kottke, T.J., Blajeski, A.L., Meng, X.W., Svingen, P.A., Ruchaud, S., Mesner, P.W., Jr., Boerner, S.A., Samejima, K., Henriquez, N.V., Chilcote, T.J., Lord, J., Salmon, M., Earnshaw, W.C., and Kaufmann, S.H. (2002). Lack of correlation between caspase activation and caspase activity assays in paclitaxel-treated MCF-7 breast cancer cells. J.Biol.Chem. *277*, 804-815.

Krajewski, S., Tanaka, S., Takayama, S., Schibler, M.J., Fenton, W., and Reed, J.C. (1993). Investigation of the subcellular distribution of the bcl-2 oncoprotein: residence in the nuclear envelope, endoplasmic reticulum, and outer mitochondrial membranes. Cancer Res. *53*, 4701-4714.

Kuo, T.H., Kim, H.R., Zhu, L., Yu, Y., Lin, H.M., and Tsang, W. (1998). Modulation of endoplasmic reticulum calcium pump by Bcl-2. Oncogene *17*, 1903-1910.

Kutay U., Hartmann E., and Rapoport T.A. (1993). A class of membrane proteins with a C-terminal anchor. Trends in Cell Biology *3*, 72-75.

Kuwana, T., Mackey, M.R., Perkins, G., Ellisman, M.H., Latterich, M., Schneiter, R., Green, D.R., and Newmeyer, D.D. (2002). Bid, Bax, and lipids cooperate to form supramolecular openings in the outer mitochondrial membrane. Cell *111*, 331-342.

Lam, M., Bhat, M.B., Nunez, G., Ma, J., and Distelhorst, C.W. (1998). Regulation of Bcl-xl channel activity by calcium. J.Biol.Chem. *273*, 17307-17310.

Lee, S.T., Hoeflich, K.P., Wasfy, G.W., Woodgett, J.R., Leber, B., Andrews, D.W., Hedley, D.W., and Penn, L.Z. (1999). Bcl-2 targeted to the endoplasmic reticulum can inhibit apoptosis induced by Myc but not etoposide in Rat-1 fibroblasts. Oncogene *18*, 3520-3528.

Lipponen, P., Pietilainen, T., Kosma, V.M., Aaltomaa, S., Eskelinen, M., and Syrjanen, K. (1995). Apoptosis suppressing protein bcl-2 is expressed in well-differentiated breast carcinomas with favourable prognosis. J.Pathol. *177*, 49-55.

Liu, D., Martino, G., Thangaraju, M., Sharma, M., Halwani, F., Shen, S.H., Patel, Y.C., and Srikant, C.B. (2000). Caspase-8-mediated intracellular acidification precedes mitochondrial dysfunction in somatostatin-induced apoptosis. J.Biol.Chem. *275*, 9244-9250.

Mashima, T., Naito, M., Noguchi, K., Miller, D.K., Nicholson, D.W., and Tsuruo, T. (1997). Actin cleavage by CPP-32/apopain during the development of apoptosis. Oncogene *14*, 1007-1012.

Minn, A.J., Kettlun, C.S., Liang, H., Kelekar, A., Vander Heiden, M.G., Chang, B.S., Fesik, S.W., Fill, M., and Thompson, C.B. (1999). Bcl-xL regulates apoptosis by heterodimerization-dependent and -independent mechanisms. EMBO J. *18*, 632-643.

Mitoma, J. and Ito, A. (1992). The carboxy-terminal 10 amino acid residues of cytochrome b5 are necessary for its targeting to the endoplasmic reticulum. EMBO J. *11*, 4197-4203.

Mizuguchi, M., Sohma, O., Takashima, S., Ikeda, K., Yamada, M., Shiraiwa, N., and Ohta, S. (1996). Immunochemical and immunohistochemical localization of Bcl-x protein in the rat central nervous system. Brain Res. *712*, 281-286.

Morishima, N., Nakanishi, K., Takenouchi, H., Shibata, T., and Yasuhiko, Y. (2002). An endoplasmic reticulum stress-specific caspase cascade in apoptosis. Cytochrome c-independent activation of caspase-9 by caspase-12. J.Biol.Chem. *277*, 34287-34294.

Motoyama, N., Wang, F., Roth, K.A., Sawa, H., Nakayama, K., Nakayama, K., Negishi, I., Senju, S., Zhang, Q., Fujii, S., and . (1995). Massive cell death of immature hematopoietic cells and neurons in Bcl-x-deficient mice. Science *267*, 1506-1510.

Muchmore, S.W., Sattler, M., Liang, H., Meadows, R.P., Harlan, J.E., Yoon, H.S., Nettesheim, D., Chang, B.S., Thompson, C.B., Wong, S.L., Ng, S.L., and Fesik, S.W. (1996). X-ray and NMR structure of human Bcl-xL, an inhibitor of programmed cell death. Nature *381*, 335-341.

Nakagawa, T. and Yuan, J. (2000). Cross-talk between two cysteine protease families. Activation of caspase-12 by calpain in apoptosis. J.Cell Biol. *150*, 887-894.

Nechushtan, A., Smith, C.L., Hsu, Y.T., and Youle, R.J. (1999). Conformation of the Bax C-terminus regulates subcellular location and cell death. EMBO J. *18*, 2330-2341.

Ng, F.W., Nguyen, M., Kwan, T., Branton, P.E., Nicholson, D.W., Cromlish, J.A., and Shore, G.C. (1997). p28 Bap31, a Bcl-2/Bcl-XL- and procaspase-8-associated protein in the endoplasmic reticulum. J.Cell Biol. *20;139*, 327-338.

Oltvai, Z.N., Milliman, C.L., and Korsmeyer, S.J. (1993). Bcl-2 heterodimerizes in vivo with a conserved homolog, Bax, that accelerates programmed cell death. Cell *74*, 609-619.

Pan, Z., Damron, D., Nieminen, A.L., Bhat, M.B., and Ma, J. (2000). Depletion of intracellular Ca2+ by caffeine and ryanodine induces apoptosis of chinese hamster ovary cells transfected with ryanodine receptor. J.Biol.Chem. *275*, 19978-19984.

Pegoraro, L., Palumbo, A., Erikson, J., Falda, M., Giovanazzo, B., Emanuel, B.S., Rovera, G., Nowell, P.C., and Croce, C.M. (1984). A 14;18 and an 8;14 chromosome translocation in a cell line derived from an acute B-cell leukemia. Proc.Natl.Acad.Sci.U.S.A *81*, 7166-7170.

Pena, J.C., Thompson, C.B., Recant, W., Vokes, E.E., and Rudin, C.M. (1999). Bcl-xL and Bcl-2 expression in squamous cell carcinoma of the head and neck. Cancer *85*, 164-170.

Petros, A.M., Medek, A., Nettesheim, D.G., Kim, D.H., Yoon, H.S., Swift, K., Matayoshi, E.D., Oltersdorf, T., and Fesik, S.W. (2001). Solution structure of the antiapoptotic protein bcl-2. Proc.Natl.Acad.Sci.U.S.A *98*, 3012-3017.

Pistor, S., Chakraborty, T., Niebuhr, K., Domann, E., and Wehland, J. (1994). The ActA protein of Listeria monocytogenes acts as a nucleator inducing reorganization of the actin cytoskeleton. EMBO J. *13*, 758-763.

Prendergast, G.C. (1999). Mechanisms of apoptosis by c-Myc. Oncogene *18*, 2967-2987.

Reutelingsperger, C.P., Dumont, E., Thimister, P.W., van Genderen, H., Kenis, H., van de, E.S., Heidendal, G., and Hofstra, L. (2002). Visualization of cell death in vivo with the annexin A5 imaging protocol. J.Immunol.Methods *265*, 123-132.

Rohlf, F.J. and Sokal R.R. **Biometry : The Principles and Practice of Statistics in Biological Research**. San Francisco: W.H. Freeman and Co., 1981.

Rudner, J., Lepple-Wienhues, A., Budach, W., Berschauer, J., Friedrich, B., Wesselborg, S., Schulze-Osthoff, K., and Belka, C. (2001). Wild-type, mitochondrial and ER-restricted Bcl-2 inhibit DNA damage-induced apoptosis but do not affect death receptor-induced apoptosis. J.Cell Sci. *114*, 4161-4172.

Sattler, M., Liang, H., Nettesheim, D., Meadows, R.P., Harlan, J.E., Eberstadt, M., Yoon, H.S., Shuker, S.B., Chang, B.S., Minn, A.J., Thompson, C.B., and Fesik, S.W. (1997). Structure of Bcl-xL-Bak peptide complex: recognition between regulators of apoptosis. Science *275*, 983-986.

Schagger, H. and von Jagow, G. (1987). Tricine-sodium dodecyl sulfate-polyacrylamide gel electrophoresis for the separation of proteins in the range from 1 to 100 kDa. Anal.Biochem. *166*, 368-379.

Schendel, S.L., Xie, Z., Montal, M.O., Matsuyama, S., Montal, M., and Reed, J.C. (1997). Channel formation by antiapoptotic protein Bcl-2. Proc.Natl.Acad.Sci.U.S.A *94*, 5113-5118.

Scorrano, L., Oakes, S.A., Opferman, J.T., Cheng, E.H., Sorcinelli, M.D., Pozzan, T., and Korsmeyer, S.J. (2003). BAX and BAK regulation of endoplasmic reticulum Ca2+: a control point for apoptosis. Science *300*, 135-139.

Sedlak, T.W., Oltvai, Z.N., Yang, E., Wang, K., Boise, L.H., Thompson, C.B., and Korsmeyer, S.J. (1995). Multiple Bcl-2 family members demonstrate selective dimerizations with Bax. Proc.Natl.Acad.Sci.U.S.A *92*, 7834-7838.

Shimizu, S., Eguchi, Y., Kosaka, H., Kamiike, W., Matsuda, H., and Tsujimoto, Y. (1995). Prevention of hypoxia-induced cell death by Bcl-2 and Bcl-xL. Nature *374*, 811-813.

Shimizu, S., Matsuoka, Y., Shinohara, Y., Yoneda, Y., and Tsujimoto, Y. (2001). Essential role of voltage-dependent anion channel in various forms of apoptosis in mammalian cells. J.Cell Biol. *152*, 237-250.

Shimizu, S., Narita, M., and Tsujimoto, Y. (1999). Bcl-2 family proteins regulate the release of apoptogenic cytochrome c by the mitochondrial channel VDAC. Nature *399*, 483-487.

Shinkai, Y., Rathbun, G., Lam, K.P., Oltz, E.M., Stewart, V., Mendelsohn, M., Charron, J., Datta, M., Young, F., Stall, A.M., and . (1992). RAG-2-deficient mice lack mature lymphocytes owing to inability to initiate V(D)J rearrangement. Cell *68*, 855-867.

Soucie, E.L., Annis, M.G., Sedivy, J., Filmus, J., Leber, B., Andrews, D.W., and Penn, L.Z. (2001). Myc potentiates apoptosis by stimulating Bax activity at the mitochondria. Mol.Cell Biol. *21*, 4725-4736.

Sternstein M. (1996). Binomial Distributions. In Statistics. AnonymousIthaca, New York: Barron's), pp. 71-80.

Sugiyama, T., Shimizu, S., Matsuoka, Y., Yoneda, Y., and Tsujimoto, Y. (2002). Activation of mitochondrial voltage-dependent anion channel by apro-apoptotic BH3-only protein Bim. Oncogene *21*, 4944-4956.

Sun, X.M., Bratton, S.B., Butterworth, M., MacFarlane, M., and Cohen, G.M. (2002). Bcl-2 and Bcl-xL inhibit CD95-mediated apoptosis by preventing mitochondrial release of Smac/DIABLO and subsequent inactivation of X-linked inhibitor-of-apoptosis protein. J.Biol.Chem. *277*, 11345-11351.

Suzuki, M., Youle, R.J., and Tjandra, N. (2000). Structure of Bax: coregulation of dimer formation and intracellular localization. Cell *103*, 645-654.

Takehara, T., Liu, X., Fujimoto, J., Friedman, S.L., and Takahashi, H. (2001). Expression and role of Bcl-xL in human hepatocellular carcinomas. Hepatology *34*, 55-61.

Teixeira, C., Reed, J.C., and Pratt, M.A. (1995). Estrogen promotes chemotherapeutic drug resistance by a mechanism involving Bcl-2 proto-oncogene expression in human breast cancer cells. Cancer Res. *55*, 3902-3907.

Thangaraju, M., Sharma, K., Leber, B., Andrews, D.W., Shen, S.H., and Srikant, C.B. (1999). Regulation of acidification and apoptosis by SHP-1 and Bcl-2. J.Biol.Chem. *274*, 29549-29557.

Thomas, D.A., Scorrano, L., Putcha, G.V., Korsmeyer, S.J., and Ley, T.J. (2001). Granzyme B can cause mitochondrial depolarization and cell death in the absence of BID, BAX, and BAK. Proc.Natl.Acad.Sci.U.S.A *98*, 14985-14990.

Vander Heiden, M.G., Li, X.X., Gottleib, E., Hill, R.B., Thompson, C.B., and Colombini, M. (2001). Bcl-xL promotes the open configuration of the voltage-dependent anion channel and metabolite passage through the outer mitochondrial membrane. J.Biol.Chem. *276*, 19414-19419.

Voet, D. and Voet, J.G. **Biochemistry: Second Edition**. Amino Acids of Proteins. Toronto: John Wiley and Sons, Inc., 1995

Walker, J.V. and Nitiss, J.L. (2002). DNA topoisomerase II as a target for cancer chemotherapy. Cancer Invest *20*, 570-589.

Wang, G.Q., Gastman, B.R., Wieckowski, E., Goldstein, L.A., Gambotto, A., Kim, T.H., Fang, B., Rabinovitz, A., Yin, X.M., and Rabinowich, H. (2001). A role for mitochondrial Bak in apoptotic response to anticancer drugs. J.Biol.Chem. *276*, 34307-34317.

Wang, X. (2001). The expanding role of mitochondria in apoptosis. Genes Dev. *15*, 2922-2933.

Wilhelm, S, Grober, B, Gluch, M, and Heinz, H. (2000) Confocal Laser Scanning Microscopy. Carl Zeiss.
Ref Type: Pamphlet

Wilson, J.W., Wakeling, A.E., Morris, I.D., Hickman, J.A., and Dive, C. (1995). MCF-7 human mammary adenocarcinoma cell death in vitro in response to hormone-withdrawal and DNA damage. Int.J.Cancer *61*, 502-508.

Wolter, K.G., Hsu, Y.T., Smith, C.L., Nechushtan, A., Xi, X.G., and Youle, R.J. (1997). Movement of Bax from the cytosol to mitochondria during apoptosis. J.Cell Biol. *139*, 1281-1292.

Wyllie, A.H. (1980). Glucocorticoid-induced thymocyte apoptosis is associated with endogenous endonuclease activation. Nature *284*, 555-556.

Yang, X.H., Sladek, T.L., Liu, X., Butler, B.R., Froelich, C.J., and Thor, A.D. (2001). Reconstitution of caspase 3 sensitizes MCF-7 breast cancer cells to doxorubicin- and etoposide-induced apoptosis. Cancer Res. *61*, 348-354.

Zhu, W., Cowie, A., Wasfy, G.W., Penn, L.Z., Leber, B., and Andrews, D.W. (1996). Bcl-2 mutants with restricted subcellular location reveal spatially distinct pathways for apoptosis in different cell types. EMBO J. *15*, 4130-4141.

Zornig, M., Hueber, A., Baum, W., and Evan, G. (2001). Apoptosis regulators and their role in tumorigenesis. Biochim.Biophys.Acta *1551*, F1-37.